

Ana Daniela Curioso Cação

Development of new L-lactic acid
copolymers: studies on the
structure/properties relationship

Master Thesis in Chemical Engineering, oriented by Professor Jorge Coelho, by
Professor Pedro Nuno Simões and by the Doctor Ana Clotilde Fonseca, submitted to
the Faculty of Sciences and Technology of the University of Coimbra

September 2013



UNIVERSIDADE DE COIMBRA

*“O futuro é construído pelas nossas decisões diárias, inconstantes e mutáveis,
e cada evento influencia todos os outros.”*

Alvin Toffler

Acknowledgments

Uma dissertação, apesar do processo individual a que qualquer aluno está destinado, reúne contributos que não podem deixar de ser reconhecidos. A conquista tem que ser partilhada com todos os que contribuíram, de forma directa ou indirecta para a concretização e conclusão do trabalho aqui apresentado. A todos quero manifestar o meu sincero agradecimento!

Desde logo à Doutora Ana Fonseca, minha orientadora, expresso o meu profundo agradecimento pelo seu auxílio em todos os momentos da realização deste trabalho, pela constante partilha de conhecimentos, pelas sugestões e pelo rigor na análise de todos os detalhes. Agradeço também a sua amizade e o modo como sempre me apoiou e especialmente pela simpatia com que sempre me recebeu. Por tudo isto, o meu sentido obrigado!

Aos meus orientadores, Professor Doutor Jorge Coelho e Professor Doutor Pedro Simões, pela preciosa ajuda em todas as questões científicas, pela disponibilidade e auxílio sempre demonstrados.

A todo o grupo de Materiais poliméricos, pelo auxílio e apoio sempre prestado. Não posso passar sem deixar um especial agradecimento ao Pedro, à Célia, à Bianca, à Cátia, à Joana e à Inês, pela preciosa ajuda e pelo óptimo ambiente que me proporcionaram durante a realização deste trabalho.

Aos meus amigos, pela sua amizade, preocupação e incentivo que sempre me transmitiram ao longo deste percurso. Em especial à Sofia e à Fabela, por toda a sua amizade, disponibilidade e companheirismo nos momentos mais críticos desta caminhada.

Ao Miguel, pela amizade, pela força e incentivo, pela paciência e compreensão reveladas ao longo da realização deste trabalho, expresso-lhe aqui o meu sincero agradecimento!

Aos meus pais, por serem o meu exemplo de vida e por me terem dado a oportunidade de chegar até aqui. Um muito obrigado por todo o apoio ao longo de todos estes anos, pelo carinho e compreensão e por acreditarem sempre nas minhas conquistas! A vocês devo tudo!

Abstract

Poly(lactic acid) (PLA) or polylactide is a biodegradable and renewable thermoplastic polyester that due to its physical and chemical properties has potential to replace conventional petrochemical-based polymers on the market, particularly in packaging. In the last years, several studies have focused on developing new technologies to produce PLA with biological, chemical and mechanical properties equivalent or superior to fossil-based polymers. The purpose of this work was: (i) synthesize PLA homopolymers and PLA copolymers with D,L-mandelic acid (MA) and vanillic acid (VA) by direct polycondensation; (ii) evaluate the structure/properties relationships of the homopolymers and copolymers; (iii) development of PLA homopolymers and PLA copolymers with high molecular weight, by chain extension reactions.

The work was organized in two parts. The first part was centered in the development of PLA homopolymers and copolymers with MA and VA, by direct polycondensation and azeotropic dehydration condensation. Different amounts of co-monomers (MA and VA) were used in the copolymerization reaction with L-lactic acid (LA) and different reaction conditions were used. The FTIR analysis revealed the presence of the ester linkages and the ^1H NMR analyses showed that the amount of co-monomers used in the feed was almost quantitatively incorporated in the final PLA copolymer.

The size exclusion chromatography (SEC) analysis indicates that the PLA copolymers have a lower molecular weight than the homopolymers, which can be attributed to a lower reactivity of the two co-monomers when compared to LA. The thermal stabilities and the thermal events below degradation temperature were evaluated by SDT, DSC and DMTA analysis, respectively. Based on the SDT results, it was concluded that the inclusion of aromatic compounds in to PLA structure increases its thermal stability. Through the DSC analysis it was possible to conclude that the PLA homopolymers present a semi-crystalline character, while the copolymers exhibit an amorphous character. The DMTA analysis allowed the determination of glass transition temperature (T_g) and the obtained results for the homopolymers and copolymers were among 80-90°C and 25-75°C, respectively. The differences in the values of T_g can be attributed to the differences in molecular weight between the copolymers and homopolymers.

The second part of the work focused on chain extension reactions L-LA oligomers and co-oligomers with diisocyanates (1,6-hexamethylene diisocyanate (HMDI) and isophorone diisocyanate (IPDI)), in order to obtain polymers of high molecular weight.. The L-LA oligomers were synthesized by melt polycondensation of monomers (LA, or LA/MA or LA/VA), in the presence of ethylene glycol and Sn(Oct)₂ as catalyst. The spectroscopic analysis (FTIR and ¹H NMR) performed on the products of chain extension indicated the success of the reaction.

The SEC analysis showed that products of chain extension present a higher molecular weight than L-LA oligomers, as expected, however not all the oligomeric chains were reinitiated. For the L-LA oligomers, the SDT analysis indicated that all the samples present a similar weight loss pattern. Regarding to the products of chain extension, SDT analysis revealed the presence of two thermal degradation stages, that can be ascribed to the rupture of C-NH urethane bond, whereas second stage corresponds to the scission of the ester linkage. Through the DSC analysis it was possible verify that both L-LA oligomers and products of chain extension present an amorphous character. Lastly, the DMTA analysis was performed in order to evaluate the samples T_g . The obtained results showed that the products of chain extension present a higher T_g which can be a direct consequence of the increase in molecular weight.

Resumo

O poli(ácido láctico) (PLA) ou lactídeo é um poliéster termoplástico biodegradável e renovável que devido às suas propriedades físicas e químicas tem potencial para substituir os polímeros convencionais de base fóssil no mercado, particularmente na área da embalagem. Nos últimos anos, vários estudos têm-se focado no desenvolvimento de novas tecnologias para produzir PLA com propriedades biológicas, químicas e mecânicas equivalentes ou superiores aos polímeros de base fóssil.

O objectivo deste trabalho foi: (i) sintetizar homopolímeros e copolímeros de PLA com ácido mandélico (D,L-MA) e ácido vanílico (VA) utilizando a policondensação directa; (ii) avaliar a relação estrutura/propriedades dos homopolímeros e copolímeros; (iii) desenvolvimento de homopolímeros e copolímeros de PLA com elevado peso molecular, através de reacções de extensão de cadeia.

O trabalho foi organizado em duas partes. A primeira parte centrou-se no desenvolvimento de homopolímeros e copolímeros de PLA com MA e VA, através de policondensação directa e condensação azeotrópica. Na reacção de policondensação foram utilizadas quantidades de monómeros (D,L-MA e VA) e condições reaccionais diferentes. A análise FTIR revelou a presença da ligação éster e a análise ^1H NMR mostrou que a quantidade de co-monómeros na alimentação foi quase incorporada quantitativamente no copolímero final de PLA.

A análise de cromatografia por exclusão de tamanhos (SEC) indicou que os copolímeros de PLA possuem um peso molecular mais baixo que os homopolímeros, o que pode ser atribuído à baixa reactividade dos dois co-monómeros quando comparados com o ácido láctico (LA). As estabilidades térmicas e os eventos térmicos abaixo da temperatura de degradação foram avaliados pelas análises SDT, DSC e DMTA, respectivamente. Baseado nos resultados da análise SDT foi concluído que a inclusão de compostos aromáticos na estrutura do PLA aumentou a sua estabilidade térmica. Através da análise DSC foi possível concluir que os homopolímeros de PLA apresentam um carácter semi-cristalino, enquanto os copolímeros exibem um carácter amorfo. A análise DMTA permitiu determinar a temperatura de transição vítrea (T_g) e os resultados obtidos para os homopolímeros e copolímeros foram entre 80-90°C e 25-75°C, respectivamente. As diferenças nos valores da T_g podem ser atribuídas à diferença no peso molecular entre os copolímeros e os homopolímeros.

A segunda parte do trabalho focou-se nas reacções de extensão de cadeia dos oligómeros e co-oligómeros de L-ácido láctico (L-LA) com di-isocianatos (1,6- hexametileno diisocianato (HMDI) e isoforona di-isocianato (IPDI)), de modo a obter polímeros de elevado peso molecular. Os oligómeros de L-LA foram sintetizados por policondensação directa dos monómeros (LA, ou LA/MA ou LA/VA), na presença de etileno glicol e de Sn(Oct)₂ como catalisador. A análise espectroscópica (FTIR e ¹H NMR) realizada aos produtos da extensão de cadeia indicou o sucesso da reacção.

A análise SEC mostrou que os produtos da extensão de cadeia apresentam um peso molecular mais elevado que os oligómeros de L-LA, como esperado, contudo, nem todas as cadeias oligoméricas foram reiniciadas. Para os oligómeros, a análise SDT indicou que todas as amostras apresentam um padrão de perda massa similar. Em relação aos produtos da extensão de cadeia, a análise SDT revelou a presença de duas fases de degradação térmica, que podem ser atribuídas à ruptura da ligação uretana C-NH, enquanto a segunda fase de degradação térmica corresponde à cisão da ligação éster. Através da análise DSC foi possível verificar que tanto os oligómeros de L-LA e os produtos da extensão de cadeia apresentam um carácter amorfo. Por último, a análise DMTA foi realizada a fim de avaliar a T_g das amostras. Os resultados obtidos mostram que os produtos da extensão de cadeia apresentam uma T_g mais elevado, o que pode ser uma consequência directa do aumento do peso molecular.

List of Acronyms

ϵ -CL – ϵ -caprolactone

DL-MA – D,L-mandelic acid

DMTA – dynamic mechanical thermal analysis

DOP – dioctyl phthalate

DSC – differential scanning calorimetry

EG – ethylene glycol

FTIR – Fourier Transform Infrared Spectroscopy

HMDI – 1,6 – hexamethylenediisocyanate

IPDI – isophorone diisocyanate

LA – lactic acid

L-LA – L-lactic acid

PBAT – poly(butylene adipate-*co*-terephthalate)

PBGA – poly(1,3-butylene glycol adipate)

PCL – poly(ϵ -caprolactone)

PDI – polydispersity

PDLA – poly(D-lactic acid)

PDLLA – poly(D,L – lactic acid)

PE – poly(ethylene)

PEG – poly(ethylene glycol)

PEPG – poly(ethylene glycol-*ran*-propylene glycol)

PET – poly(ethylene terephthalate)

PHAs – poly(hydroxyalkanoates)

PHB – poly(β -hydroxybutyrate)

PLA – poly(lactic acid)

PLLA – poly(L-lactic acid)

PP – polypropylene

PPG – polypropylene glycol

PS – polystyrene

PVC – poly(vinyl chloride)

RI – refractive index

SEC – size-exclusion chromatography

SSP – solid state polymerization

ROP – ring opening polymerization

TBC – tributyl citrate

THF – tetrahydrofuran

TMS – tetramethylsilane

VA – vanillic acid

Nomenclature

T_c : decomposition temperature, °C

T_m : melting temperature, °C

T_g : glass transition temperature, °C

T_{on} : extrapolated onset temperature, °C

\overline{M}_n : number average molecular weight, g mol⁻¹

\overline{M}_w : weight average molecular weight, g mol⁻¹

Contents

1. Introduction	1
1.1. Evaluation of biodegradability of polymers	2
1.2 Poly(Lactic Acid).....	4
1.3 Lactic Acid – PLA monomer	7
1.4 PLA Synthesis	8
1.5 Physical and chemical properties of PLA	15
1.6 PLA advantages and limitations	16
1.6.1. Advantages	16
1.6.2. Limitations	16
1.7 Pathways to change PLA properties	17
1.7.1 Copolymerization	17
1.7.2 Chain extension	18
1.7.3 Polymer blends	19
1.7.4 Plasticization	20
2 Characterization Techniques	21
2.1 Fourier Transform Infrared Spectroscopy (FTIR)	21
2.2 Nuclear Magnetic Resonance (NMR).....	22
2.3 Molecular Weight Determination by Gel Permeation Chromatography (GPC)	23
2.4 Thermogravimetric Analysis (TGA)	24
2.5 Differential Scanning Calorimetry (DSC)	25
2.6 Dynamic Mechanical Thermal Analysis (DMTA)	26
3 Experimental Methods	27
3.1 Materials.....	27
3.2 Synthesis Procedures	27
3.2.1 Melt polycondensation.....	27
3.2.2 Azeotropic dehydration condensation	29
3.2.3 Chain extension	30

3.3	Characterization techniques	32
3.3.1	Chemical Structure identification	32
3.3.2	Molecular Weight Distribution.....	33
3.3.3	Thermal properties.....	33
4	Results and Discussion.....	35
4.1	PLA homopolymers and copolymers.....	35
4.1.1	Chemical Structure Identification.....	35
4.1.2	Molecular Weight Distribution by GPC	38
4.1.3	Thermal analysis.....	41
4.2	PLA chain extension.....	47
4.2.1	Chemical Structure Identification.....	47
4.2.2	Molecular Weight Distribution by GPC	54
4.2.3	Thermal analysis.....	57
5	Final remarks	66
5.1	Conclusions	66
5.2	Future work	67
	Annexes.....	71
A.	FTIR analysis.....	I
B.	¹ H NMR Analysis	V
C.	GPC Analysis	XIII
D.	SDT Analysis.....	XVI
E.	DSC Analysis	XXIV
F.	DMTA Analysis.....	XXVIII

List of Figures

Figure 1 – The different classifications of bioplastic materials. (Adapted from reference ^[3]). .	2
Figure 2 - The life cycle of PLA in nature ^[10]	4
Figure 3 - Different isomeric forms of LA.....	7
Figure 4 - Microbial fermentation of LA; SFF represents simultaneous saccharification and fermentation ^[16]	8
Figure 5 - Different isomers of lactide.....	12
Figure 6 - Molecular structure of PLA, a chiral molecule.	15
Figure 7 - Schematics of block copolymer structures: a) diblock; (b) triblock; (c) alternating multiblock; (d); dendrimer-like copolymer; (e) star-like copolymer (Adapted from reference ^[36]	18
Figure 8 - A typical correlation figure for the infrared modes of polymers ^[53]	22
Figure 9 - ¹ H NMR peaks of the PLA formulations, main functional groups (Adapted from ^[53]).....	23
Figure 10 - Image of a typical size-exclusion chromatograph column.....	24
Figure 11 - Typical losses mass and derivative curve in a polymer system ^[53]	25
Figure 12 - Typical DSC curve for a polymer ^[53]	26
Figure 13 – Schematic representation of the melt polycondensation apparatus.....	28
Figure 14 - Schematic representation of the azeotropic dehydration polycondensation apparatus.....	29
Figure 15 - FTIR spectra of the PLA homopolymer (AC2), PLA-co-MA copolymer (AC5) and PLA-co-VA copolymer (AC7).....	35
Figure 16 – ¹ H NMR of the PLA homopolymer (AC2), PLA-co-MA copolymer (AC5) and PLA-co-VA copolymer (AC7).	37
Figure 17 – Normalized RI signal vs. retention volume for PLA homopolymer and copolymers.	39
Figure 18 - Normalized RI signal vs. retention volume for PLA homopolymers.	40
Figure 19 - Thermoanalytical curves obtained in simultaneous of PLA homopolymers and copolymers; (A) PLA homopolymer (AC2); (B) PLA-co-MA (AC5); (C) PLA-co-VA (AC7).	41
Figure 20 - DSC thermograms of PLA homopolymer (AC2) and PLA-co-PMA copolymer (AC5).....	44

Figure 21 – DMTA traces (glass transition zone) of PLA homopolymer and copolymers, at two frequencies: (A) PLA homopolymer (AC2); (B) PLA- <i>co</i> -MA (AC5); (C) PLA- <i>co</i> -VA (AC7).....	46
Figure 22 - FTIR spectra of the PLA oligomers with hydroxyl end groups.	48
Figure 23 - FTIR spectra of PLA oligomer (AC-OLA1) and the products of chain extension (AC-CE1 and AC-CE2).	49
Figure 24 - ¹ H NMR of the PLA oligomers and co-oligomers with hydroxyl end groups.	51
Figure 25 - ¹ H NMR of the PLA oligomer (AC-OLA1) and products of chain extension (AC-CE1 and AC-CE2).	53
Figure 26 - Normalized RI signal vs. retention volume for LA oligomers and co-oligomers.	54
Figure 27 - Normalized RI signal vs. retention volume for PLA oligomer (AC-OLA1) and products of chain extension (AC-CE1 and AC-CE2).	55
Figure 28 - Simultaneous thermoanalytical curves of LA oligomer and co-oligomers; (A) LA oligomer (AC-OLA1);(B) O(LA- <i>co</i> -MA) (AC-OLA2); (C) O(LA- <i>co</i> -VA) (AC-OLA4).	57
Figure 29 - Simultaneous thermoanalytical curves of LA oligomer and products of chain extension; (A) LA oligomer (AC-OLA1); (B) Product of chain extension (AC-CE1); (C) Product of chain extension (AC-CE2).	59
Figure 30 - DSC curves of the LA oligomers.....	61
Figure 31 – DSC thermograms of LA oligomer and products of chain extension.	62
Figure 32 - DMTA traces (glass transition zone) of the LA oligomers. (A) LA oligomer (AC-OLA1); (B) O(LA- <i>co</i> -MA) (AC-OLA2); (C) O(LA- <i>co</i> -VA) (AC-OLA4), at two frequencies.	63
Figure 33 - DMTA traces (glass transition zone) of products of chain extension. (A) LA oligomer (AC-OLA1); (B) product of chain extension with IPDI (AC-CE1); (C) product of chain extension with HMDI (AC-CE2), at two frequencies.	64
Figure A1 - FTIR spectra for PLA samples obtained by melt polycondensation; (A) PLA homopolymers; (B) PLA copolymer.....	I
Figure A2 - FTIR spectra for PLA samples obtained by azeotropic dehydration condensation; (A) PLA homopolymers; (B) PLA copolymers.....	II
Figure A3 - FTIR spectra of the PLA oligomers and products of chain extension.	III
Figure B1 - ¹ H NMR of the PLA homopolymers (AC3 and AC4) and copolymer (PLA- <i>co</i> -MA) (AC6).	V

Figure B2 - ^1H NMR of the PLA homopolymers obtained by Azeotropic dehydration condensation.....	VI
Figure B3 - ^1H NMR of the PLA oligomer (AC-OLA2) and products of chain extension (AC-CE3) and AC-CE4).....	VII
Figure B4 - ^1H NMR of the PLA oligomer (AC-OLA3) and products of chain extension (AC-CE5) and AC-CE6).....	VIII
Figure B5 - ^1H NMR of the PLA oligomer (AC-OLA4) and products of chain extension (AC-CE7) and AC-CE8).....	IX
Figure B6 - ^1H NMR of the PLA oligomer (AC-OLA5) and products of chain extension (AC-CE9) and AC-CE10).....	X
Figure B7 - ^1H NMR of the PLA oligomer (AC-OLA6) and products of chain extension (AC-CE11) and AC-CE12).....	XI
Figure B8 - ^1H NMR of the PLA oligomer (AC-OLA7) and products of chain extension (AC-CE13) and AC-CE14).....	XII
Figure C1- Normalized RI signal vs. retention volume for PLA samples obtained by melt polycondensation; (A) PLA homopolymers; (B) PL- <i>co</i> -MA.....	XIII
Figure C2 - Normalized RI signal vs. retention volume for PLA homopolymer and copolymer obtained by azeotropic dehydration condensation.....	XIV
Figure C3 - Normalized RI signal vs. retention volume for LA oligomers and products of chain extension.....	XV
Figure D1 - Simultaneous thermoanalytical curves of monomers; (A) Mandelic acid; (A) Vanillic acid.....	XVI
Figure D2 - Simultaneous thermoanalytical curves of PLA homopolymers and copolymers; (A) PLA homopolymer; (B) PLA homopolymer; (C) PLA- <i>co</i> -MA.....	XVII
Figure D3 Simultaneous thermoanalytical curves of LA co-oligomer and products of chain extension; (A) OLA- <i>co</i> -MA (AC-OLA2); (B) Product of chain extension (AC-CE3); (C) Product of chain extension (AC-CE4).....	XVIII
Figure D4 - Simultaneous thermoanalytical curves of LA co-oligomer and products of chain extension; (A) OLA- <i>co</i> -MA (AC-OLA3); (B) Product of chain extension (AC-CE5); (C) Product of chain extension (AC-CE6).....	XIX

Figure D5 - Simultaneous thermoanalytical curves of LA co-oligomer and products of chain extension; (A) OLA-co-VA (AC-OLA4); (B) Product of chain extension (AC-CE7); (C) Product of chain extension (AC-CE8).	XX
Figure D6 - Simultaneous thermoanalytical curves of LA oligomer and products of chain extension; (A) LA oligomer (AC-OLA5); (B) Product of chain extension (AC-CE9); (C) Product of chain extension (AC-CE10).	XXI
Figure D7 - Simultaneous thermoanalytical curves of LA co-oligomer and products of chain extension; (A) OLA-co-MA (AC-OLA6); (B) Product of chain extension (AC-CE11); (C) Product of chain extension (AC-CE12).	XXII
Figure D8 - Simultaneous thermoanalytical curves of LA co-oligomer and products of chain extension; (A) OLA-co-VA (AC-OLA7); (B) Product of chain extension (AC-CE13); (C) Product of chain extension (AC-CE14).	XXIII
Figure E1 - DSC thermogram (second heating cycle) of the PLA homopolymers (AC3 and AC4) and copolymer (AC6) obtained by melt polycondensation.	XXIV
Figure E2 - DSC thermogram (second heating cycle) of the PLA homopolymers (AC8 and AC9) and copolymer (AC10) obtained by azeotropic dehydration condensation.	XXV
Figure E3 - DSC curves of LA oligomers and products of chain extension.	XXVI
Figure F1 - DMTA traces (glass transition zone) of PLA homopolymers and copolymer, at two frequencies; (A) PLA homopolymer (AC3); (B) PLA homopolymer (AC4); (C) PLA-co-MA (AC6).	XXVIII
Figure F2 - DMTA traces (glass transition zone) of PLA homopolymers and copolymer, at two frequencies; (A) PLA homopolymer (AC8); (B) PLA homopolymer (AC9); (C) PLA-co-MA (AC10).	XXIX
Figure F3 - DMTA traces (glass transition zone) of LA oligomer and products of chain extension, at two frequencies; (A) LA oligomer (AC-OLA2); (B) Product of chain extension (AC-CE3); (C) Product of chain extension (AC-CE4).	XXX
Figure F4 - DMTA traces (glass transition zone) of LA oligomer and products of chain extension, at two frequencies; (A) LA oligomer (AC-OLA3); (B) Product of chain extension (AC-CE5); (C) Product of chain extension (AC-CE6).	XXXI

Figure F5 - DMTA traces (glass transition zone) of LA oligomer and products of chain extension, at two frequencies; (A) LA oligomer (AC-OLA4); (B) Product of chain extension (AC-CE7); (C) Product of chain extension (AC-CE8). XXXII

Figure F6 - DMTA traces (glass transition zone) of LA oligomer and products of chain extension, at two frequencies; (A) LA oligomer (AC-OLA5); (B) Product of chain extension (AC-CE9); (C) Product of chain extension (AC-CE10).XXXIII

Figure F7 - DMTA traces (glass transition zone) of LA oligomer and products of chain extension, at two frequencies; (A) LA oligomer (AC-OLA6); (B) Product of chain extension (AC-CE11); (C) Product of chain extension (AC-CE12).XXXIV

Figure F8 - DMTA traces (glass transition zone) of LA oligomer and products of chain extension, at two frequencies; (A) LA oligomer (AC-OLA7); (B) Product of chain extension (AC-CE13); (C) Product of chain extension (AC-CE14). XXXV

List of Tables

Table 1 - Business segments and applications for products based on NatureWorks™ PLA and Ingeo™ fibers ^[13]	5
Table 2 - Industrial production of PLA ^[7]	6
Table 3 - Mechanical properties of PLA, compared with PET and PS (Adapted from reference ^[14] .)	6
Table 4 - Physical and chemical properties of PLA stereoisomers ^[11]	16
Table 5 - Typical chain extenders and their structures.	19
Table 6 - Plasticizers used and their effects.	20
Table 7 - Reagents used in the synthesis of PLA homopolymers and copolymers.	27
Table 8 - Monomers, catalysts and reactional conditions used in melt polycondensation.	28
Table 9 - Monomers, catalysts and reactional conditions used in azeotropic dehydration condensation.	30
Table 10 - Monomers, catalysts and reactional conditions used in synthesis of lactic acid oligomers and co-oligomers.	31
Table 11 - Oligomers, chain extenders and reactional conditions used in chain extension reactions.....	32
Table 12 - Main IR bands of PLA homopolymer and PLA copolymer and respective assignments.....	36
Table 13 - Amount of acids incorporated in the L-LA chain.	38
Table 14 - Molecular weight and PDI values for PLA homopolymer and copolymers obtained by melt polycondensation and calculated by conventional calibration.....	39
Table 15 - Molecular weight and PDI values for PLA homopolymers.	41
Table 16 - Characteristic temperatures (average) obtained from simultaneous thermal analysis for homopolymers and copolymers. T_{on} : extrapolated onset temperature (TG); $T_{5\%}$: temperature corresponding to 5% of mass loss; $T_{10\%}$: temperature corresponding to 10% of mass loss; T_p : peak temperature (DTG); T_d : degradation temperature.....	43
Table 17 - T_m values for the PLA homopolymer and copolymers obtained by DSC	45
Table 18 - T_g values for the PLA homopolymer and copolymers obtained by DMTA.	47
Table 19 - Main IR bands of LA oligomers with hydroxyl end groups and respective assignments.....	48

Table 20 - Main IR bands of PLA oligomer (AC-OLA1) and the products of chain extension (AC-CE1 and AC-CE2) and respective assignments.....	50
Table 21 - Amount of hydroxyacids incorporated in the L-LA oligomeric chain.....	52
Table 22 - Molecular weight and PDI values for PLA oligomers.	55
Table 23 - Molecular weight and PDI values for LA oligomers and products of chain extension.....	56
Table 24 - Characteristic temperatures (average) obtained from simultaneous thermal analysis for homopolymers and copolymers. T_{on} : extrapolated onset temperature (TG); $T_{5\%}$: temperature corresponding to 5% of mass loss; $T_{10\%}$: temperature corresponding to 10% of mass loss; T_p : peak temperature (DTG); T_d : degradation temperature.....	58
Table 25 - Characteristic temperatures (average) obtained from simultaneous thermal analysis for homopolymers and copolymers. T_{on} : extrapolated onset temperature (TG); $T_{5\%}$: temperature corresponding to 5% of mass loss; $T_{10\%}$: temperature corresponding to 10% of mass loss; T_p : peak temperature (DTG); T_d : degradation temperature.....	60
Table 26 - T_g values for the LA oligomers obtained by DMTA.....	63
Table 27 - T_g values for the products of chain extension obtained by DMTA.....	65
Table A1 - Main IR bands of PLA homopolymer and copolymers and respective assignments.	I
Table A2 - Main IR bands of PLA homopolymers and copolymers and respective assignments.....	II
Table A3 - Main IR bands of PLA oligomers and respective assignments.	IV
Table A4 - Main IR bands of products of chain extension and respective assignments.....	IV

List of schemes

Scheme 1 - Direct polycondensation polymerization mechanism (Adapted from reference ^[23]).	
.....	10
Scheme 2 - Azeotropic Dehydration Condensation mechanism ^[23] .	10
Scheme 3 - The Melt/Solid Polymerization mechanism ^[22] .	11
Scheme 4 - ROP mechanism.	13
Scheme 5 - Coordination insertion ROP mechanism in the presence of stannous (II) octoate and a monoalcohol.	13
Scheme 6 - Anionic ROP mechanism.	14
Scheme 7 - Cationic ROP mechanism.	14
Scheme 8 - The Chain extension process of a lactic acid prepolymer and a diisocyanate.	19
Scheme 9 - Structure of homopolymer and copolymers.	29
Scheme 10 - Structures of the LA oligomers and co-oligomers.	30
Scheme 11 - Structures of the chain extended oligomers.	32

Motivation and objectives

In the last years there has been a significant growth in the amount of plastics used in various sectors of the economy, particularly in food packaging. Durability, safety, low price and good aesthetic properties are important and decisive factors of rapid growing in the use of plastics in packaging. More than a third of all plastics production is used for packaging purposes.

Until now, packaging materials have been made from petrochemical-based polymers such as polyethylene (PE), poly(ethylene terephthalate) (PET), polypropylene (PP), polystyrene (PS), and poly(vinyl chloride) (PVC). These materials have been used as packaging materials because of their availability at low cost and because of their good mechanical properties (*e.g.*, tensile and tear strength), and their good barrier properties to oxygen and carbon dioxide.

However, their use has been regulated because they are not biodegradable, which lead to serious environmental problems. The presence of these materials in the environment causes the lack of landfill space, the poisoning of soil and contributes to the global warming, due to the poisonous gases generated during the incineration. Furthermore, petroleum resources are becoming limited and have floatable prices. Thus, it will be very important to find durable plastics substitutes, particularly in short-term packaging. Because of that there has been an increasing interest in the development of biodegradable materials for use in packaging, agriculture, medicine and other areas.

A biodegradable material that has showed growing industrial interest in packaging area is an aliphatic polyester generated from lactic acid (LA), poly(lactic acid) (PLA). PLA has received much attention due to its mechanical properties similar to fossil-based materials like PET and PP and due to its biodegradability, biocompatibility and bio-absorbability. Besides, it is made from renewable raw materials. Nevertheless, PLA has some unsatisfactory characteristics, namely brittleness, poor water permeability, low glass transition temperature ($T_g \approx 64$ °C), low toughness, and poor thermal stability, which hamper its broad use in several applications where normally petroleum-based polymers are used. Thus, it is of prime importance to develop new lactic acid (LA) based copolymers that could overcome some of the PLA disadvantages. In this work, the two co-monomers chosen were D,L-mandelic acid (MA) and vanillic acid (VA). Both monomers have an aromatic ring in the structure, which may

contribute to an enhancement of the PLA properties (e.g., thermo-mechanical), and can be obtained from renewable raw materials.

Thus, the present work had as main objectives: (i) development of PLA homopolymers and PLA copolymers with MA and VA by direct polycondensation; (ii) study of the structure/properties relationships of the homopolymers and copolymers; (iii) development of LA homopolymers and LA copolymers with high molecular weight, by chain extension reactions.

1. Introduction

The plastic industry is an important consumer of oil market. The constant rising of oil prices have obliged the plastics industry to increasingly invest in research and development of bioplastics^[1]. The current consumption of plastics in the world is more than 200 million tons, and bioplastics constitute nearly 300,000 tons of the global plastic market^[2]. Bioplastics emerged in search of new material solutions and with the goal of sustainable production and consumption. For these reasons they have several potential advantages. The use of renewable resources to produce bioplastics is their main advantage due to: increasing resource efficiency, saving fossil resources and reducing the carbon footprint and greenhouse gas (GHG) emissions of some materials and products^[3]. Today, bioplastics are already in several areas: packaging, catering, agriculture and horticulture, automotive industry, consumer electronics, textiles and fibers, toys and sports^[3-5]. According to European Bioplastics, a plastic is defined as a bioplastic if it is biobased (derived from renewable biomass), biodegradable, or both^[3]. Biobased plastics are those materials that are (partly) derived from biomass and biodegradable plastics are those materials that are converted into natural substances such as water and carbon dioxide, by the action of microorganisms (*e.g.*, bacteria, fungi and algae), under specific conditions.

Biobased plastics can be classified into three groups, each one with its own properties: (i) biobased or partly biobased; (ii) biobased and biodegradable plastics such as PLA, poly(hydroxyalkanoates) (PHAs) and cellulose; (iii) fossil-based and biodegradable plastics including aromatic copolyesters (poly(butylene adipate-*co*-terephthalate), PBAT) and aliphatic copolyesters (poly(butylene succinate),PBS) (Figure 1). One of the most significant bioplastic is PLA, also known as poly(lactide)^[3].

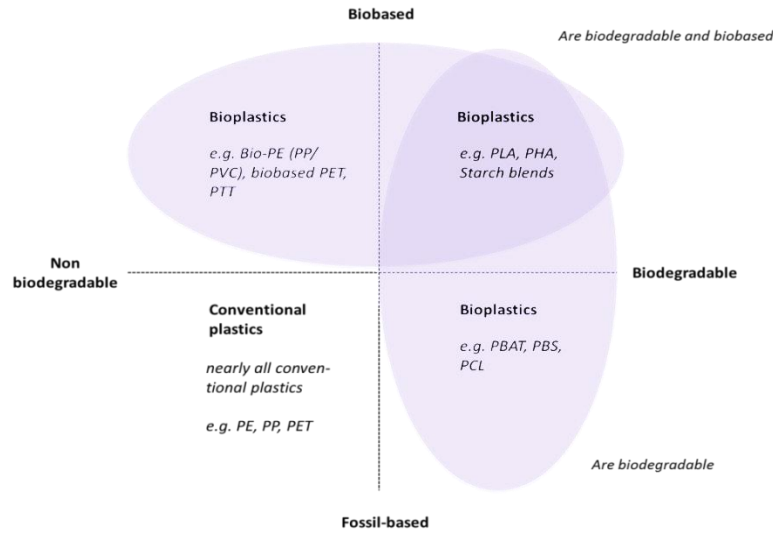


Figure 1 – The different classifications of bioplastic materials. (Adapted from reference [3]).

1.1. Evaluation of biodegradability of polymers

Biodegradation of a polymer can be understood as a deterioration of physical and chemical properties of a polymer and can be made through several processes. This process can occur under aerobic conditions, where the organic material is degraded in the presence of oxygen, and under anaerobic conditions, without oxygen [6-9].

Polymer's biodegradation is influenced by chemical composition and chemical bonding, effect of substituents, hydrophobic character, size of molecules, methods of synthesis, molecular weight and degree of crystallinity. In biodegradation of solid polymers, the degree of crystallinity is the determining factor. In order to study the biodegradation of polymers some standard tests were developed [8, 9]. These tests comprise the following analysis: (i) visual observations, (ii) weight loss measurements, (iii) changes in mechanical properties and molar mass, (iv) clear-zone formation, (v) enzymatic degradation, and (vi) controlled composting test [9]. The visual observations have the purpose to be a first indication that there was microbial attack. Usually, in this type of test the surface roughness, formation of holes or cracks, de-fragmentation, color change, or formation of bio-film on the surface of a sample are evaluated. The second analysis, weight loss measurement, is also not enough conclusive about the occurrence of biodegradation in the polymer. It is an analysis that is prone to some errors that include incorrect cleaning of the sample and excessive disintegration of the material. For this test the samples are used in the form of films or bars. After such tests, the

samples are subjected to evaluation of mechanical properties and molecular weight. For instance, tensile strength is quite sensitive to alterations in polymers' molecular weight (due to degradation), and changes in such mechanical property indicate that the polymer was effectively degraded.

The clear-zone test is a simple semi-quantitative method and it is also a test for easy detection of biodegradation. The principle of using this method is the following: the polymer is placed in a synthetic medium, agar, which becomes opaque in contact with the polymer. After inoculation with microorganisms, a clear halo around the colony of the microorganisms can be formed indicating the occurrence of biodegradation.

Enzymatic degradation occurs through a hydrolysis process that decrease molecular weight of polymer. This process originates smaller polymer chains, for example, oligomers and dimers.

The composting tests are an essential tool for treat and recycle organic waste material. The typical conditions for composting tests are: high temperature (58°C) under aerobic conditions, suitable water content (approximately 50%) and mature compost as a source of nutrients. Composting has as principle of operation the determination of net CO₂ evolution, in other words, the CO₂ evolved from the mixture of polymer-compost minus the CO₂ evolved from the unchanged compost (blank) tested in another reactor. The difference between the CO₂ evolved from the mixture of polymer-compost and blank compost gives the biodegradation degree.

1.2 Poly(Lactic Acid)

PLA is a highly versatile, biodegradable, aliphatic thermoplastic polyester synthesized from 100% renewable resources, which makes it environmentally and ecologically safe (Figure 2).

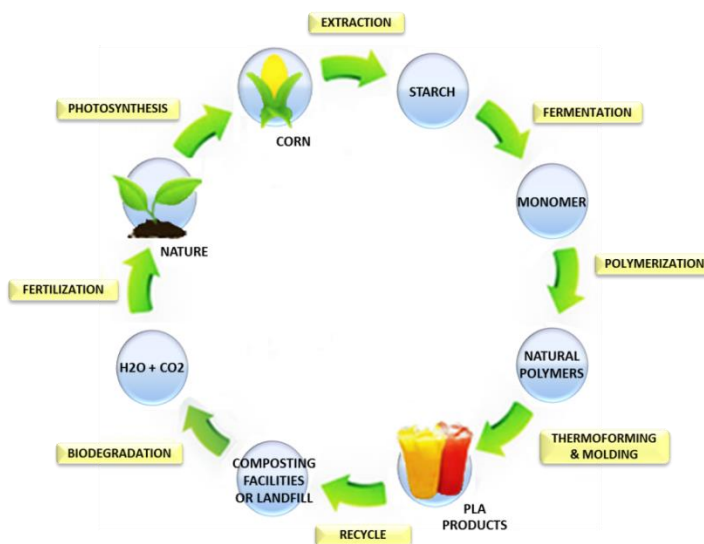


Figure 2 - The life cycle of PLA in nature ^[10].

Contrary to common belief, PLA is not a new material. In 1932, Wallace Carothers, a scientist from DuPont, produced a low molecular weight PLA by heating lactic acid under vacuum ^[11].

In 1954, DuPont patented a high molecular weight PLA, and thereafter many companies have begun to produce PLA ^[2, 12]. However, only in 1980, PLA was developed as a material with good characteristics for general use thanks to a project of Cargill, Inc.. This project encouraged the partnership with Dow Chemical Co., and later they launched its PLA product under the name NatureWorks. In 2005, Cargill bought Dow's participation in the partnership and the company is now known simply as NatureWorks, with the PLA being marketed under the trade name IngeoTM ^[2, 11, 12]. Currently, Nature Works LLC is the leader in PLA technology and market. This company develops LA based products of two types, the polylactide-based resins (NatureWorksTM PLA), used for plastics or packaging applications, and the IngeoTM polylactide-based fibers that are used in specialty textiles and fiber applications. Table 1 shows the business of Cargill Dow and applications of the two types of poly(lactide)s ^[13].

Table 1 - Business segments and applications for products based on NatureWorks™ PLA and Ingeo™ fibers⁽¹³⁾.

	Business segment	Commercial available applications
Ingeo™	Apparel	Casual (sports-), active- and underwear and fashion
	Non-wovens	Wipes, hygiene products, diapers, shoe liners, automotive head and door liners and paper reinforcement
	Furnishings	Blankets and panel, upholstery and decorative fabrics
	Industrial	Agricultural and geo textiles
	Carpet	Residential/institutional broadloom and carpet tiles
	Fiberfill	Pillows, conforters, mattresses, duvets and furniture
NatureWorks™ PLA	Rigid thermoforms	Clear fresh fruit and vegetable clamshells Deli meat trays Opaque dairy (yogurt) containers Bakery, fresh herb and candy containers Consumer displays & electronics packaging Disposable articles and cold drink cups
	Biaxially-oriented films	Candy twist and flow wrap Envelope and display carton windows Lamination film Product (gift basket) overwrap Lidding stock Die cut labels Floral wrap Tapes Shrink sleeves Stand-up pouches Cake mix, cereal and bread bags
	Bottles	Short shelf-life milk Edible oils Bottled water

Other PLA from other companies are also on the market, as shown in Table 2.

Table 2 - Industrial production of PLA ^[7].

Company name/location	Trade name	Production capacity (metrictons/year)	Mw (Da)	Mn (Da)	Process used
NatureWorks (Cargill/Teijin)/NB,USA	NatureWorks PLA (Eco PLA)	140,000	NA	1.22x10 ⁴ (94% L-LA content)	Solvent free Melt PC/ ROP
Toyota (Shimadzu Co.)/Kyoto, Japan	LACTYTM 5000	>100,000	2.89x10 ⁵	1.7x10 ⁵	ROP
	LACTYTM 2012		1.6x10 ⁵	1.883x10 ⁵ (100% L-LA content)	
DuPont/USA	Medisorb	NA	1.0x10 ⁵	NA	ROP
Purac plc./Netherlands	Purasorb ® PL	NA	3.5x10 ⁵	1.5x10 ⁵	ROP/Solution PC
Mitsui Chemicals Co./Japan	LACEA	500,000	NA	NA	Solution PC
Birmingham Polymers / AL., USA	LACTEL	NA	NA	NA	NA
Toyobo / Japan	Vyloecol	NA	43x10 ³	NA	NA
Hisun Biomaterials Co. Ltd. /China	REVODE	5,000	NA	70x10 ³	NA

NA- Not Available

PLA has attracted large attention due to its biodegradability and mechanical properties similar to PET, PP and other common petroleum-based plastics. It is a thermoplastic polymer with high mechanical strength and flexural modulus higher than PS, as can be seen from Table 3.

Table 3 - Mechanical properties of PLA, compared with PET and PS (Adapted from reference ^[14].)

Property	Unit	PLA	PS	PET
Tensile strength	[MPa]	68	45	57
Elongation at break	[%]	4	3	300
Flexural strength	[MPa]	98	76	88
Flexural modulus	[MPa]	3700	3000	2700
Izod impact	[J/m ³]	29	21	59
Vicat softening point	[°C]	58	98	79
Density	[g/cm ³]	1.26	1.05	1.4

[†] PLA (LACEA Mitsui Chemicals)

Until the last decade, PLA was only used in medical applications such as tissue engineering scaffolds, internal sutures, and bone fixation devices in orthopedic and oral surgeries, due to its limited molecular weight, low availability and high cost. Recently, new methods were investigated in order to develop a cost-effective production process of high molecular weight PLA allowing the extension of its application fields. Now PLA offers great promise in a large range of commodity applications (*e.g.*, exterior parts of electric devices, parts of automobiles, and food packages).

1.3 Lactic Acid – PLA monomer

LA (2-hydroxypropanoic acid) is the simplest α -hydroxy acid. It presents a chiral carbon atom and exists as two optical isomers, L- and D-LA, as illustrated in Figure 3.

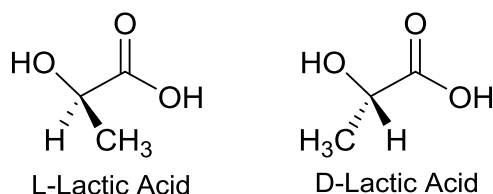


Figure 3 - Different isomeric forms of LA.

The two enantiomeric forms differ in their optical rotation. For L-LA, the plane is rotated to the right (*dextro*) direction, while the D-LA rotates to the left (*laevo*) direction ^[11]. The stereochemical composition of lactic acid monomers determines the final properties of the polymer ^[15]. Melting and glass transition temperatures are the most affected properties by the stereochemical composition ^[11].

LA can be produced in two ways: chemical synthesis or fermentation. It can be chemically synthesized by the hydrolysis of lactonitrile by strong acids and produces only the racemic mixture of D- and L-LA. In contrast, the fermentative production of lactic acid provides almost exclusively the L-lactic acid. The fermentation of lactic acid has many advantages compared to chemical synthesis such as low production temperature, low cost of substrates and low energy consumption. The main advantage of this process is the eco-friendly nature due to the use of renewable resources instead of fossil compounds ^[15, 16]. In the literature are listed many raw materials for the production of lactic acid, such as whey, corn, potato, rice, wood, waste paper, rye, and corncob ^[16].

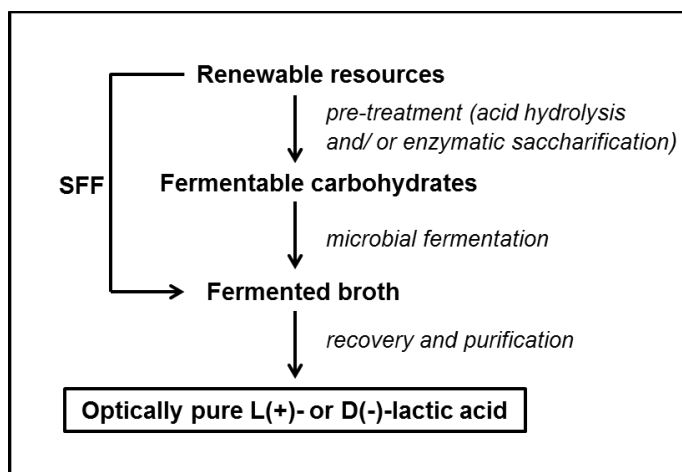


Figure 4 - Microbial fermentation of LA; SFF represents simultaneous saccharification and fermentation [16].

1.4 PLA Synthesis

There are several methods that can be employed in the polymerization of LA. The main methods include the polycondensation and ring opening polymerization (ROP).

1.4.1 Polycondensation methods

The structure of LA, since it contains alcohol and carboxylic acid functionalities, allows it to participate in polycondensation reactions. However, as this is an equilibrium reaction, and water is continuously formed as a sub-product during the reaction, high molecular weights are difficult to obtain. To overcome this problem, vacuum can be applied during the reaction in order to favor water removal from the reaction medium or an organic solvent that has the ability to form an azeotrope with water can be used. These two processes will be explained in detail below. Usually, the polycondensation method produces oligomers with molecular weights in the range of thousands [15, 17]. To increase the molecular weight, LA oligomers can be linked together by isocyanates and epoxides to produce polymers having a larger range of molecular weights, as it will be described below [18].

The polycondensation methods include direct polycondensation, azeotropic dehydration polycondensation and solid state polymerization.

Direct Polycondensation

Direct polycondensation is relatively simpler and cheaper than the other methods, but it is a process that does not allow the obtainment of high molecular weight polymers^[11, 19-21]. This process has been sorely studied by many scientists, but high molecular weight PLA could not be synthesized, due to an unfavorable equilibrium between free acids, water and polymer^[19, 20]. This process can be improved if the following aspects are taken into consideration: kinetics control, efficient removal of water and minimization of depolymerization reactions^[19].

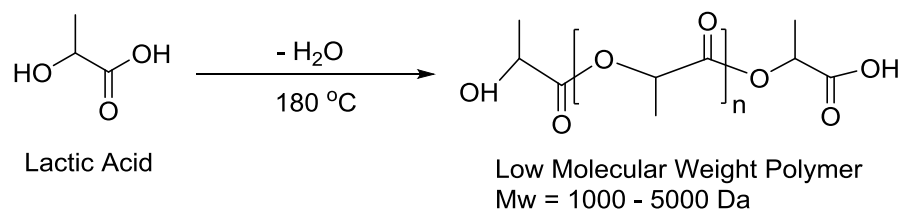
The direct polycondensation method involves the removal of water using specific conditions such as high temperature and high vacuum. Normally, the polycondensation of LA is carried out in bulk with or without a catalyst. This method can be divided into three main stages: (i) removal of free water, (ii) oligomer formation, and (iii) melt polycondensation to yield high molecular weight PLA^[2, 14, 22, 23].

In the first stage, the free water is removed from the mixture, because the feedstock, besides the LA, contains also free water. Due to the equilibrium between LA and water, the linear oligomers of LA (e.g., dimer, trimer) can be formed in low amount in this stage. Therefore, to convert the LA into PLA, first the free water has to be removed^[11]. For this, it is necessary a system having good heat transfer, in order to successfully remove the water^[11, 23].

LA is converted into low molecular weight PLA in the second stage. The water removal in this stage is not critical because the reaction mixture presents a low viscosity. The important factor in this step is the chemical reaction, which is significantly affected by the catalyst used. Various kinds of catalysts can be used in polycondensation. The most used are stannous chloride, stannous oxide, tetraphenyl tin, tin powder, isopropyltitanate, tetrachlorotitanate, titanium-*n*-butoxide, antimony oxide, antimony chloride, lead oxide, calcium oxide, aluminum oxide, iron oxide, calcium chloride, zinc acetate, *p*-toluene sulfonic acid, among others^[20]. At the end of this step, it is obtained a prepolymer of LA with low molecular weight^[11, 18, 23].

In the last stage, melt polycondensation, the removal of water becomes critical. In this step, the water removal should be efficient to promote the polycondensation reaction and not the transesterification reactions. In this phase, the determining factor is the mass transfer of water.

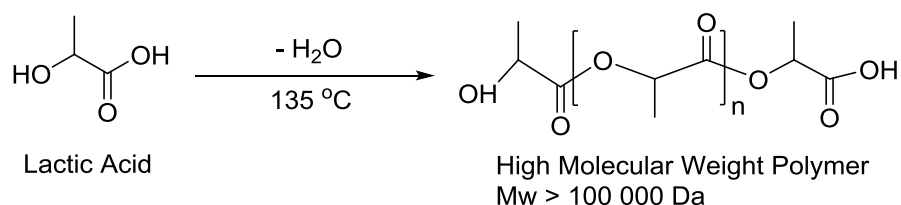
To obtain a high molecular weight PLA, the apparatus requires a system that can manipulate high-viscosity mass. For this, the apparatus should generate good surface renewal to increase the mass transfer of the formed water ^[11]. The mechanism of direct polycondensation is shown in Scheme 1.



Scheme 1 - Direct polycondensation polymerization mechanism (Adapted from reference ^[23]).

Azeotropic dehydration condensation

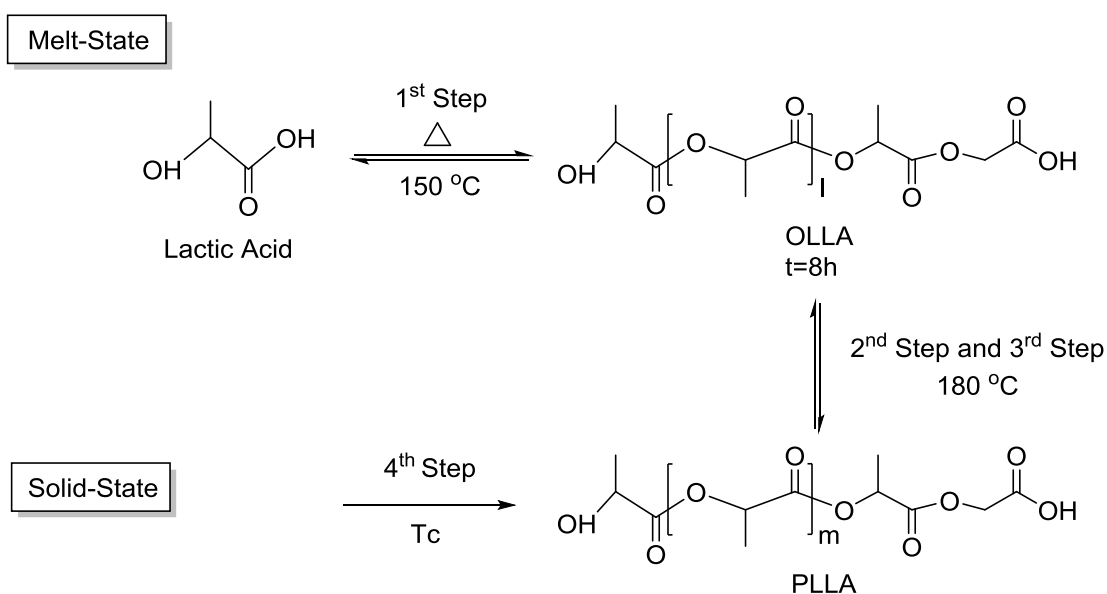
PLA can also be synthesized by azeotropic dehydration condensation (Scheme 2), using usually tin based catalysts (Sn powder, SnO, and SnCl₂), nickel(II) acetate, and *p*-toluene sulfonic acid ^[11]. In this method, an organic solvent that forms an azeotrope with water is used and thus an efficient water removal from the reaction medium is ensured and a PLA of high molecular weight is obtained. The main solvents used are xylene, toluene and methoxybenzene ^[24]. In this polymerization, the depolymerization and racemization during the reaction are easier to avoid because the polymerization reaction occurs at lower temperatures when compared to those used in direct polycondensation ^[14]. Nevertheless, the use of organic solvents brings some disadvantages to the process, namely the fact that the polymer was to be purified at the end of the reaction. Additionally, the environmental concerns are also present ^[11, 14, 23].



Scheme 2 - Azeotropic Dehydration Condensation mechanism ^[23].

Solid State polymerization

Solid state polymerization (SSP) can also be employed in the synthesis of PLA and allows the obtainment of high molecular weight PLA. In this polymerization process are present the same stages of direct polycondensation (removal of free water content, oligomer formation, melt polycondensation) with an additional fourth stage. In the fourth stage, the melt polycondensed PLA is cooled below its melting temperature to solidify. Subsequently the solid particles are subjected to a crystallization process. In this process it is possible to identify two phases: a crystalline phase and an amorphous phase ^[11, 22, 25]. Then, the reaction proceeds in the solid state to attain a PLA with high molecular weight. The reaction scheme for the SSP method is shown in Scheme 3.



Scheme 3 - The Melt/Solid Polymerization mechanism ^[22].

In SSP, the most suitable catalysts are metals, such as Sn, Ti, and Zn or metal salts. The SSP is an environmentally-friendly process. Due to the lower temperature employed in the solid state polymerization (*ca.* 150 °C), the side reactions are prevented as well as the thermal, oxidative and hydrolytic degradation of the polymer.

Ring-opening polymerization

The most used method in the synthesis of PLA is the ROP. The ROP can be carried out either in bulk, in solution or in dispersion. In this polymerization it is necessary a catalyst or initiator to start the reaction^[26].

In this method, PLA is made by the polymerization of its respective cyclic dimer, lactide. Lactide, 3,6-dimethyl-1,4-dioxane-2,5-dione, is formed during the dehydration process of LA^[14, 26]. As LA has two stereoisomeric forms, therefore lactide is formed in three stereoisomeric forms, DD-, LL- and DL-lactide (Figure 5).

Lactide should be used with a high purity because the impurities can interfere with the course of the reaction, leading to the formation of polymers with low molecular weight and a high degree of racemization. Thus, before the polymerization, lactide must be purified^[14, 26].

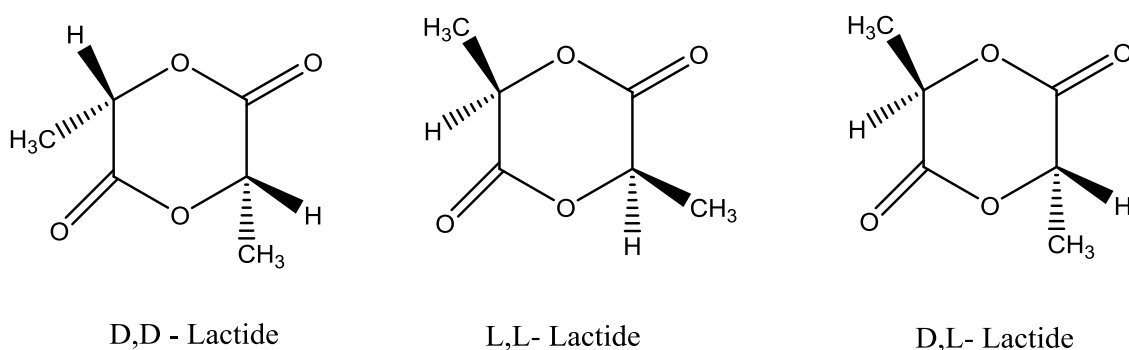
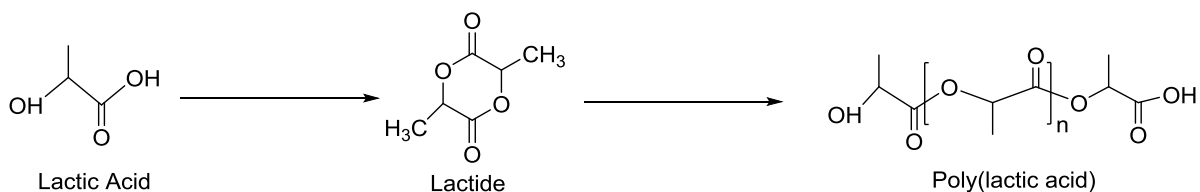


Figure 5 - Different isomers of lactide.

The ROP involves two main steps: the conversion of LA into lactide and polymerization of lactide to form PLA^[14]. This process is more complex than the above referred methods (time and labor consumptive), but it allows the obtainment of PLA with higher molecular weight and good properties.

The reaction scheme for the ROP method is shown in Scheme 4.



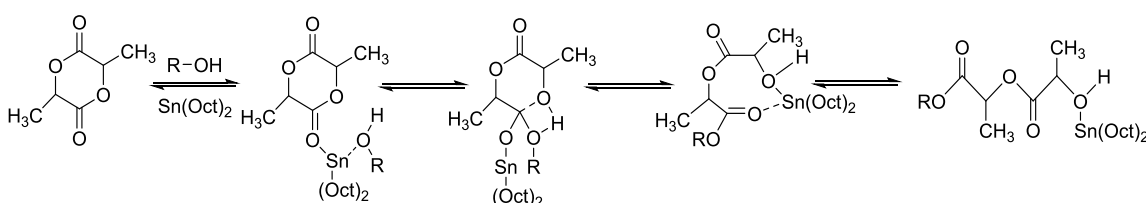
Scheme 4 - ROP mechanism.

The ROP can be carried out via three different mechanisms: coordination-insertion, that is the most studied, anionic and cationic ^[11, 14].

Coordination-Insertion ROP

The coordination-insertion mechanism is the most widely studied method for the synthesis of high molecular weight PLA, allowing a good control over the polymerization reaction ^[14].

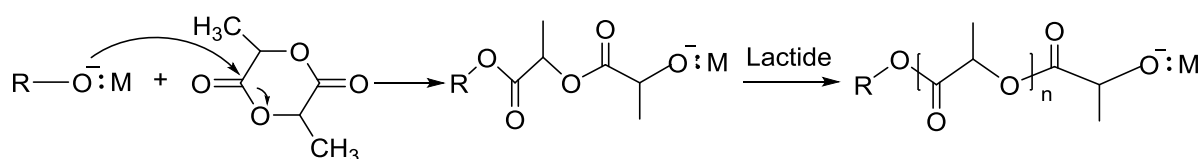
The ROP begins with the exocyclic oxygens of the lactide become temporarily coordinated with the metal atom of the initiator. Next, the acyl-oxygen bond (between the carbonyl group and the endocyclic oxygen) of the lactide is broken and the lactide chain produced is inserted into the metal-oxygen bond of the initiator. The polymerization continues as the lactide molecules are opened and inserted into the bond between the metal atom and its adjacent oxygen atom, while the other end becomes a dead chain end ^[11, 14, 27]. The most used catalysts in this type of ROP are aluminium alkoxides and stannous (II) octoate. The reaction mechanism of coordination insertion in the presence of stannous (II) octoate and a monoalcohol is shown in Scheme 5.



Scheme 5 - Coordination insertion ROP mechanism in the presence of stannous (II) octoate and a monoalcohol.

Anionic ROP

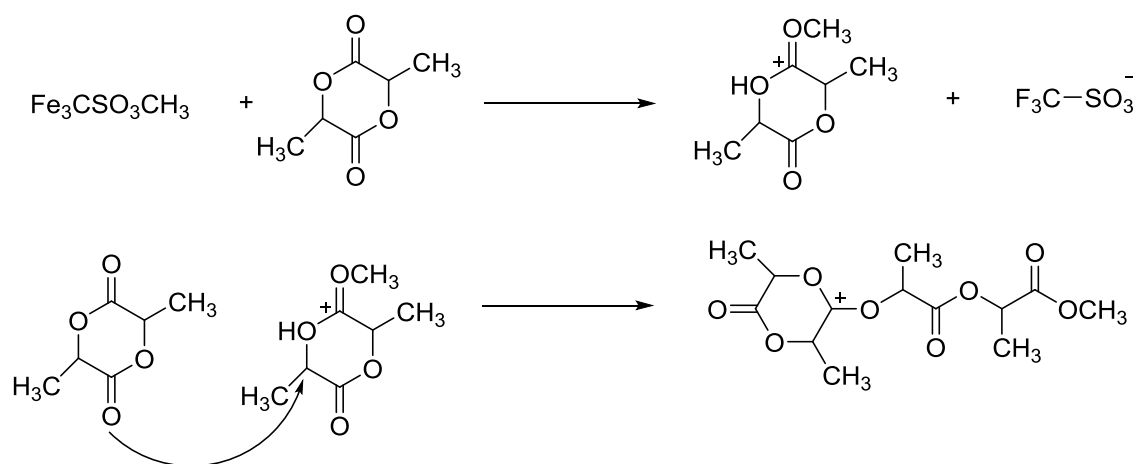
Anionic ROP is initiated when the nucleophilic anion of the initiator attacks the carbonyl group of the lactide, which cleaves the linkage between the carbonyl carbon and endocyclic oxygen bond. This oxygen becomes a new anion, which continues to propagate. This method, due to highly active catalysts at high temperatures, results in racemization and other side reactions ^[14, 26]. Due to these aspects, this polymerization produces a low molecular weight PLA. The reaction mechanism of anionic polymerization method is illustrated in Scheme 6.



Scheme 6 - Anionic ROP mechanism.

Cationic ROP

Cationic ROP is initiated when the exocyclic oxygen of one of the lactide carbonyl is either alkylated or protonated by the initiator, which causes the resulting O-CH bond to become positively charged. Nucleophilic attack occurs by a second monomer molecule to break this bond and create another electrophilic carbocation, and thus the reaction propagates as additional monomers continue this attack ^[14, 26, 27]. The reaction mechanism of cationic polymerization method is shown in Scheme 7.



Scheme 7 - Cationic ROP mechanism.

This polymerization is difficult to control and only low molecular weight polymers are formed ^[26].

1.5 Physical and chemical properties of PLA

PLA belongs to the aliphatic polyesters family and it is a chiral polymer that has a helical conformation containing an asymmetric carbon atom. The chemical structure of PLA is illustrated in Figure 6 ^[11].

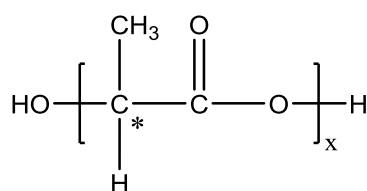


Figure 6 - Molecular structure of PLA, a chiral molecule.

Due to the chirality present in α -carbon atom, L-, D-, and D, L- isomers of the polymer are possible. Polymers like PLA that have a stereocenter (*) in the chain can show two structures of maximum order: isotactic and syndiotactic structures, depending on the direction of the methyl group with respect to the direction of propagation of the chain. In isotactic polymers all the substituents are positioned on the same side of the chain while in syndiotactic polymers the substituents have alternate positions along the chain. PLA can be produced with different enantiomeric composition, depending upon the L- and D- content in the polymer chains, also referred as polymer optical purity. Due to this aspect, PLA shows properties varying in a range of values as a function of the enantiomeric composition. Depending on the application, polymers ranging from amorphous (50% D content) to highly crystalline (>99% L content) can be selected. PLA has a glass transition temperature (T_g) ranging from 50 to 80°C and melting temperature (T_m) ranging from 130 to 180°C. Physical and mechanical properties and degradation rates are greatly affected by the chain stereochemistry ^[11]. Some physical and chemical properties of PLA stereoisomers are presented in Table 4.

Table 4 - Physical and chemical properties of PLA stereoisomers ^[11].

Properties	PDLA	PLLA	PDLLA
Solubility	All are soluble in benzene, chloroform, acetonitrile, tetrahydrofuran (THF), dioxane etc., but insoluble in ethanol, methanol, and aliphatic hydrocarbons		
Crystalline structure	Semi-Crystalline	Semi-crystalline	Amorphous
T_m (°C)	180	180	do not present T_m
T_g (°C)	55 - 60	55 - 60	Variable
Decomposition temperature (°C)	200	200	185 - 200
Elongation at break (%)	20 - 30	20 - 30	Variable
Breaking strength (g/d)	4.0 - 5.0	5.0 - 6.0	Variable
Half-life in 37°C normal saline	4 - 6 months	4 - 6 months	2 - 3 months

1.6 PLA advantages and limitations

As mentioned before, PLA has important advantages that can be seen as strengths in the replacement of petroleum based polymers. However, it has also some drawbacks that have to be taken into consideration.

1.6.1. Advantages

Here are presented some of the most important advantages of PLA utilization.

Energy savings – PLA production requires less energy than fossil-based polymers production (about 25 – 55% less energy) ^[28, 29].

Eco-friendly – PLA is recyclable, compostable, and biodegradable and its production consumes CO₂. Furthermore, it is derived from 100% renewable resources ^[28, 29].

Processability – Compared with other polymers including PHAs, poly(ethylene glycol) (PEG), poly(ϵ -caprolactone) (PCL), among others, PLA has better thermal processing capacity. There are several methods in which PLA can be processed such as injection molding, film extrusion, blow molding, thermoforming, fiber spinning, and film forming ^[28, 29].

1.6.2. Limitations

Slow degradation rate – The degradation rate has influence in several aspects. For example, slow degradation rate brings a long *in vivo* life time. It is a critical problem at the level of

biomedical applications and the disposal of consumer commodities. Properties such as molecular weight, molecular weight distribution, crystallinity degree, morphology, water diffusion rate into the polymer and the stereoisomeric content affect the PLA degradation rate [28].

Poor toughness – Despite being a strong candidate to replace the fossil-based polymers due to its tensile strength and elastic modulus, the poor toughness limits PLA use in applications that need plastic deformation at higher stress levels. PLA is brittle presenting a low elongation at break [28].

Lack of reactive side-chain groups – PLA has no reactive side-chain groups which makes difficult its surface and bulk modification [28].

1.7 Pathways to change PLA properties

Some polymers to be used in a specific application have to be modified in order to fulfill a set of requisites. Such modifications can be chemical (e.g., copolymerization) or physical (e.g., blending, plasticization). In this section, the most common modifications of PLA are presented.

1.7.1 Copolymerization

Lactic acid or lactide has been copolymerized with different monomers in order to modify and improve the properties of the homopolymers, such as stiffness, permeability, crystallinity and thermal stability [11]. The most extensively used and studied monomers are ϵ -caprolactone (ϵ -CL) [30-32], glycolide [32, 33], δ -valerolactone [34] and trimethylene carbonate [32, 35].

The properties of PLA homopolymers may suffer only slight modifications, through the variation of molecular weight and crystallinity, and the role of copolymers is to provide materials with a larger range of properties. The PLA copolymers can present all the conventional structures, namely diblock, triblock, alternating multiblock, dendrimer-like copolymer and star-like copolymer (Figure 7) [36].

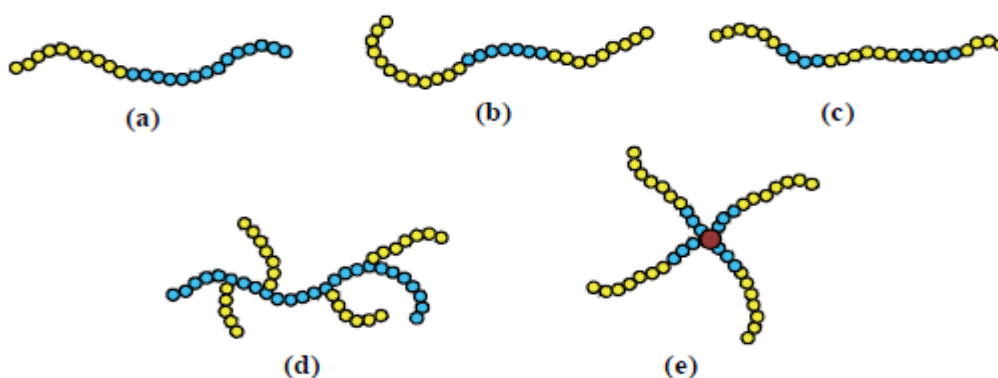


Figure 7 - Schematics of block copolymer structures: a) diblock; (b) triblock; (c) alternating multiblock; (d); dendrimer-like copolymer; (e) star-like copolymer (Adapted from reference ^[36]).

Copolymers of (ϵ -CL)/LA have found great importance in biomedical applications, due to the lack of toxicity and great permeability of ϵ -caprolactone and due to biocompatibility and fast biodegradability of LA polymers. These copolymers have a vast range of mechanical properties, ranging from elastomeric to rigid, depending on the composition and the average sequence length ^[30, 31].

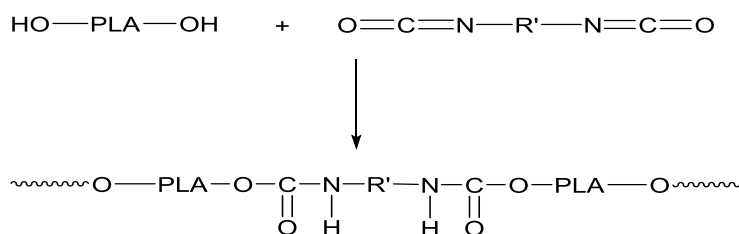
Several studies have been made to increase the T_g of PLA and only a few monomers showed to be adequate for such purpose. Fukuzaki and co-workers^[37] used α -hydroxy acids containing aromatic rings in the main chain or in the side groups to stiffen the oligomer chain. The α -hydroxy acids used in copolycondensation of lactic acid were *p*-hydroxybenzoic acid, *p*-hydroxyphenylacetic acid, and *p*-3-(hydroxyphenyl) propionic acid, D, L-mandelic acid and L-3-phenyllactic acid.

Soo Hyun Kin and co-workers ^[20] increased the T_g by synthesizing a higher molecular weight PLA, with a star-shape, by direct polycondensation. The co-monomer used was dipentaerythritol. This work allowed the obtainment of a PLA polymer with an excellent tensile strength, allowing its utilization as a biodegradable material in packaging films.

1.7.2 Chain extension

High molecular weight PLA is difficult to obtain through the polycondensation method, even using high temperatures and under vacuum conditions. The lack of structural regularity of aliphatic polyesters combined with low molecular weights lead to materials with low degree of crystallinity, limited strength and weak mechanical properties. To overcome these failures, chain extension reaction of LA-prepolymers has been suggested to achieve high molecular

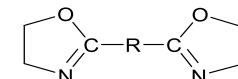
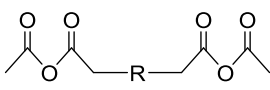
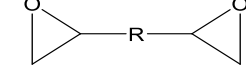
weights. Chain extension offers the possibility of introducing different functional groups into the polymeric chain. Improved mechanical properties and flexibility in the manufacture of copolymers are also associated with the use of chain extending agents. Typical chain extenders are diisocyanates, bisoxazolines, dianhydrides, and diepoxides. An example of this method is the formation of a poly(ester-urethane) (Scheme 8) ^[38-41].



Scheme 8 - The Chain extension process of a lactic acid prepolymer and a diisocyanate.

Typical chain extenders and their structure are present in Table 5.

Table 5 – Typical chain extenders and their structures.

Chain extenders	Structure
Diisocyanates	O=C=N-R-N=C=O
Bisoxazolines	
Dianhydrides	
Diepoxides	

Touminen and Seppälä ^[42] prepared a poly(ester-amide) (PEA), where LA prepolymers were chain extended with 2,2'-bis(2-oxazoline). The authors obtained a PEA based on PLA with good mechanical properties that could provide an alternative to PLA based polymers.

1.7.3 Polymer blends

Polymer blending is a versatile and simple alternative to produce new polymeric materials with tailored properties without synthesizing new materials. The products can show new properties due to interactions between the different components. PLA has been blended with many different polymers, either biodegradable or non-biodegradable, being the most

representative examples: PEG ^[43], PCL ^[44], chitosan and starch ^[45], poly(vinyl acetate) ^[46], poly(ethylene oxide) ^[47] and poly[(R)-3-hydroxybutyrate] ^[48]. Blending PLA with non-biodegradable polymers has been mainly directed to overcome some disadvantages of PLA such as fragility, poor barrier properties, and low heat deflection temperature. Recently, the objective of these blends was to create specific morphologies for medical applications ^[11].

1.7.4 Plasticization

Plasticizers are added to polymers to improve processability and flexibility, by increasing the mobility of the end groups in the amorphous region. However, other properties can also be modified. One of the essential features of a plasticizer is that it should be miscible with PLA, in order to obtain a homogeneous blend that can be created by polar interactions. The plasticizers should not be too volatile, to avoid evaporation during processing. Further, they should not be susceptible to migration phenomena of because that could cause contamination of the materials in contact with the plasticized PLA ^[7]. Several PLA plasticizers have been investigated, namely citrate esters, dimethyladipate, tributylcitrate, acetyltributylcitrate and prolactone (Table 6).

Table 6 – Plasticizers used and their effects.

Type of plasticizer	Plasticizer	Effects	Reference
Renewable resource based plasticizers	Citrate ester (tri-acetyl n-butyl citrate), tributylcitrate glucose monoesters, glycerol, partial fatty acid esters, oligomeric lactic acid.	T_g/T_m decreases and elongation at break increases.	[44, 49]
Biocompatible plasticizers	PEG, PEG monolaurate.	Improvement of flexibility and impact resistance; gains deformation and resilience.	[50]
Multiple plasticizer	Blends of low molecular weight triaceton (TAC) and oligomeric poly(1,3-butylene glycol adipate) (PBGA).	T_g/T_m decreases and elongation at break increases.	[51]

Other plasticizers like polypropylene glycol (PPG), poly(ethylene glycol-*ran*-propylene glycol) (PEPG), dioctyl phthalate (DOP), tributyl citrate (TBC) and adipic acid have also been studied ^[52].

PLA can be also plasticized with its own monomers and oligomers. The use of a plasticizer such as lactide and lactic acid is favorable to produce more flexible materials, but it has the disadvantage of the fast migration of the rather small molecules that result in irregularities in films and sticking during processing ^[44].

2 Characterization Techniques

The characterization of a polymeric sample is of prime importance, since it allows the establishment of the structure-properties relationships. Structural characterization can be accomplished by Nuclear Magnetic Resonance (NMR) and Fourier Transform Infrared (FTIR) Spectroscopies, whereas the physical properties can be evaluated by Thermogravimetric Analysis (TGA), Differential Scanning Calorimetry (DSC) and Dynamic Mechanical Thermal Analysis (DMTA).

2.1 Fourier Transform Infrared Spectroscopy (FTIR)

Infrared Spectroscopy is a general technique for polymers' characterization, allowing the identification and analyses of the functional groups present in liquid, solid and gaseous samples ^[53].

Most infrared spectroscopy analysis is carried out by Fourier Transform Infrared (FTIR) Spectrometers. FTIR is usually used for qualitative identification of various functionalities in a given sample. This technique is based on the emission of infrared radiation through a beam which passes through the sample to be analyzed. Some of this radiation is absorbed by the sample, while the remaining is transmitted. This specific behavior of the beam is correlated with the reference, originating the FTIR spectrum. The infrared spectrum can be divided into three regions, specifically the far-infrared, the mid-infrared and the near-infrared, but the region most employed is mid-infrared region ($400 - 4000 \text{ cm}^{-1}$) ^[53]. In the FTIR technique, the identification of a chemical compound or a substituent group present in the sample is made by analogy with historical data, which relates the wavelength of the radiation and the respective type of molecule or group (Figure 8) ^[53].

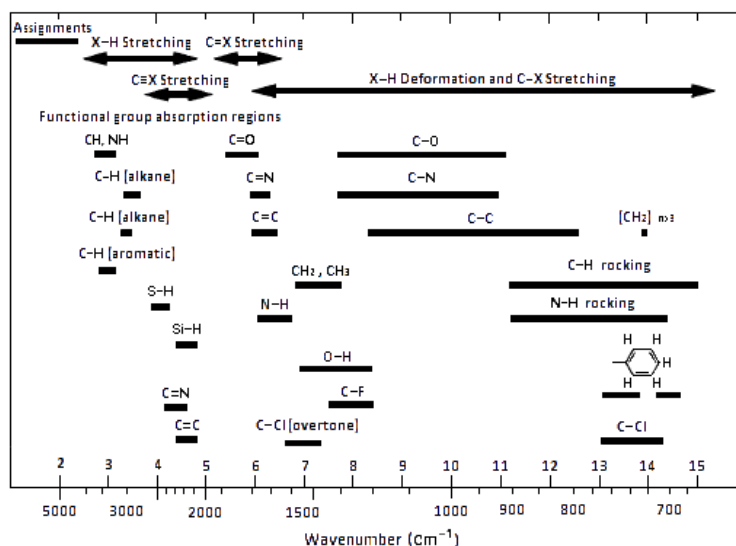


Figure 8 - A typical correlation figure for the infrared modes of polymers ^[53].

2.2 Nuclear Magnetic Resonance (NMR)

Nuclear Magnetic Resonance (NMR) is a spectrometric technique used in the study of polymer structures, in solution or in solid state. The polymer characterization is performed combining the data associated with the chemical shift and spin-spin splitting. This technique has as operating principle the generation of an external magnetic field which radiates electromagnetic energy. The atomic nucleus (consists of protons and neutrons) in the presence of an external magnetic field tends to align with the applied field. The magnetic nuclei of not null nuclear spin can be oriented in the same direction or in the opposite direction to the applied field, when subjected to the magnetic field. When the nuclei are irradiated by electromagnetic radiation, their spins transit to a higher energy level and the energy absorbed and emitted by the nucleus is quantified and represented in a NMR spectrum. The covalent bonds between the atoms in a molecule generate shielding effects that interfere with magnetic resonance phenomena. The greater the electron density around a proton, the greater is the degree of shield and lesser is the field strength where we have electromagnetic energy absorption. Thus, each proton, depending on its molecular position, will have a different position in the NMR spectrum, i.e., different chemical shifts. Chemical shifts are measured relative to a standard, typically tetramethylsilane (TMS) and expressed in parts per million (ppm). Another phenomenon that interferes with the analysis of the NMR spectrum is the split

of the signal. This reflects the magnetic influence generated by hydrogen atoms, neighbors of the atom responsible for the signal depending on the position of molecular proton, this type of interaction originates doublets, triplets and so on ^[53, 54].

The most common nucleuses analyzed by NMR are ^1H and ^{13}C . Through the NMR spectrum it is possible to analyze the peaks corresponding to each functional group (Figure 9) ^[53].

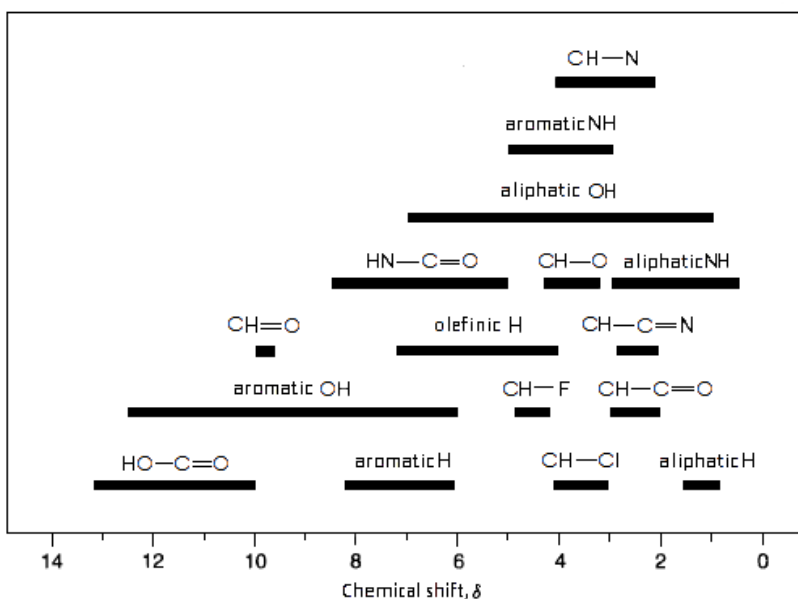


Figure 9 - ^1H NMR peaks of the PLA formulations, main functional groups (Adapted from ^[53]).

2.3 Molecular Weight Determination by Gel Permeation Chromatography (GPC)

The molecular weight is one of the most important characteristic of polymers, since it influences many of their properties (e.g., thermal and mechanical) ^[53]. There are many methods to analyze polymer's molecular weight, such as osmometry, cryoscopy, light-scattering, neutron scattering, ultra centrifugation, solution viscosimetry, and size-exclusion chromatography (SEC) or gel permeation chromatography (GPC). GPC is one of the most widely used analytical techniques in the determination of molecular weight of polymers. This is a chromatographic technique in which particles are separated based on their hydrodynamic volume. This separation is carried out by passing a polymeric solution through a chromatographic column filled with a porous bed. The hydrodynamic volume of a polymer

determines its path along the column. Smaller molecules penetrate into the majority of pores, following a longer path. In contrast, larger molecules are not retained in the pores following a shortest path, as can be seen from **Erro! A origem da referência não foi encontrada.** ^[53].

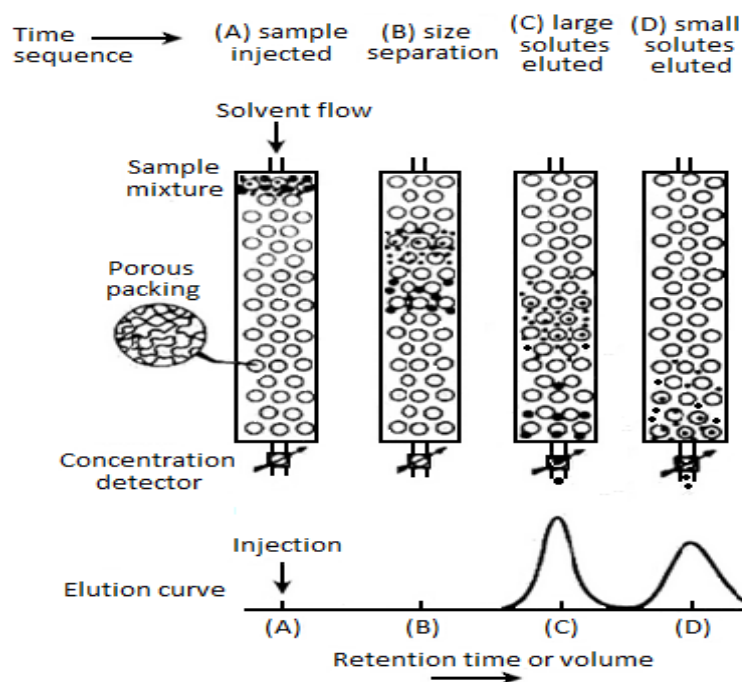


Figure 10 - Image of a typical size-exclusion chromatograph column.

2.4 Thermogravimetric Analysis (TGA)

Thermogravimetric analysis (TGA) or Thermogravimetry (TG) is a thermoanalytical method that involves the measurement of the amount and rate of change in the mass of a material as a function of temperature or time in a controlled atmosphere. Measurements are used primarily to determine the composition of materials and to predict their thermal stability. TGA is used to quantify the mass change in a polymer associated with transitions or degradation processes ^[53].

TGA curve can be represented in two forms: sample mass loss vs. temperature, or mass loss derivative over time vs. temperature. The curve of mass loss derivative is known as DTG curve and represents the degradation rate. This DTG curve has a peak that represents the maximum rate of mass loss ^[53]. Figure 11 gives a representation of a typical output result from a TGA analysis.

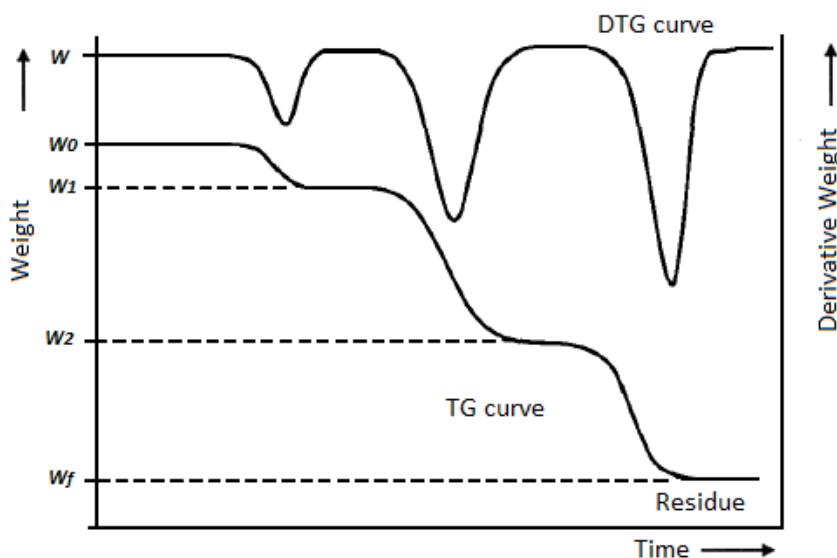


Figure 11 - Typical losses mass and derivative curve in a polymer system ^[53].

This technique has the advantage of analyzing samples in a wide range of temperatures, with the use of only a small amount of sample and has sensibility to changes of the surrounding atmosphere (*e.g.*, nitrogen, air) ^[53].

2.5 Differential Scanning Calorimetry (DSC)

Differential scanning calorimetry (DSC) is a thermoanalytical technique that measures the heat flux associated to materials' transitions as a function of temperature. In a DSC experiment, energy is supplied simultaneously to a sample cell and a reference cell. Both cells are subjected to the same heating or cooling program, which is rigorously controlled. The difference in the input energy required to match the temperature of the sample to that of the reference would be the amount of excess heat absorbed (endothermic process) or released by the sample (exothermic process).[53] DSC is used to measure the glass transition temperatures (T_g), melting temperature (T_m), decomposition temperature (T_c) and heat of fusion of polymers (Figure 12) ^[53].

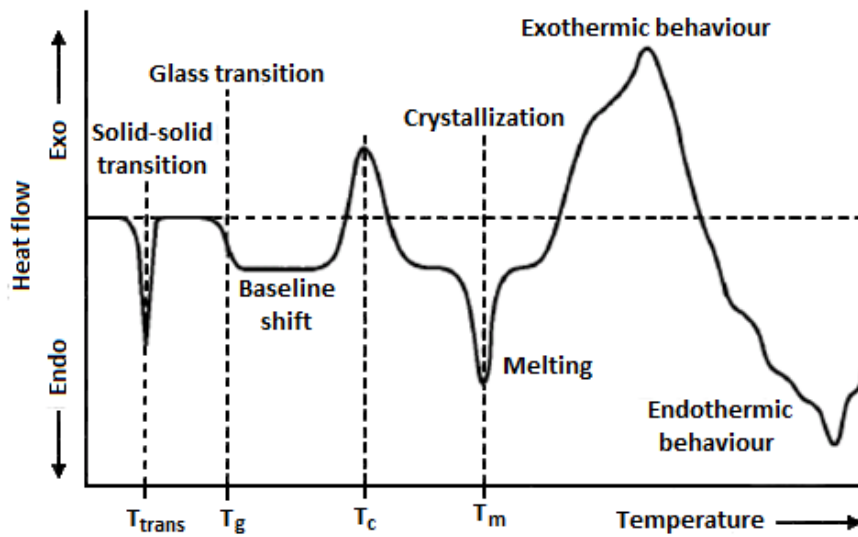


Figure 12 - Typical DSC curve for a polymer ^[53].

2.6 Dynamic Mechanical Thermal Analysis (DMTA)

Dynamic mechanical thermal analysis (DMTA) is the most versatile method for thermal analysis ^[53].

In the DMTA technique, the storage modulus (elastic response) and loss modulus (viscous response) of a sample, under an oscillating load, are monitored as a function of time, temperature or frequency of oscillation, while the temperature of the sample is programmed ^[53].

This technique allows the determination and analysis of glass transition temperatures, secondary transitions (β , γ), crystallinity, phase separation (polymer blends, copolymers, polymer alloys), curing of networks, and effect of additives (plasticizers, moisture) ^[53].

3 Experimental Methods

This section presents the experimental procedures to synthesize the PLA homopolymers and copolymers, the materials used, and describe the parameters used in the different characterization techniques.

3.1 Materials

Table 7 lists all reagents used in the experimental work.

Table 7 - Reagents used in the synthesis of PLA homopolymers and copolymers.

Material	T_b (°C)	T_m (°C)	Density (g/cm ³)	MW (g/mol)
L-Lactic acid aqueous solution (80 %) (Sigma-Aldrich)	122	NA	NA	90.1
D,L-Mandelic acid (98.5%) (Acros Organics)	321.8	131-133	1.30	152.2
Vanillic acid (99%) (Acros Organics)	NA	208-210	NA	168.1
Xylene (98%) (Panreac)	138-139	-48	0.84	106.2
Ethylene glycol (99%) (Sigma-Aldrich)	195-198	-13	1.1	62.1
Tin octanoate (95%) (Sigma-Aldrich)	NA	NA	1.3	405.1
Toluene (99.99%) (Panreac)	110-111	-93	0.9	92.1
Isophorone diisocyanate (IPDI) (98%) (Sigma-Aldrich)	158-159	NA	1.05	222.3
1,6-Hexamethylenediisocyanate (HMDI) (99%) (Acros Organics)	82 - 85	-67	1.05	168.2
Tetrahydrofuran (Panreac))	65-67	-108	0.89	77.1
Deuterated chloroform (99.5%) (Eur isotop)	60.9	-64	1.5	120.4
Deuterated DMSO (Eur isotop)	189	18.5	1.1	78.1
Deuterated THF (Eur isotop)	65-66	-106	0.99	80.2

NA – Not Available

3.2 Synthesis Procedures

3.2.1 Melt polycondensation

The monomers (LA, or LA/ DL-MA or LA/VA) were placed in a reactor equipped with a mechanical stirrer, a nitrogen inlet and a condenser (Figure 13). The reactional mixture was heated up to 180 °C and after a predetermined time the catalyst Sn(Oct)₂ was added to the mixture.

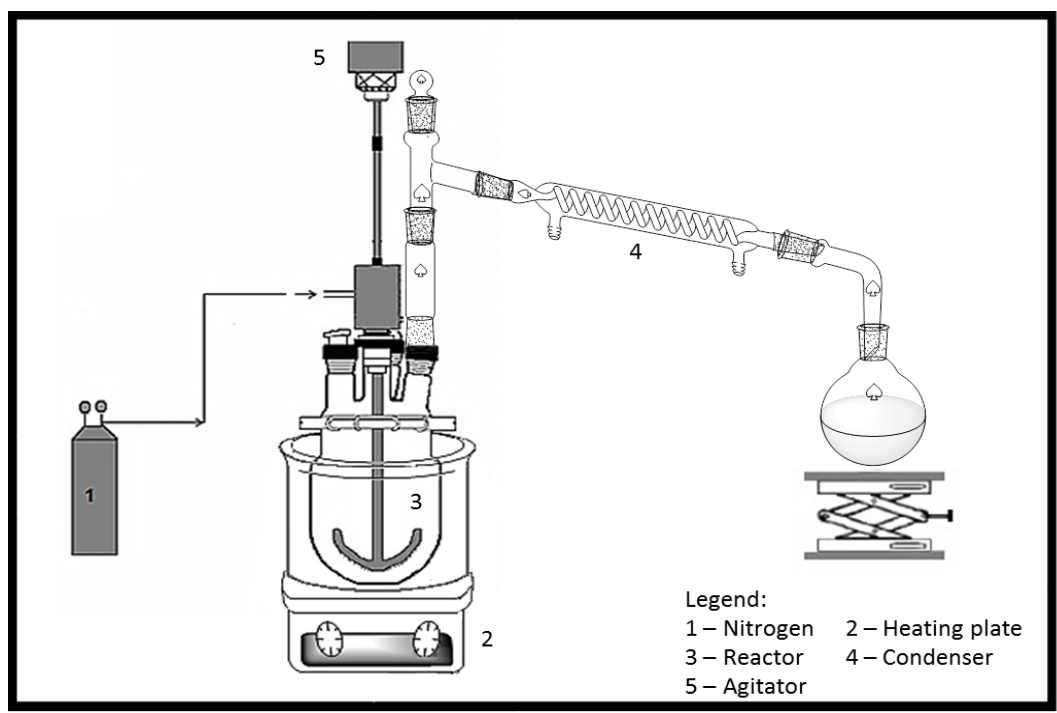


Figure 13 – Schematic representation of the melt polycondensation apparatus.

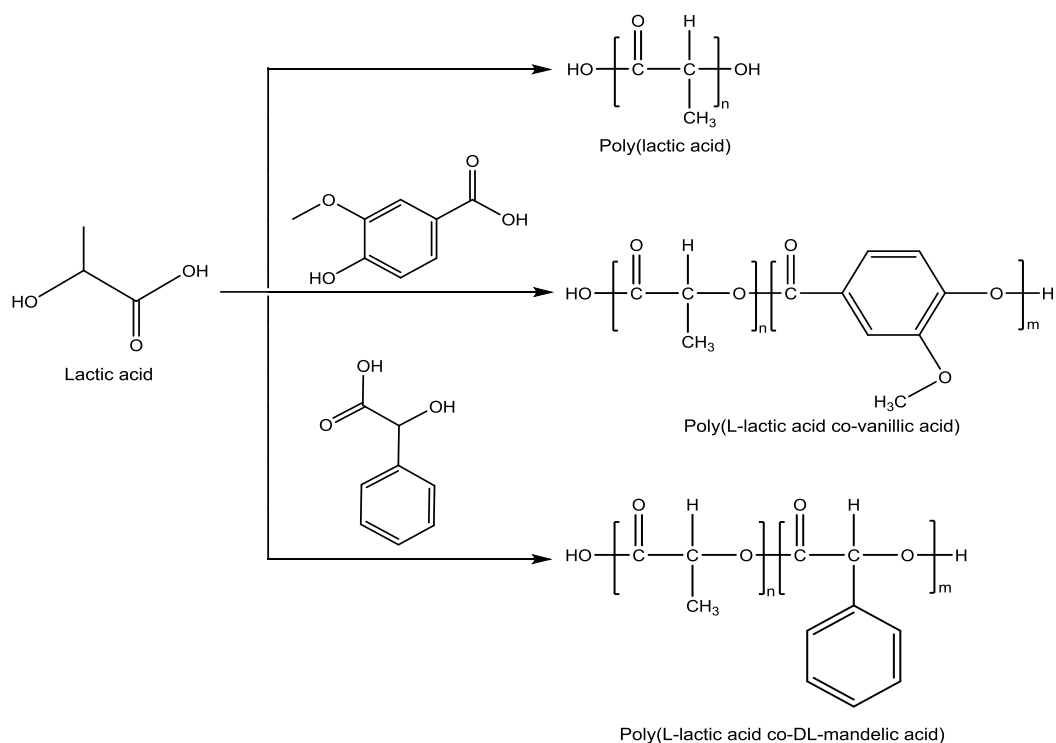
The quantities of monomers, catalyst, temperatures and times of reaction are shown in Table 8.

Table 8 – Monomers, catalysts and reactional conditions used in melt polycondensation.

Experience	n(LA)/n(CM) ¹	Monomer			Catalyst (g)	T (°C)	Time Reaction (h)
		LA (ml)	DL-MA (g)	VA (g)			
AC1 ²	100/0	100			x	180	12
AC2	100/0	100			0,06	180	24
AC3	100/0	100			0,06	180	24
AC4	100/0	100			0,05	180	36
AC5	90/10	90	20,27		0,06	180	24
AC6	75/25	90	60,81		0,08	180	24
AC7	90/10	90		22,4	0,06	180	24
AC7.1	90/10	90		22,4	0,07	180	24

¹ CM stands for Co-monomer ² very low molecular weight

The structures of the obtained polymers are presented in Scheme 9.



Scheme 9 - Structure of homopolymer and copolymers.

3.2.2 Azeotropic dehydration condensation

In azeotropic dehydration condensation the same monomers were used (LA, or LA/ DL-MA or LA/VA) and apparatus used is presented in Figure 14.

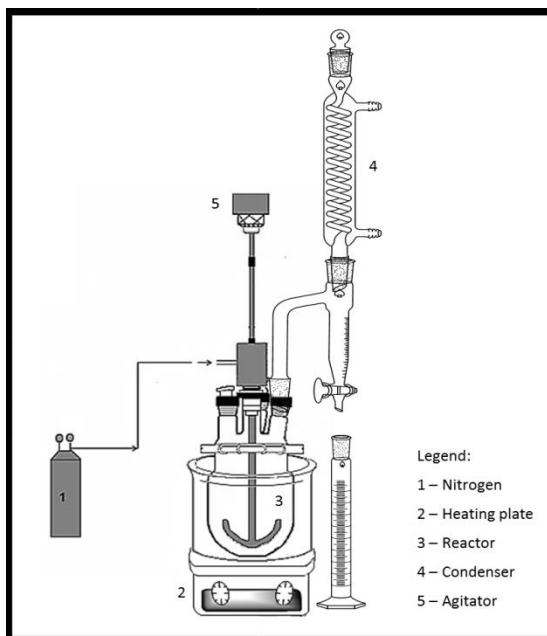


Figure 14 - Schematic representation of the azeotropic dehydration polycondensation apparatus.

The quantities of monomers, catalyst and solvent (xylene) and the reaction conditions are presented in Table 9.

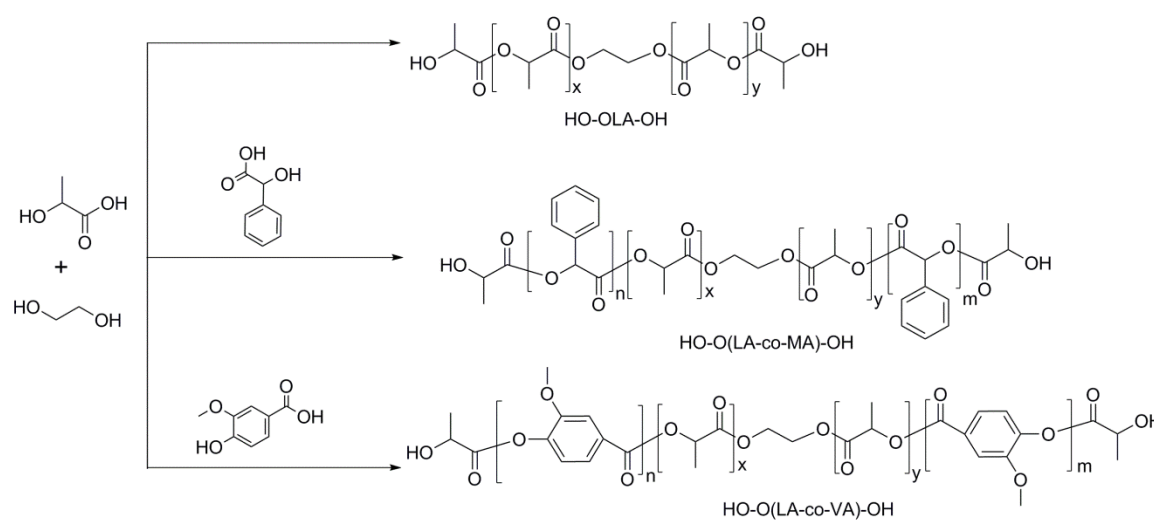
Table 9 - Monomers, catalysts and reactional conditions used in azeotropic dehydration condensation.

Experience	n(LA)/n(CM) ¹	Monomer			Catalyst (g)	Solvent (ml)	T (°C)	Time Reaction (h)
		LA (ml)	DL-MA (g)	VA (ml)				
AC8.0	100/0	50			0,03	100	150	24
AC8.1	100/0	50				100	150	24
AC9	100/0	50			0,03	100	150	24
AC10	90/10	45	10,13		0,03	100	150	24
AC11	90/10	45		11,2	0,03	100	150	24
AC11.1	90/10	45		11,2	0,03	100	150	24

¹ CM stands for Co-monomer

3.2.3 Chain extension

To accomplish the chain extension with diisocyanates it was necessary to first synthesize oligomers of LA with hydroxyl terminal groups. The LA oligomers were synthesized by melt polycondensation of monomers (LA, or LA/ MA or LA/VA) and in the presence of ethylene glycol (EG), using Sn(Oct)₂ as catalyst (Scheme 10). The reactional mixture is heated up to 160°C and was maintained at this temperature for 4 hours. Next, the temperature was raised to 180 °C and after 4 hours the catalyst was added ^[55]. Then the reaction was allowed to proceed for 16 hours. Possible structures of the obtained oligomers are presented in Scheme 10.



Scheme 10 – Structures of the LA oligomers and co-oligomers.

The quantities of monomers, catalyst, temperatures and times of reaction are shown in Table 10.

Table 10 - Monomers, catalysts and reactional conditions used in synthesis of lactic acid oligomers and co-oligomers.

Experience	n(LA)/n(CM) ¹	Monomer			EG (g)	Catalyst (g)	T(°C)	t(h)	M _n ^{a)} (g/mol)
		LA (ml)	DL-MA (g)	VA (g)					
AC-OLA1	100/0	100			11,11	0,07	160/180	24	600
AC-OLA2	90/10	90	26,1		11	0,07	160/180	24	600
AC-OLA3	75/25	90	60,8		13,33	0,09	160/180	24	600
AC-OLA4	90/10	90		22,4	11,11	0,07	160/180	24	600
AC-OLA5	100/0	90			2,76	0,07	160/180	24	2000
AC-OLA6	90/10	90	20,3		3,08	0,07	160/180	24	2000
AC-OLA7	90/10	90		22,4	3,08	0,07	160/180	24	2000

¹ CM stands for Co-monomer; ^{a)} Theoretical molecular weight.

To obtain the targeted molecular weight, equation 1^[39] was used to estimate the required amount of monomer and initiator.

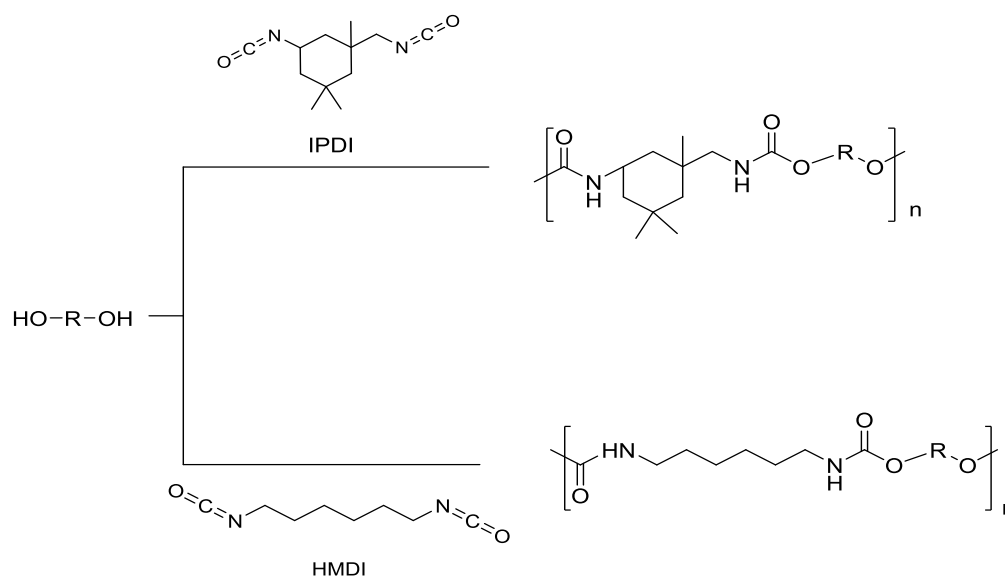
$$M_{n, \text{Theo}} = \frac{n(L - LA)}{n(\text{initiator})} \times 72 + 88 + 2 \quad \text{Eq. (1)}$$

Where $n(L - LA)/n(\text{initiator})$ is the feed molar ratio of lactic acid to EG, 72 and 2 are the masses of repeating unit of PLA and the hydrogens at the ends of lactic acid oligomers, respectively, and 88 is the mass of residue of EG. For the LA co-oligomers, the same equation was used, since the co-monomers were used in small percentages.

The chain extension was performed with isophorone diisocyanate (IPDI) and 1,6-hexamethylenediisocyanate (HMDI). The LA oligomers were dissolved in dry THF, in a round bottom flask. After dissolution of the oligomers, IPDI or HMDI was added and the mixture was stirred for 10 min. Then, a catalytic amount of DBTL was added. The reaction flask was transferred to a thermostatic bath at 60°C, and the reaction was allowed to proceed for 24 h, under a nitrogen atmosphere. The product of reaction was recovered by precipitation in *n*-hexane, followed by filtration and drying under vacuum, at 40°C^[56]. The reaction conditions are listed in Table 11 and Scheme 11 presents the structures of the obtained chain extended polymers.

Table 11 - Oligomers, chain extenders and reactional conditions used in chain extension reactions.

Experience	Oligomer	m _{oligomer} (g)	IPDI (g)	HMDI (g)	DBTL (g)	THF (ml)	t (h)	T (°C)
AC-CE1	AC-OLA1	5	1,825		0,0035	50	24	60
AC-CE2	AC-OLA1	5		1,402	0,0032	50	24	60
AC-CE3	AC-OLA2	5	1,825		0,0034	50	24	60
AC-CE4	AC-OLA2	5		1,402	0,0032	50	24	60
AC-CE5	AC-OLA3	5	1,825		0,0035	50	24	60
AC-CE6	AC-OLA3	5		1,402	0,0034	50	24	60
AC-CE7	AC-OLA4	5		1,402	0,0034	50	24	60
AC-CE8	AC-OLA4	5	1,825		0,0034	50	24	60
AC-CE9	AC-OLA5	5	0,556		0,0028	50	24	60
AC-CE10	AC-OLA5	5		0,421	0,0027	50	24	60
AC-CE11	AC-OLA6	5	0,956		0,0028	50	24	60
AC-CE12	AC-OLA6	5		0,421	0,0027	50	24	60
AC-CE13	AC-OLA7	5	0,558		0,0028	50	24	60
AC-CE14	AC-OLA7	5		0,421	0,0028	50	24	60

**Scheme 11 – Structures of the chain extended oligomers.**

3.3 Characterization techniques

3.3.1 Chemical Structure identification

FTIR spectra were obtained in the range 4000–500 cm^{-1} at room temperature using a Jasco FT/IR-4200 spectrometer, equipped with a Golden Gate Single Reflection Diamond ATR. Data collection was performed with 64 accumulations and 4 cm^{-1} spectral resolution.

^1H NMR spectra of the polymers were obtained at 25 °C on a Bruker Avance III 400 MHz spectrometer, using a 5 mm TIX triple resonance detection probe, in CDCl_3 or THF-d_8 . ^1H NMR spectra of the oligomers and chain extended polymers were obtained at 25 °C on a Varian Unity 600 MHz Spectrometer using a 3 mm broadband NMR probe, in DMSO-d_6 . Tetramethylsilane (TMS) was used as internal standard.

3.3.2 *Molecular Weight Distribution*

The molecular weight distribution of the samples was determined using high-performance gel permeation chromatography (HPSEC; Viscotek TDMax) with a differential viscometer (DV); right-angle laser-light scattering (RALLS, Viscotek); low-angle laser-light scattering (LALLS, Viscotek) and refractive-index (RI) detectors. The column set consisted of a PL 10 mm guard column ($50 \times 7.5 \text{ mm}^2$) followed by one Viscotek T200 column (6 μm), one MIXED-E PLgel column (3 μm), and one MIXED-C PLgel column (5 μm). HPLC dual piston pump was set with a flow rate of 1 mL min^{-1} . The eluent (THF) was previously filtered through a 0.2 μm filter. The system was also equipped with an on-line degasser. The tests were done at 30 °C using an Elder CH-150 heater. Before the injection (100 μL), the samples were filtered through a polytetrafluoroethylene (PTFE) membrane with 0.2 μm pore. The system was calibrated with narrow PS standards.

3.3.3 *Thermal properties*

Firstly, the thermal stability was evaluated by simultaneous thermal analysis (heat-flux DSC and thermogravimetric analysis (TGA)), using a TA Instruments SDT Q600 equipment (thermobalance sensibility: 0.1 μg), which was previously calibrated in the range 25 °C to 1000 °C by running tin and lead as melting standards, at a heating rate (ϕ) of $10 \text{ }^\circ\text{Cmin}^{-1}$, using open alumina crucibles and a dry nitrogen purge flow of 100 mL min^{-1} . Sample weights ranging from 8 to 10 mg were used.

The thermal behavior of the samples was further studied by DSC in a TA Instruments Q100 model equipped with a RCS90 cooling unit. The heat flow and the heat capacity were calibrated at $5 \text{ }^\circ\text{C min}^{-1}$ using, respectively, indium and sapphire standards. The samples were analyzed in aluminum pans with an ordinary aluminium lid loosely placed. Sample weights ranging from 5 to 10 mg were used. A dry nitrogen purge flow of 50 mL min^{-1} was used in all

measurements. The samples were heated at $5\text{ }^{\circ}\text{C min}^{-1}$ from -80 to $200\text{ }^{\circ}\text{C}$, after performing a cycle in which the samples were heated from $25\text{ }^{\circ}\text{C}$ to $150\text{ }^{\circ}\text{C}$ and cooled to $-85\text{ }^{\circ}\text{C}$ to erase the samples' thermal history.

DMTA was carried out using a Tritec 2000 DMA. The runs were performed using the samples in powder form, placed in stainless steel material pockets, in single cantilever bending geometry. The tests were carried out from $-150\text{ }^{\circ}\text{C}$ to 190°C , in multifrequency mode, with a heating rate of $5\text{ }^{\circ}\text{C min}^{-1}$.

4 Results and Discussion

4.1 PLA homopolymers and copolymers

4.1.1 Chemical Structure Identification

FTIR

The FTIR analysis was performed in order to identify the main functional groups and chemical bonds present in the structure of the PLA homopolymers and copolymers. For the obtainment of the copolymers, L-LA was made to react with two different monomers, DL-MA or VA, in the presence of $\text{Sn}(\text{Oct})_2$ as catalyst. Figure 15 presents the FTIR spectra for PLA homopolymer and copolymers (PLA-co-MA and PLA-co-VA). The FTIR spectra of the remaining PLA homopolymers and copolymers are in Annex A.

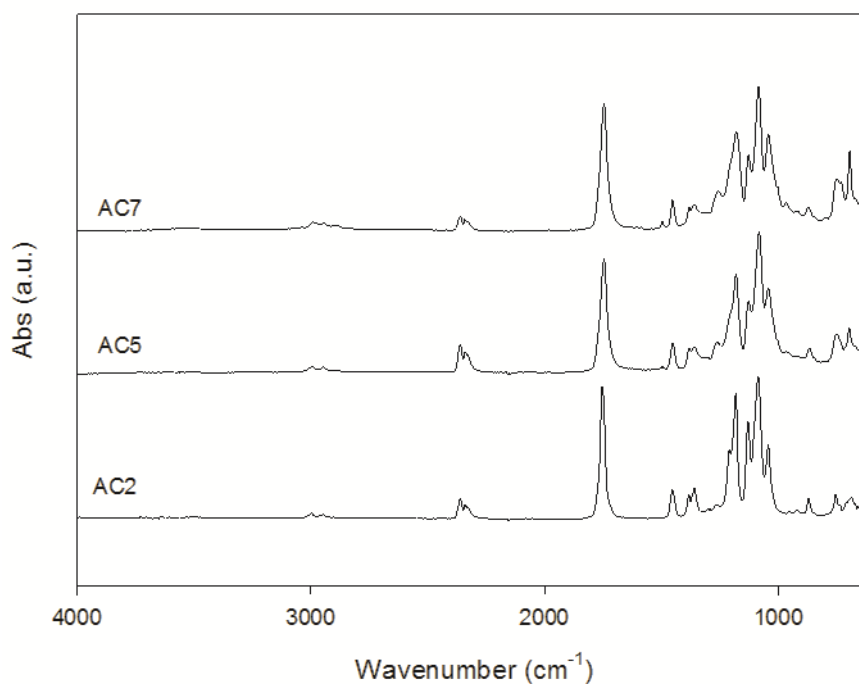


Figure 15 - FTIR spectra of the PLA homopolymer (AC2), PLA-co-MA copolymer (AC5) and PLA-co-VA copolymer (AC7).

In the spectra of Figure 15 one can verify the presence of the characteristic bands of $\nu_{\text{C=O}}$ vibration of the ester group, located among $1750\text{-}1725\text{cm}^{-1}$.

Table 12 summarizes the main bands present in the spectra of Figure 15 and respective assignments.

Table 12 – Main IR bands of PLA homopolymer and PLA copolymer and respective assignments.

Samples	Infrared bands (cm ⁻¹)		
	ν -CH ₃ , -CH ₂ , -CH	ν C=O _{ester}	ν C-O-C _{ester}
AC2	2919-3024	1758	1086
AC5	2873-3022	1752	1083
AC7	2923-3039	1746	1085

AC2 – PLA-homopolymer; AC5 – PLA-co-MA; AC7– PLA-co-VA

It should be mentioned that in the FTIR spectra of the samples AC5 and AC7 it is difficult to identify the characteristic bands of the aromatic ring (1615-1580 cm⁻¹) present in the MA and VA structures. Thus, in order to fully clarify the structure of the homopolymers and copolymers, ¹H NMR analysis was carried out.

¹H NMR

The technique mentioned above identified the main groups presented in the PLA and LA copolymers. ¹H NMR allows understanding the composition of the synthesized polymers and serves as a complement to the FTIR technique. First of all, it is important to emphasize important aspects of this technique; the signals are represented as a function of tetramethylsilane, at $\delta=0$ ppm, so that the nuclei are distributed according to this reference; the functional groups and chemical bonds have resonance peaks at specific chemical shifts, and depending on the structure of the molecule and the type of interaction that exists, these peaks may unfold in multiplets. Figure 16 presents the ¹H NMR spectra of the PLA homopolymer (AC2) and copolymers (AC5 and AC7). The ¹H NMR spectra of the remaining homopolymers and copolymers are shown in Annex B.

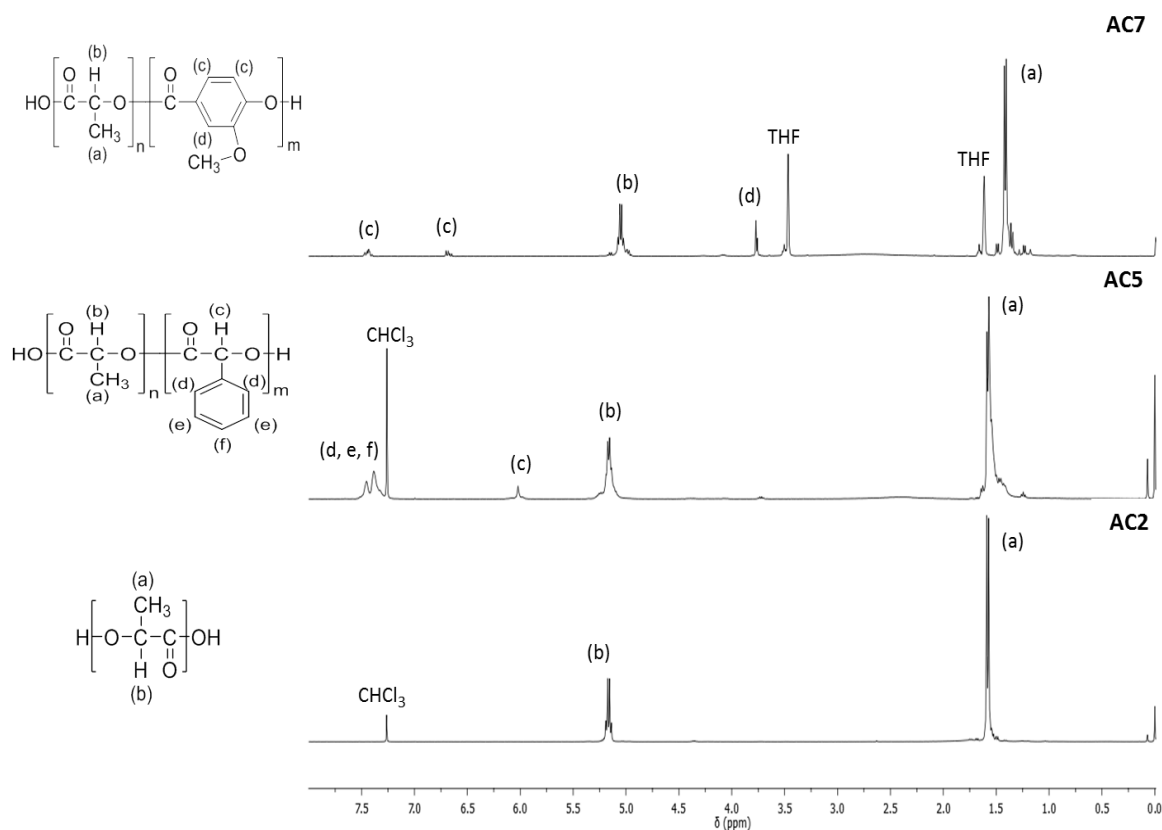


Figure 16 – ^1H NMR of the PLA homopolymer (AC2), PLA-co-MA copolymer (AC5) and PLA-co-VA copolymer (AC7).

The ^1H NMR spectra of the PLA homopolymer and copolymers is in accordance with the expected chemical structure. For the three samples it is possible to observe the resonances of the $-\text{CH}$ (b) (5.3-5 ppm) and $-\text{CH}_3$ (a) (1.5-1 ppm) groups of L-LA units. In AC5 it is possible to visualize two resonances in 7.5-7 ppm (d,e,f) and 5.5-5 ppm (c) that can be ascribed to the aromatic ring of the MA. In AC7, the resonances in 7.5-6.5 ppm (c) correspond to the resonances of the protons belonging to the aromatic ring and at 3.75 ppm (d) it is possible to observe the resonance of the protons belonging to the group $-\text{OCH}_3$ linked to the aromatic ring.

The amount of MA and VA incorporated in the L-LA chain was determined by ^1H NMR (

Table 13), through the integral ratio between the resonances belonging to L-LA chain and the hydroxyacids (Eq. (2)):

$$\% n(DL - MA \text{ or } VA) = \frac{n(DL - MA \text{ or } VA)}{n(DL - MA \text{ or } VA) + n(L - LA)} \times 100 \quad \text{Eq. (2)}$$

Where,

$$n(DL - MA) = \frac{\int d, e, f}{3} \quad \text{Eq. (3)}$$

$$n(VA) = \frac{\int c}{1} \quad \text{Eq. (4)}$$

$$n(L - LA) = \frac{\int b}{1} \quad \text{Eq. (5)}$$

Table 13 – Amount of acids incorporated in the L-LA chain.

Samples	Feed		Real	
	n_{L-LA}/n_{MA}	n_{L-LA}/n_{VA}	n_{L-LA}/n_{MA}	n_{L-LA}/n_{VA}
AC2	100		100	
AC5	90/10		91/9	
AC6	75/25		75/25	
AC7		90/10		92/8

The values obtained for the amount of MA and VA incorporated in the L-LA chain indicates that the initial quantity of the hydroxyacids was almost incorporated. Differences in the values can be attributed to errors inherent to the quantification by ^1H NMR or to the loss of monomers during the reaction.

4.1.2 Molecular Weight Distribution by GPC

The molecular weight distribution (MWD) of the PLA homopolymers and copolymers was measured by SEC, using the conventional calibration. Figure 17 the SEC trace (RI signal) obtained for the PLA homopolymer and copolymers.

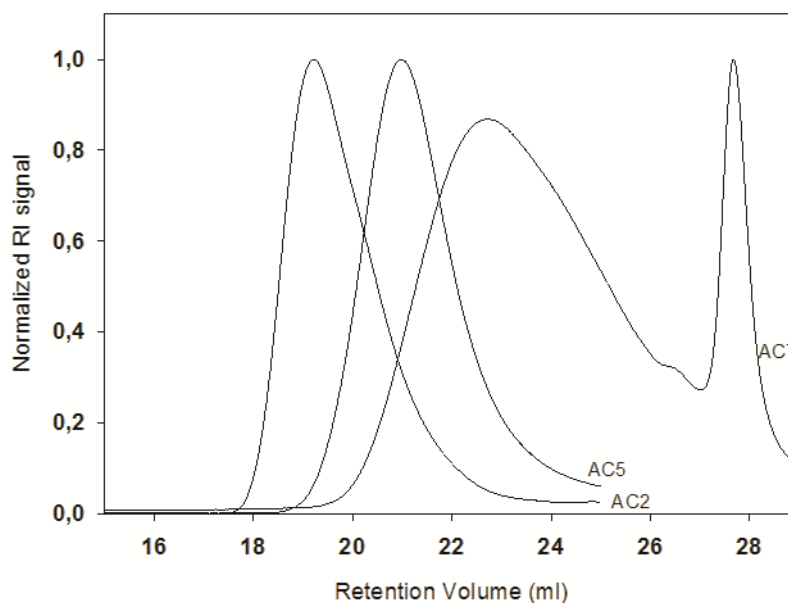


Figure 17 – Normalized RI signal vs. retention volume for PLA homopolymer and copolymers.

It is possible to observe in Figure 17 that the copolymers curves are deviated to the right relative to the homopolymer curve, which indicates the lower molecular weight of copolymers. It is also possible to visualize that the sample AC7 has a broad molecular weight distribution comparing with the other samples. It should be mentioned that AC7 sample has an additional peak that most probably is due to the presence of oligomers with very low molecular weight.

Table 14 presents the molecular weights (conventional calibration) of the PLA homopolymer and copolymers synthesized along the work by melt polycondensation.

Table 14 - Molecular weight and PDI values for PLA homopolymer and copolymers obtained by melt polycondensation and calculated by conventional calibration.

Samples	\bar{M}_n (g/mol)	PDI
AC2	8,006	2.18
AC3	8,094	1.93
AC4	11,089	1.72
AC5	4,142	1.38
AC6	984	2.76
AC7	972	2.38

The differences observed in the values of molecular weight can be ascribed to the different reactivities of the monomers during the reaction. Most probably the aromatic rings present in

MA or VA hinder sterically the -OH and -COOH groups turning them less reactive than those of LA.

The results obtained for the PDI are above 1.3, which is accordance with the values presented in literature for polycondensation reactions ^[57].

Figure 18 presents the SEC trace (RI signal) for PLA homopolymers obtained through bulk polycondensation (AC2) and azeotropic dehydration condensation (AC8).

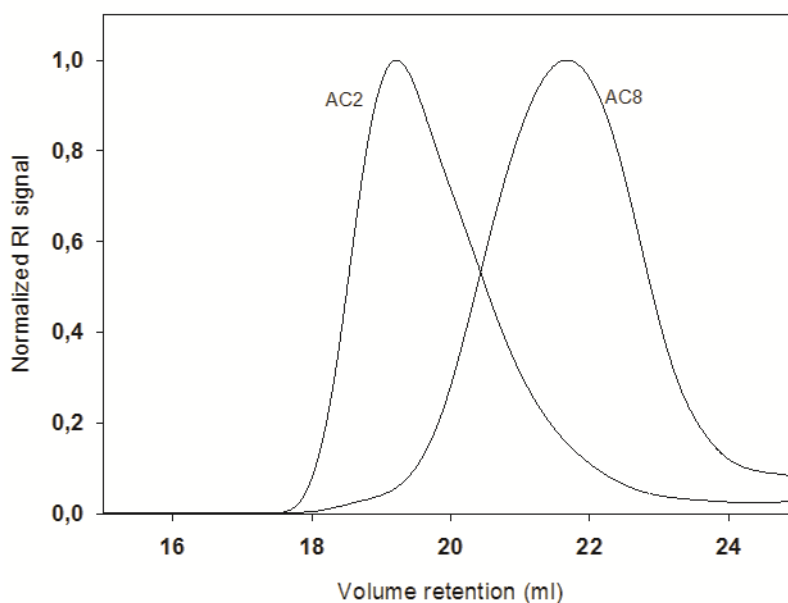


Figure 18 - Normalized RI signal vs. retention volume for PLA homopolymers.

Figure 18 shows that the sample AC8 that was obtained through azeotropic dehydration condensation is more deviated to the right, indicating that this has a lower molecular weight than the AC2 sample, which is somewhat contradictory. According to the literature, it was expected to obtain higher molecular weights for the samples obtained by azeotropic dehydration condensation, since in this type of polymerization the water is more efficiently removed than in bulk polycondensation, allowing the polymeric chain to increase considerably its molecular weight. Unfortunately, in any of the azeotropic dehydration condensation experiments it was possible to efficiently distill off the water formed during the reaction. For this reason, this strategy was abandoned.

Table 15 presents the molecular weights of the PLA homopolymers and copolymers obtained from the azeotropic dehydration condensation method.

Table 15 - Molecular weight and PDI values for PLA homopolymers.

Samples	\overline{M}_n (g/mol)	PDI
AC8	1,905	2.39
AC9	3,076	1.16
AC10	2,546	1.54

4.1.3 Thermal analysis

SDT

Simultaneous thermal analysis (DSC-TGA) was conducted to evaluate the thermal stability of the PLA homopolymers and copolymers. Figure 19 gives a general overview of the thermal behavior of the PLA homopolymer and copolymers and Table 16 summarizes the main temperatures obtained from the simultaneous thermal analysis for all homopolymers and copolymers synthesized along this work. In Annex D are presented the thermoanalytical curves of the remaining PLA homopolymers and copolymers.

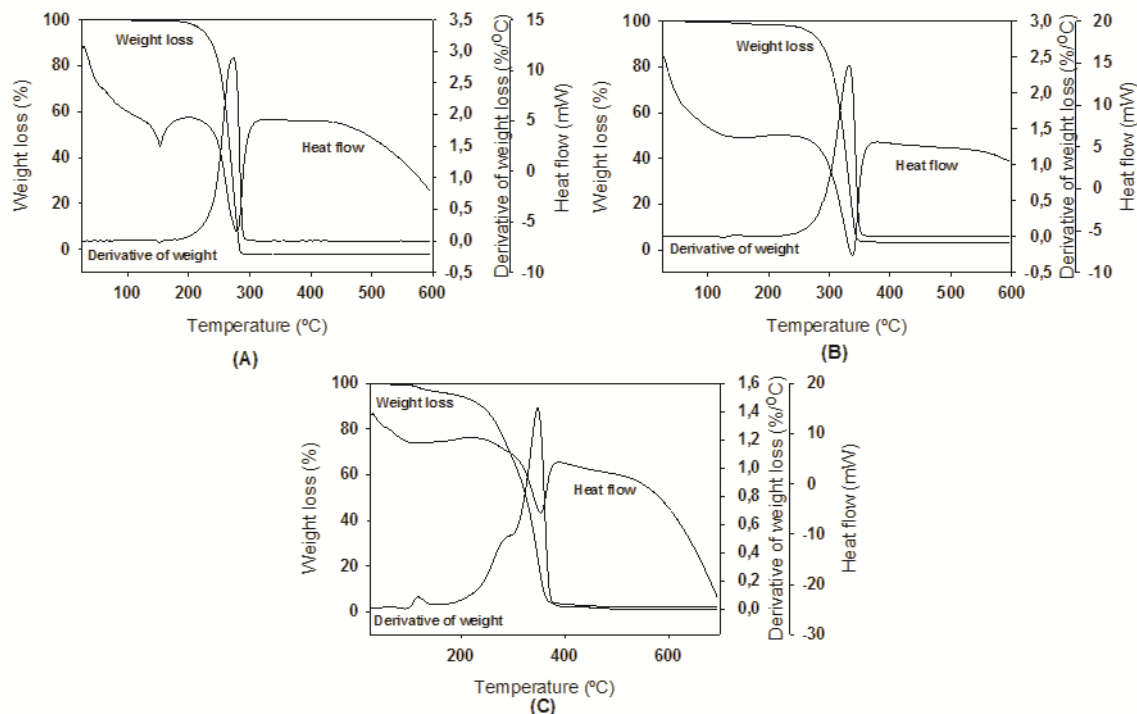


Figure 19 - Thermoanalytical curves obtained in simultaneous of PLA homopolymers and copolymers; (A) PLA homopolymer (AC2); (B) PLA-co-MA (AC5); (C) PLA-co-VA (AC7).

Figure 19 shows that AC2 and AC5 exhibit a similar weight loss pattern, with one degradation stage, which can be attributed to the scission of the ester linkage ^[58]. In turn, the DTG curve of AC7 sample evidence three distinct degradation stages. In the simultaneous thermal analysis performed to the monomer (present in Annex D) is possible to verify that this only begins to degrade at temperatures above 200°C, which suggests that the first weight loss is not due to monomer degradation. Thus, this first stage of degradation can be attributed to the volatilization of water present in the sample. The second and the third stages can be justified by the loss of ester bonds and the scission of –OCH₃ linkage.

Regarding the heat flow curve it is possible to observe that AC2 sample presents a clear peak that can be attributed to the melting. PLA copolymers (AC5 and AC7) do not present any melting peak, demonstrating their amorphous character. This will be appropriately discussed in DSC analysis.

Table 16 – Characteristic temperatures (average) obtained from simultaneous thermal analysis for homopolymers and copolymers. T_{on} : extrapolated onset temperature (TG); $T_{5\%}$: temperature corresponding to 5% of mass loss; $T_{10\%}$: temperature corresponding to 10% of mass loss; T_p : peak temperature (DTG); T_d : degradation temperature.

Samples	T_{on1} (°C)	T_{on2} (°C)	T_{p1} (°C)	T_{p2} (°C)	T_{p3} (°C)	$T_{5\%}$ (°C)	$T_{10\%}$ (°C)	T_m (°C)	T_d (°C)
AC2	247±1.2	----	270.5±3.6	----	----	223.2±1.5	236.9±0.6	152.5±0.4	277.3±2.0
AC3	257.2±1.8	----	282.7±2.4	----	----	235.9±5.8	247.3±3.7	148.3±0.0	287±2.0
AC4	253±1.5	----	281.5±0.9	----	----	232.6±0.4	244.5±0.5	154.8±0.5	285.8±0.5
AC5	302.8±0.3	----	332.6±0.8	----	----	267.6±3.7	286.3±1.5	----	338.3±0.8
AC6	113.7±0.6	288.3±0.4	129.7±3.3	320.6±0.9	----	228.1±9.2	265.3±2.3	----	323.5±0.5
AC7	111.7±3.6	298.9±0.3	117.7±1.4	292.1±3.8	350.1±3.8	185.6±7.9	239.5±1.6	----	355.3±3.3
AC8	285.4±3.1	----	324.7±0.8	363±2.0	----	254.6±0.5	281±0.5	134.4±1.2	367.8±2.4
AC9	260.4±0.7	----	290.4±0.5	----	----	213.8±2.1	238.7±1.4	126.9±1.3	296.2±0.2
AC10	135±4.4	244.9±.9	146.9±4.4	274.8±3.2	321.6±0.4	220.5±3.4	242.5±2.6	----	276.8±1.2

Analyzing Table 16 it is possible to verify that the homopolymers samples (AC2, AC3, AC4, AC8 and AC9) presents a similar thermal stability. The small difference in the thermal stability can be justified to the difference in the corresponding molecular weight of the samples.

The AC6, AC7 and AC10 samples present two T_{on} , being the first ascribed to the vaporization of water present in the samples. Nevertheless, analyzing the T_{on2} value for these samples it is possible to note that their thermal stability is greater than that of homopolymers. It should be also pointed out that AC5 has a T_{on} value significantly higher than that of the homopolymers. This behavior can be explained by the increase in the thermal stability by the introduction of aromatic compounds.

DSC

DSC was used to examine the thermal behavior of the synthesized PLA homopolymer and copolymers, below the degradation temperature. Figure 20 presents the DSC traces recorded during the second heating cycle of the samples. The DSC traces of the remaining polymers are presented in Annex E.

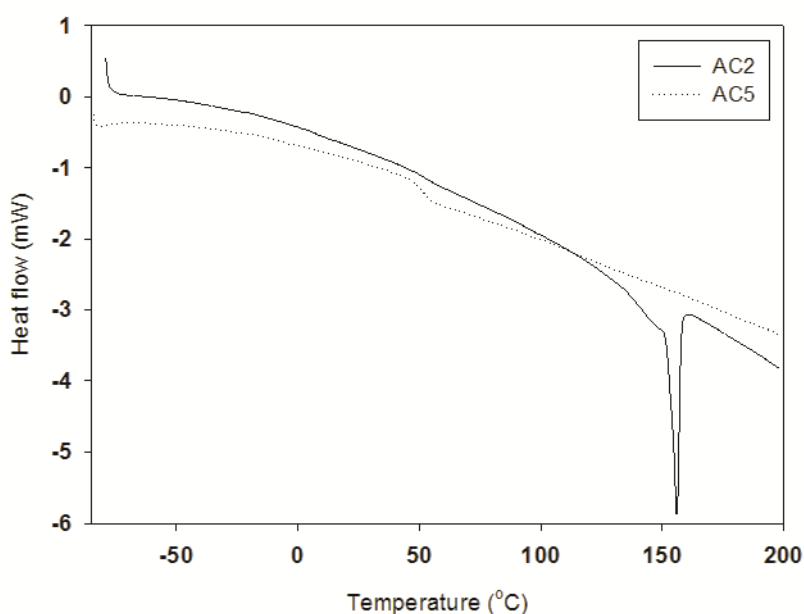


Figure 20 - DSC thermograms of PLA homopolymer (AC2) and PLA-co-PMA copolymer (AC5).

In Figure 20 it is possible to observe that AC2 sample presents a well-defined melting endotherm, at *ca* 155°C (peak temperature), indicating that it has a semi-crystalline character. PLA copolymer with MA (AC5) does not present any melting peak, demonstrating its amorphous character. The AC7 sample showed a weight loss for temperatures below 100 °C in SDT analysis. Although, this can be attributed to the evaporation of residual moisture, for precaution this sample was not analyzed by DSC. Nevertheless, the SDT analysis revealed the absence of peaks in the heat flow curve (below the degradation), suggesting that AC7 has an amorphous character.

The melting temperatures (T_m) of PLA homopolymers and copolymers prepared in this work and determined by DSC are present in Table 17.

Table 17 - T_m values for the PLA homopolymer and copolymers obtained by DSC

Samples	T_m (°C)
AC2	152.5
AC3	148.3
AC4	154.8
AC5	----
AC6	----
AC7	----
AC8	134.4
AC9	126.9
AC10	----

Table 17 indicates that only the homopolymers samples present a melting endotherm, indicating a semi-crystalline character. In turn, the introduction of aromatic rings in the chain of copolymers induces disturbances in regularity of copolymer structure impairing a close chain packaging, and preventing crystallization to take place ^[59].

DMTA

DMTA analysis was used to determine the glass transition temperatures (T_g) and secondary thermal transitions of the PLA homopolymer and copolymers. The analysis was performed in multifrequency mode (1, 10 Hz), at 5 °C min. The results obtained for the samples AC2 (PLA homopolymer), AC5 (PLA-co-MA) and AC7 (PLA-co-VA) are presented in Figure 21. The results obtained for the other polymers are presented in Annex F.

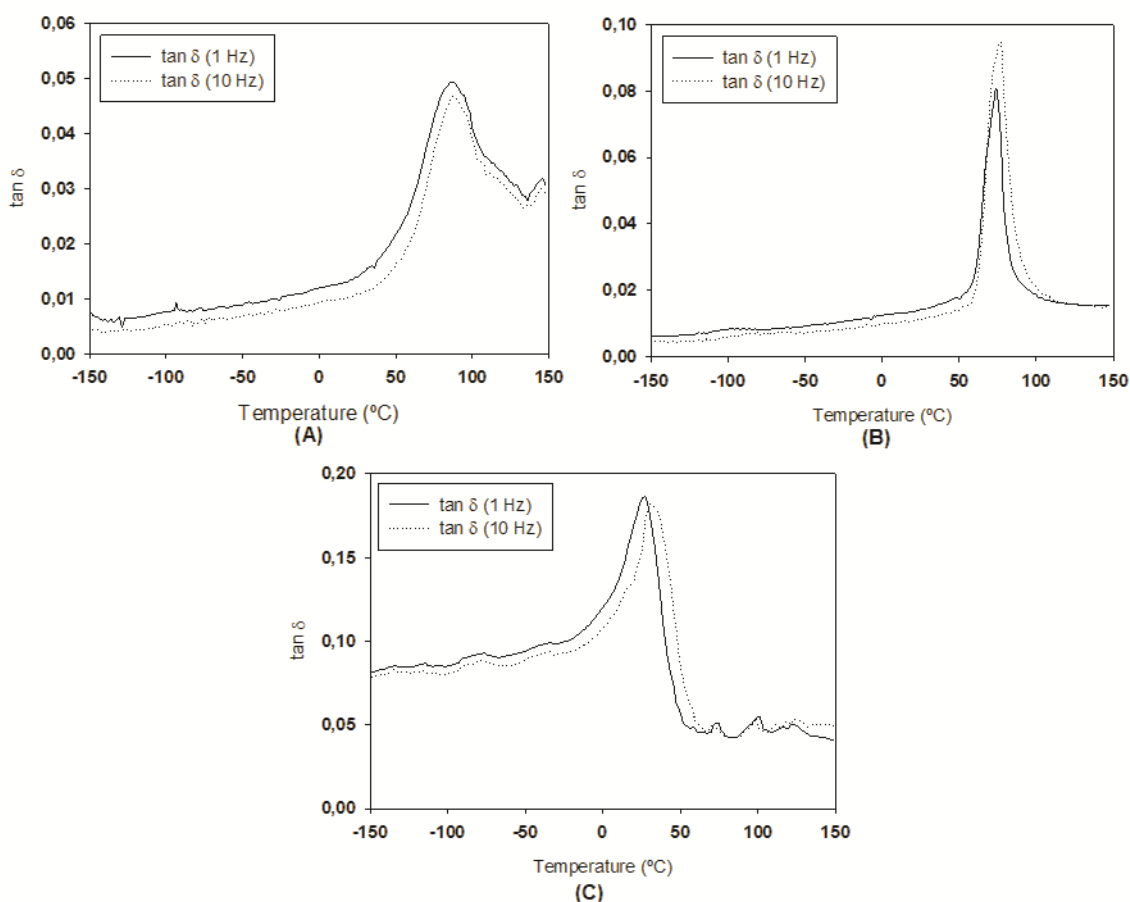


Figure 21 – DMTA traces (glass transition zone) of PLA homopolymer and copolymers, at two frequencies: (A) PLA homopolymer (AC2); (B) PLA-co-MA (AC5); (C) PLA-co-VA (AC7).

Both the PLA homopolymer and copolymers present a peak sensitive to frequency. This peak is associated to the α -relaxation and corresponds to the glass transition ^[60]. It is worth to be mentioned that this temperature coincides with the abrupt fall of the storage modulus (E') (curve not presented).

It is also possible to observe that the AC2 and AC7 (PLA-co-PMA and PLA-co-PVA, respectively) samples exhibit more peaks beyond the T_g peak. These peaks can be ascribed to the local movements of the polymer main chain, lateral groups movements or even rotation/vibration of the terminal groups ^[60].

The T_g values of all the PLA homopolymers and copolymers obtained from the DMTA analysis are shown in Table 18.

Table 18 - T_g values for the PLA homopolymer and copolymers obtained by DMTA.

Samples	T_g (°C)
AC2	87.3
AC3	81.9
AC4	85.9
AC5	74.4
AC6	54.7
AC7	25.3
AC8	90.3
AC9	88.2
AC10	59.1

Analyzing Table 18 it is possible to note that the homopolymers samples (AC2, AC3, AC4, AC8 and AC9) present a higher T_g than the copolymers samples. This seems a little contradictory, since it was expected that the introduction of the aromatic moieties (from MA and VA) would stiffen the polymeric chain, contributing to motion restrictions, with a consequent increase in the T_g value. The reason behind such unexpected behavior can be attributed to the differences in molecular weight. The SEC analysis showed that the PLA copolymers had a significantly lower molecular weight than the homopolymers. Nevertheless, this fact could only be clarified if copolymers of molecular weight similar to homopolymers were prepared.

4.2 PLA chain extension

4.2.1 Chemical Structure Identification

FTIR

Before carry out the chain extension it was necessary to synthesize the LA oligomers with hydroxyl end groups. The synthesis of LA oligomers was performed through melt polycondensation of monomers (LA, LA/MA or LA/VA) in the presence of EG and with $\text{Sn}(\text{Oct})_2$ as catalyst. It is supposed that the L-LA oligomeric chain react with the diol in order to produce oligomeric chains with hydroxyl end groups. Figure 22 illustrates FTIR spectra of L-LA oligomers with hydroxyl end groups.

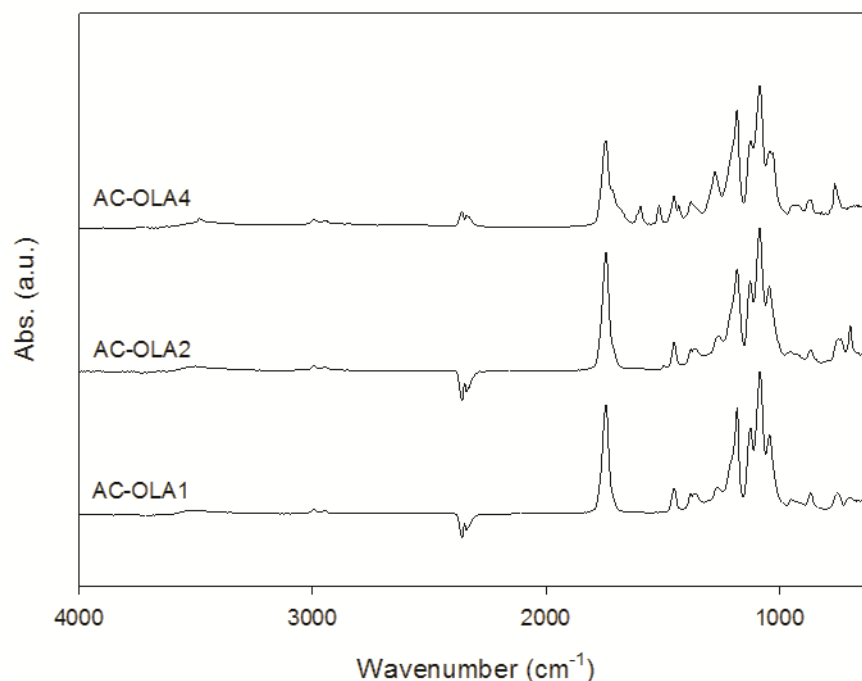


Figure 22 - FTIR spectra of the PLA oligomers with hydroxyl end groups.

It is possible to observe the bands corresponding to the main functional groups in the three samples, the ester group ($\nu_{\text{C=O}}$) and the hydroxyl group (ν_{OH}), located among $1750\text{-}1725\text{cm}^{-1}$ and $3550\text{-}3500\text{cm}^{-1}$, respectively. Table 19 shows the main bands present in spectra of Figure 22 and respective assignments.

Table 19 - Main IR bands of LA oligomers with hydroxyl end groups and respective assignments.

Samples	Infrared bands (cm^{-1})			
	$\nu_{\text{CH}_3, \text{CH}_2, \text{CH}}$	$\nu_{\text{C=O ester}}$	$\nu_{\text{C-O-C ester}}$	ν_{OH}
AC-OLA1	2797-3008	1745	1084	3512
AC-OLA2	2871-3090	1743	1085	3501
AC-OLA4	2930-3023	1746	1085	3503

In Annex A are presented the FTIR spectra and respective assignments of the remaining LA oligomers.

The chain extension was carried out by reacting the LA oligomers with HMDI and IPDI. The isocyanates have a very high reactivity, which makes them strong candidates for use in chain extension reactions with hydroxyl terminated moieties ^[41, 61]. The FTIR spectra of PLA oligomer (AC-OLA1) and the products of chain extension with IPDI and HMDI (AC-CE1

and AC-CE2, respectively) (Figure 23) present the characteristic bands of ester and urethane groups.

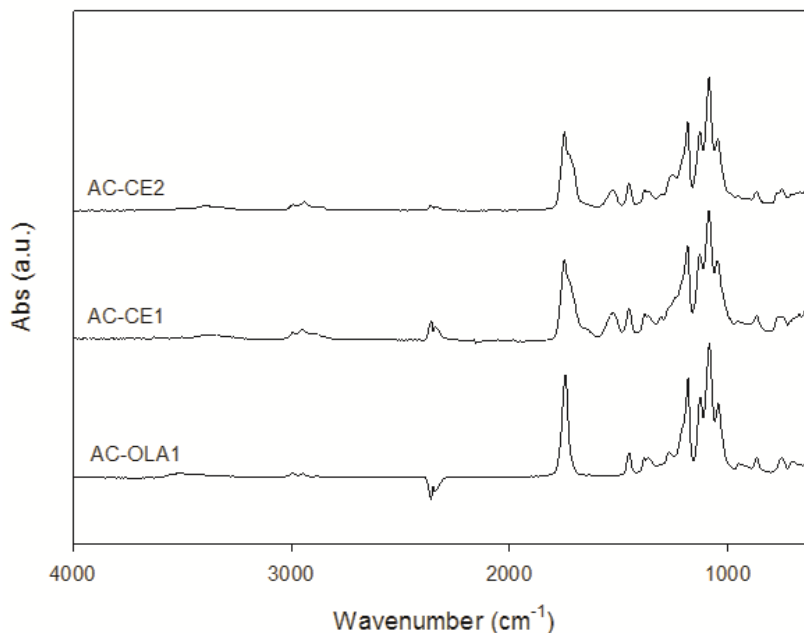


Figure 23 - FTIR spectra of PLA oligomer (AC-OLA1) and the products of chain extension (AC-CE1 and AC-CE2).

For the three samples it is possible to observe a peak at *ca.* 1745 cm^{-1} correspondent to the $\nu_{\text{C=O}}$ of the ester group. A shoulder at *ca.* 1710 cm^{-1} is observed in the spectra of AC-CE1 and AC-CE2, which corresponds to the $\nu_{\text{C=O}}$ of the urethane linkage. A new band at *ca.* 1525 cm^{-1} appears in the spectra of AC-CE1 and AC-CE2 and is due to the $\nu_{\text{-NH}} + \nu_{\text{-CN}}$ vibration of the urethane linkage. At *ca.* 3300 cm^{-1} appear the band corresponding to the $\nu_{\text{-NH}}$. It is worth to be mentioned the absence of bands at *ca.* 2270 cm^{-1} ($\nu_{\text{-N=C=O}}$), which is indicative of the inexistence of free isocyanate within the sample.

Table 20 shows the wavenumbers and respective assignments of the main bands identified in FTIR spectra of Figure 23.

Table 20 - Main IR bands of PLA oligomer (AC-OLA1) and the products of chain extension (AC-CE1 and AC-CE2) and respective assignments.

Samples	Infrared bands (cm ⁻¹)					
	$\nu_{\text{-NH}}$	$\nu_{\text{-CH}_3, \text{-CH}_2, \text{-CH}}$	$\nu_{\text{C=Oester}}$	$\nu_{\text{C=Ourethane}}$	$\nu_{\text{NH}} + \nu_{\text{CN}}$	$\nu_{\text{C-O-Cester}}$
AC-OLA1	-----	2797-3008	1745	-----	-----	1084
AC-CE1	3303	2883-3034	1748	1733-1698 (sh)	1524	1085
AC-CE2	3302	2904-3010	1748	1730-1695 (sh)	1526	1085

The FTIR spectra and respective bands assignment of the remaining chain extended polymers are shown in Annex A.

NMR

Further insights onto the L-LA oligomers and co-oligomers were given by ¹H NMR analysis. Figure 24 presents the ¹H NMR spectra of the LA oligomer (AC-OLA 1) and co-oligomers with MA and VA (AC-OLA 2 and AC-OLA 4, respectively). The spectra of the remaining oligomers and co-oligomers are shown in Annex B.

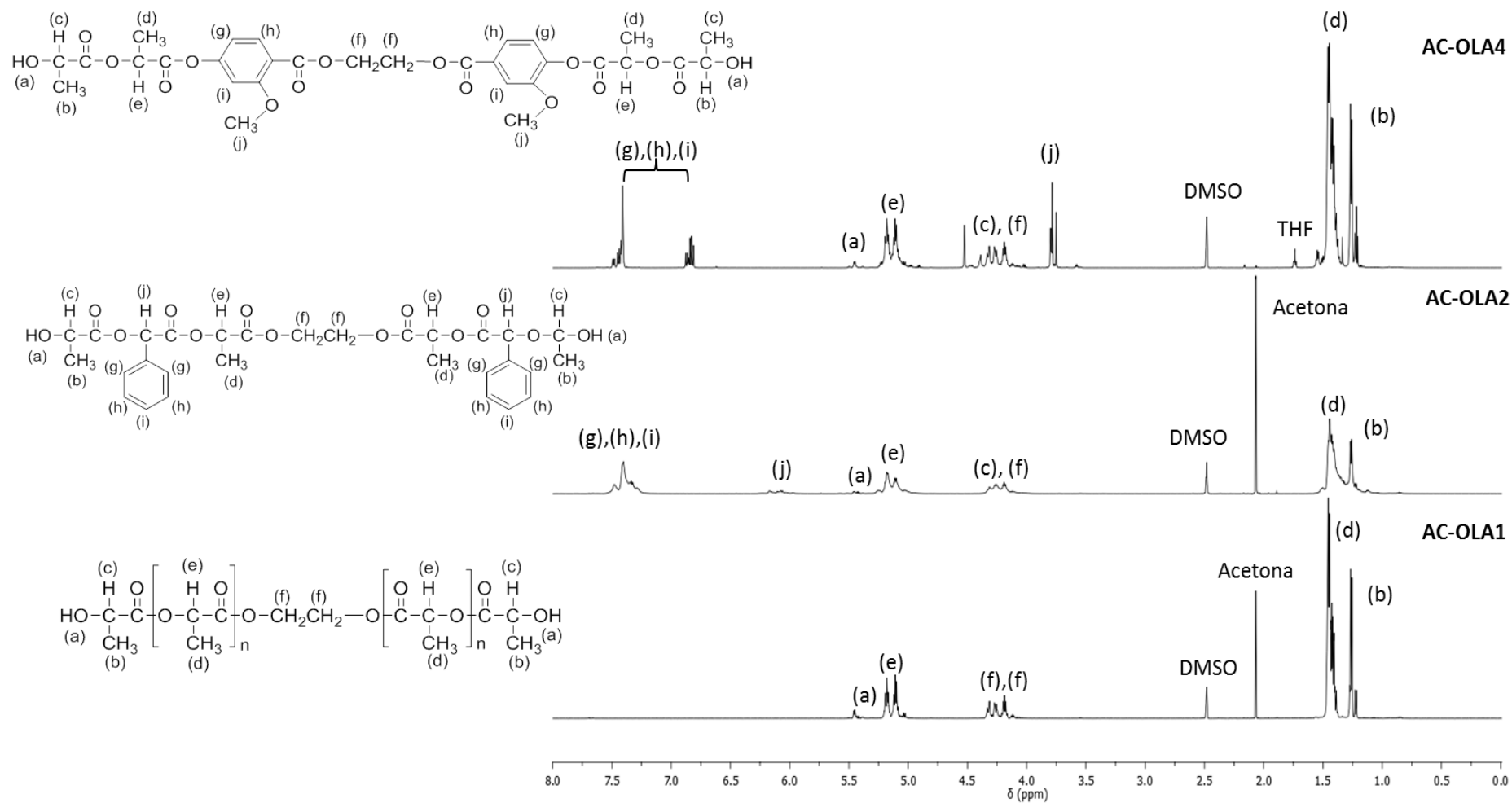


Figure 24 - ^1H NMR of the PLA oligomers and co-oligomers with hydroxyl end groups.

The ^1H NMR (Figure 24) presents the resonances of the protons of the LA oligomers and co-oligomers and respective assignments. The resonance of $-\text{OH}$ groups of L-LA (a) is visible at 5.5-5.35 ppm for all the samples. Here it is possible to detect the resonances of the central units of L-LA oligomers and the resonances of the protons linked to the hydroxyl end groups. The resonances in the 5.5-5.0 ppm (e) range and in the 1.5-1.3 ppm (d) are assigned to the $-\text{CH}$ and $-\text{CH}_3$ groups of L-LA central units, respectively. The signals in the 4.3-4.1 ppm (c) correspond to the $-\text{CH}$ groups from the hydroxyl end groups, together with the $-\text{CH}_2$ protons (f) of the EG linked to the L-LA oligomeric chain. In the 1.3-1.1 ppm (b) it is possible to observe the resonances of the $-\text{CH}_3$ protons linked to the hydroxyl end groups.

The amounts of MA and VA incorporated in the oligomers were calculated by ^1H NMR, using the Eq. (2), presented above. The results obtained are presented in Table 21.

Table 21 - Amount of hydroxyacids incorporated in the L-LA oligomeric chain.

Samples	Feed		Real	
	$n_{\text{L-LA}}/n_{\text{MA}}$	$n_{\text{L-LA}}/n_{\text{VA}}$	$n_{\text{L-LA}}/n_{\text{MA}}$	$n_{\text{L-LA}}/n_{\text{VA}}$
AC-OLA1	100			
AC-OLA2	90/10		81/19	
AC-OLA3	75/25		65/35	
AC-OLA4		90/10		86/14
AC-OLA5	100			
AC-OLA6	90/10		81/19	
AC-OLA7		90/10		90/10

The values obtained demonstrate that the acids incorporation was well succeeded. The difference between the quantities calculated and those used in the feed can be explained by some evaporation of L-LA during the reaction and also due to errors inherent to the calculations using the integrals calculated by ^1H NMR.

Figure 25 presents the ^1H NMR spectra of the LA oligomer (AC-OLA1) and the products of chain extension with IPDI and HMDI (AC-CE1 and AC-CE2, respectively).

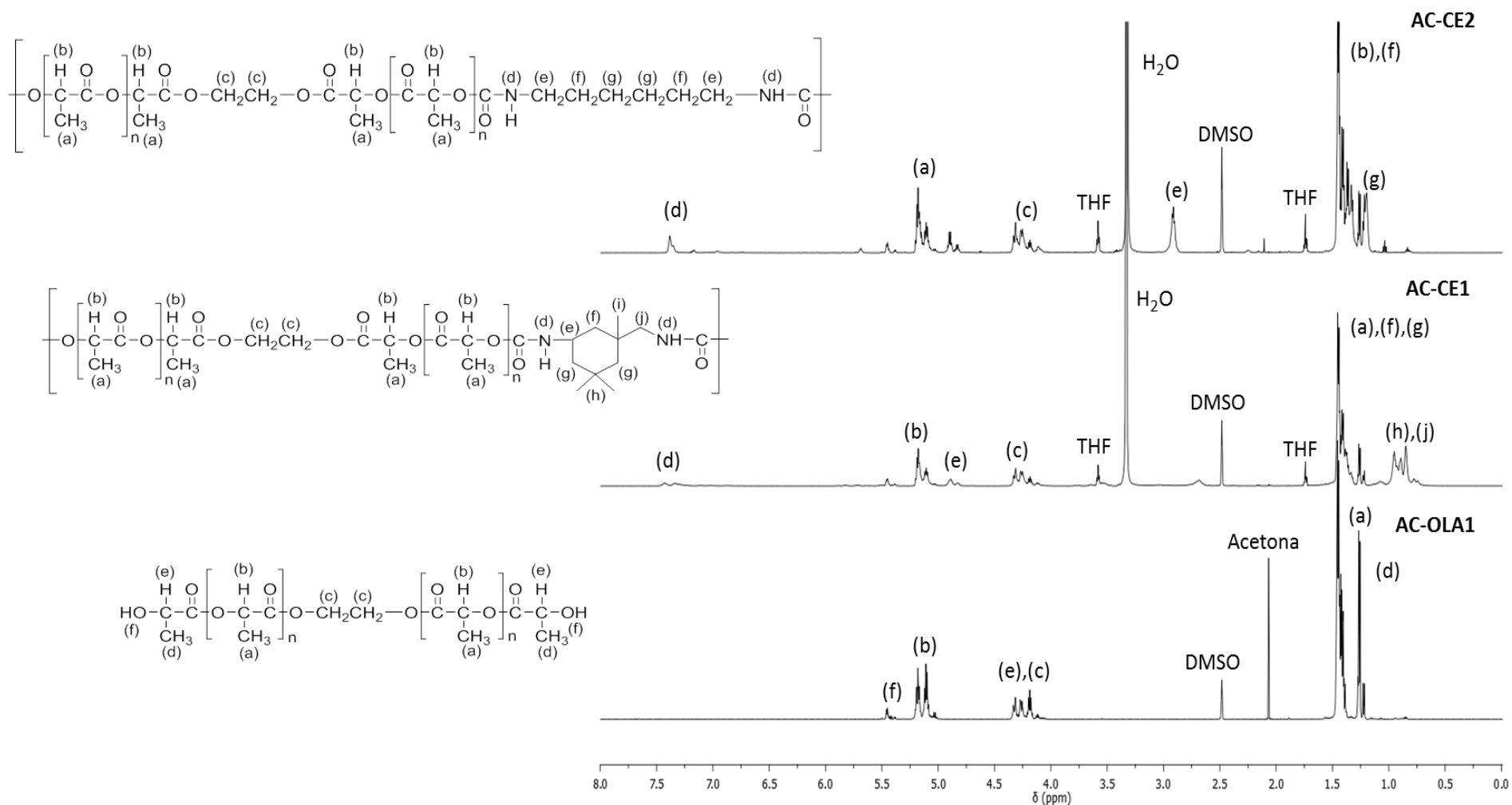


Figure 25 - ^1H NMR of the PLA oligomer (AC-OLA1) and products of chain extension (AC-CE1 and AC-CE2).

The spectroscopic analysis is in accordance with the expected structure. The ^1H HMR spectra of products of chain extension (AC-CE1 and AC-CE2) it is possible observe a set of new resonances (d, e, f, g) resulting from the addition of IPDI and HMDI to the structure of L-LA oligomers, through a urethane linkage. The signal $\delta \approx 7.5$ ppm (d) is ascribed to the protons of urethane linkage. It should be also noted that for AC-CE1 and AC-CE2, the resonance corresponding to the $-\text{CH}$ and $-\text{CH}_3$ groups of hydroxyl end groups does not appear. Thus, this suggests that the chain extension reaction was performed successfully.

4.2.2 Molecular Weight Distribution by GPC

The molecular weight distribution (MWD; Figure 26) of the LA oligomers and co-oligomers was measured by SEC, using conventional calibration.

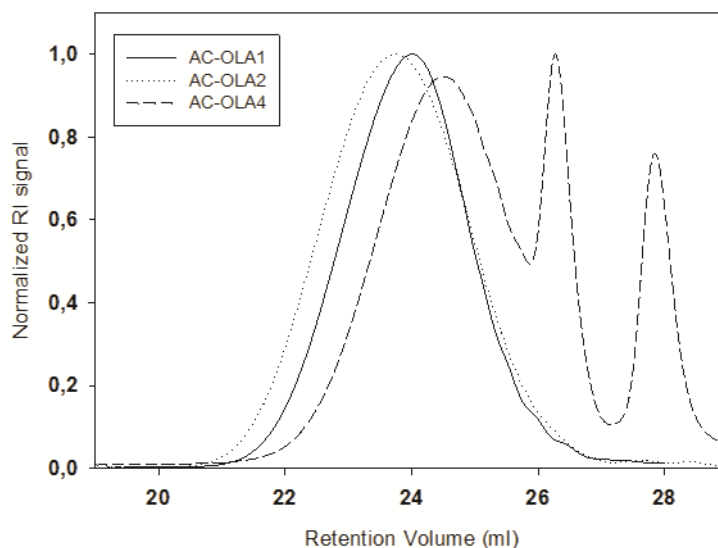


Figure 26 - Normalized RI signal vs. retention volume for LA oligomers and co-oligomers.

It is possible observe that the three samples have a broad molecular weight distribution (see PDI values in Table 22), which was expected since we are in presence of an oligomeric mixture. Once again, the co-oligomer presenting VA in the structure has the lowest molecular weight and the broadest MWD, with additional peaks. This fact can be attributed to the presence of oligomers of very low molecular weight.

Table 22 shows the values of molecular weight and PDI for LA oligomers and co-oligomers synthesized along the work.

Table 22 - Molecular weight and PDI values for PLA oligomers.

Samples	\overline{M}_n (g/mol)	PDI
AC-OLA1	741	1.63
AC-OLA2	608	2.26
AC-OLA3	1,076	1.63
AC-OLA4	197	3.45
AC-OLA5	2,122	1.36
AC-OLA6	2,566	1.62
AC-OLA7	695	2.97

It should be mentioned that the values of molecular weight are somewhat away from the predicted values (600 g/mol to AC-OLA1-AC-OLA4 and 2000 g/mol to AC-OLA5-AC-OLA7), which can be related with the different reactivities of the monomers used.

Figure 27 presents the SEC trace (RI signal) obtained for the LA oligomer (AC-OLA1) and products of chain extension with IPDI (AC-CE 1) and HMDI (AC-CE 2).

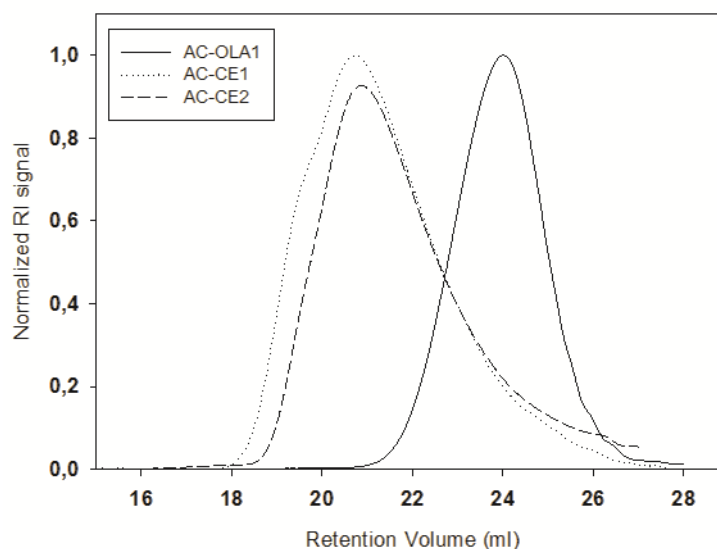


Figure 27 - Normalized RI signal vs. retention volume for PLA oligomer (AC-OLA1) and products of chain extension (AC-CE1 and AC-CE2).

It is possible to note a clear deviation for the left of the products of chain extension when compared to the LA oligomer, indicating an increase in the molecular weight. The molecular weight distribution appears identical for the three samples. Nevertheless, it should be

mentioned the incomplete shift of the AC-CE1 and AC-CE2 curves relatively to AC-OLA1, which indicates that not all the oligomeric chains were reinitiated. This fact can be related to an unbalance between the stoichiometric ratio between the hydroxyl groups and isocyanate groups. The same behavior was observed for all the products of chain extension with the different LA oligomers and co-oligomers (see Annex C).

Table 23 summarizes the data of molecular weight and PDI for the LA oligomer and co-oligomers and products of chain extension. For comparison purposes, the values of molecular weight of the oligomers are also presented.

Table 23 - Molecular weight and PDI values for LA oligomers and products of chain extension.

Samples	\overline{M}_n (g/mol)	PDI
AC-OLA 1	741	1.63
AC-CE1	2,785	2.67
AC-CE2	2,121	2.69
AC-OLA2	608	2.26
AC-CE3	3,325	1.59
AC-CE4	3,447	2.68
AC-OLA3	1076	1.63
AC-CE5	1,258	4.58
AC-CE6	a)	
AC-OLA4	197	3.45
AC-CE7	515	4.97
AC-CE8	553	7.28
AC-OLA5	2122	1.36
AC-CE9	3,874	1.89
AC-CE10	b)	
AC-OLA6	2,566	1.62
AC-CE11	3,207	1.48
AC-CE12	b)	
AC-OLA7	695	2.97
AC-CE13	1,676	2.53
AC-CE14	1,469	2.16

^{a)} The sample did not dissolve in the eluent (THF) of the SEC analysis. ^{b)} Impossible to calculate due to software issues.

The values for the \overline{M}_n support what was observed in Figure 27, the oligomer molecular weight is lower than that the products of chain extension.

4.2.3 Thermal analysis

SDT

The thermal stabilities of the LA oligomers with hydroxyl terminal groups were evaluated by simultaneous thermal analysis. Figure 28 shows the thermal behavior of the LA oligomers (AC-OLA1) and co-oligomers (AC-OLA2 and AC-OLA4), and Table 24 presents the relevant temperatures obtained from the simultaneous thermal analysis. The thermogravimetric curves of the remaining LA oligomers and co-oligomers are presented in Annex D.

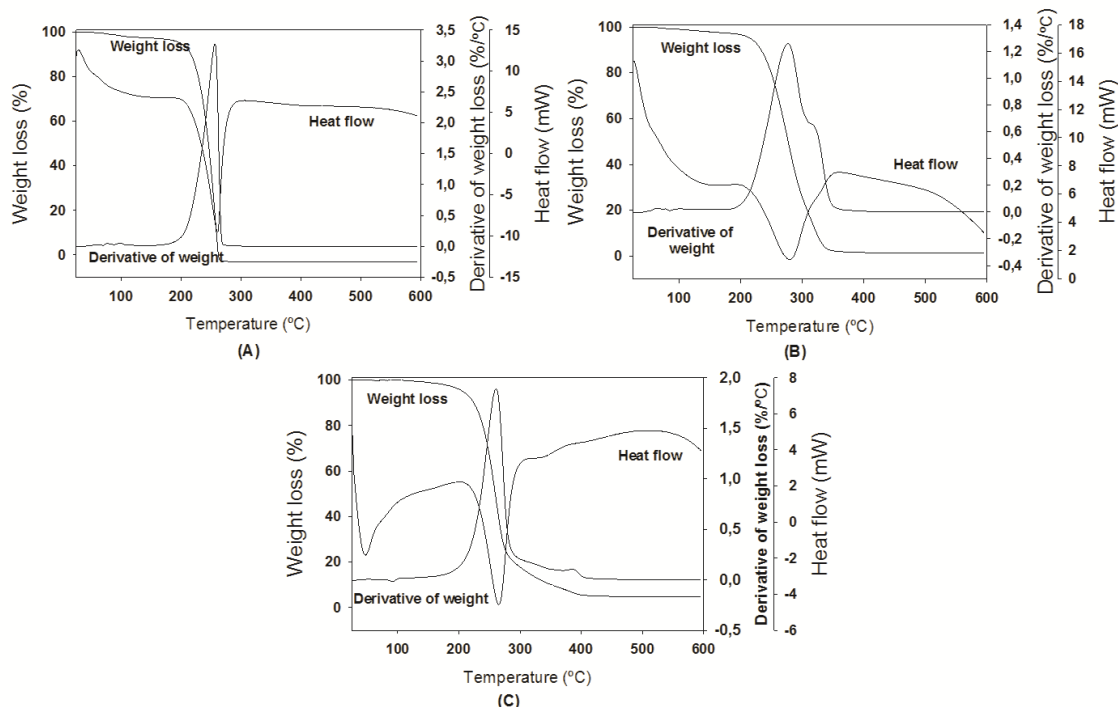


Figure 28 - Simultaneous thermoanalytical curves of LA oligomer and co-oligomers; (A) LA oligomer (AC-OLA1);(B) O(LA-co-MA) (AC-OLA2); (C) O(LA-co-VA) (AC-OLA4).

Figure 28 shows that the AC-OLA1 and AC-OLA4 samples present a similar weight loss pattern, with one thermal degradation stage, that most probably correspond to the degradation of the ester linkages. AC-OLA2 sample, in turn, undergoes a two-step thermal degradation with the first step occurring between 230 – 300 °C and the second step among 310 – 350°C. The data in literature regarding the thermal behavior of such co-oligomers is scarce and for that reason it is not possible to advance with an explanation for such fact.

Table 24 - Characteristic temperatures (average) obtained from simultaneous thermal analysis for homopolymers and copolymers. T_{on} : extrapolated onset temperature (TG); $T_{5\%}$: temperature corresponding to 5% of mass loss; $T_{10\%}$: temperature corresponding to 10% of mass loss; T_p : peak temperature (DTG); T_d : degradation temperature.

Samples	T_{on1} (°C)	T_{p1} (°C)	T_{p2} (°C)	$T_{5\%}$ (°C)	$T_{10\%}$ (°C)	T_d (°C)
AC-OLA1	233.5±1.7	256.9±0.4	----	211.5±4.6	221.8±3.1	261.7±0.0
AC-OLA2	239.6±1.4	272.8±6.0	314.5±3.2	219±2.8	234.9±0.6	276.5±4.0
AC-OLA3	235±0.7	275.9±2.4	326.1±0.4	183.3±27	228.6±1.7	282.7±4.0
AC-OLA4	232.5±2.8	258.6±3.6	----			260.6±6.4
AC-OLA5	233.3±2.4	256±3.3	----	212.9±1.5	222.9±1.6	260.6±3.2
AC-OLA6	228.1±5.5	266±4.4	309.7±5.2	208.8±1.4	223.5±3.1	269.4±4.4
AC-OLA7	238.6±3.2	277.9±5.2	350.2±2.4	198.7.6±4.8	221±6.7	283±5.2

Analyzing the T_{on} values on Table 24 it is possible to verify that all LA oligomers and co-oligomers present a similar thermal stability.

The thermal behaviors and thermal stabilities of products of chain extension were also evaluated by simultaneous thermal analysis. Figure 29 shows the thermogravimetric curves for LA oligomer (AC-OLA1) and products of chain extension with IPDI (AC-CE1) and HMDI (AC-CE 2). The thermogravimetric curves of the remaining chain extended oligomers are presented in Annex D. Table 25 presents the main temperatures obtained from the simultaneous thermal analysis.

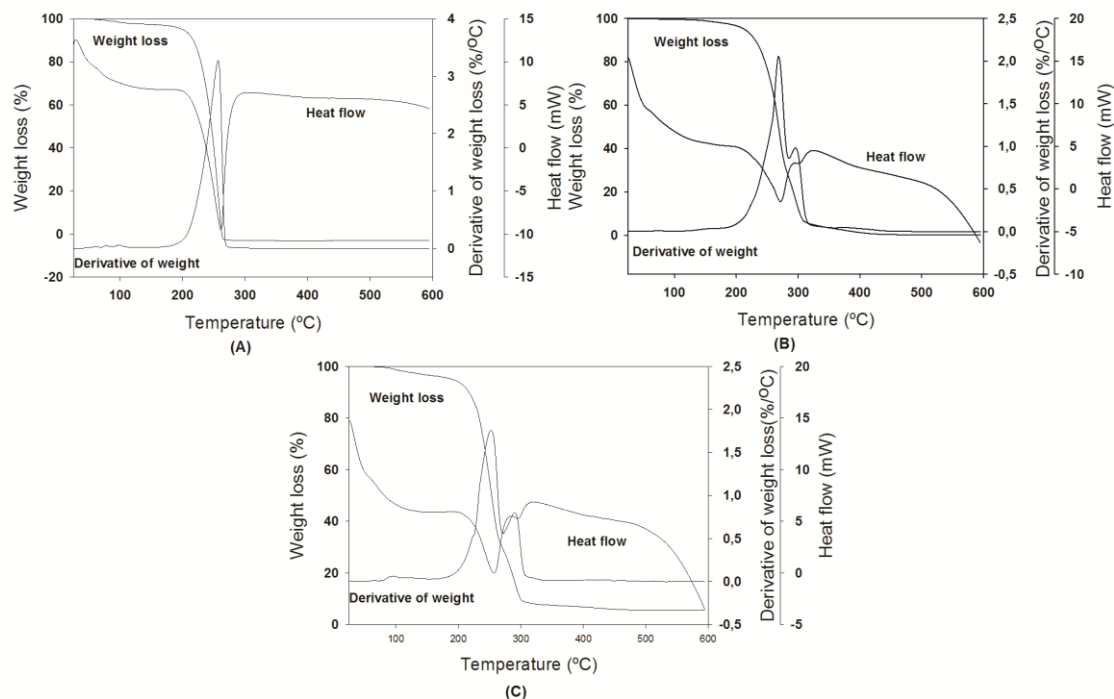


Figure 29 - Simultaneous thermoanalytical curves of LA oligomer and products of chain extension; (A) LA oligomer (AC-OLA1); (B) Product of chain extension (AC-CE1); (C) Product of chain extension (AC-CE2).

Through the Figure 29 it is possible observe that the LA oligomer (AC-OLA1) sample present one thermal degradation stage, while the products of chain extension (AC-CE1 and AC-CE2) exhibits two thermal degradation stages. The first thermal degradation stage can be attributed to the rupture of C-NH urethane bond and the second stage corresponds to the scission of the ester linkage at the alkyl-oxygen bond ^[62]. Similar weight loss curves were also observed for other products of chain extension synthesized from lactic acid oligomers with IPDI and HMDI [39, 62].

Table 25 - Characteristic temperatures (average) obtained from simultaneous thermal analysis for homopolymers and copolymers. T_{on} : extrapolated onset temperature (TG); $T_{5\%}$: temperature corresponding to 5% of mass loss; $T_{10\%}$: temperature corresponding to 10% of mass loss; T_p : peak temperature (DTG); T_d : degradation temperature.

Samples	T_{on1} (°C)	T_{on2} (°C)	T_{p1} (°C)	T_{p2} (°C)	T_{p3} (°C)	$T_{5\%}$ (°C)	$T_{10\%}$ (°C)	T_d (°C)
AC-CE1	242±4.1	----	274.2±8.0	298.6±3.2	----	231.6±0.5	231±0.5	276.8±6.8
AC-CE2	229.9±2.2	----	255.2±4.4	295.2±7.2	----	201.6±0.4	221.4±1.8	259.7±4.4
AC-CE3	237.8±2.6	----	158.8±3.6	268.8±5.2	307.1±7.2	223±2.0	238.6±3.7	271.1±5.2
AC-CE4	230.9±0.1	----	150.9±5.2	263.1±2.0	297.5±2.4	200.5±1.4	231.2±4.5	265±1.6
AC-CE5	252.2±0.1	----	288.9±0.0	393.9±5.6	----	231.5±2.8	252.2±0.9	287±1.2
AC-CE6	244.9±4.4	----	281.3±1.2	422.8±0.8	----	203.7±9.4	236.6±3.1	277±0.0
AC-CE7	227.2±4.8	----	152±3.5	254.1±6.0	293.8±8.2	182.7±24	218.7±11	258.3±5.6
AC-CE8	247.9±0.4	----	272.8±0.4	----	----	223.6±0.1	243.1±0.3	275.6±1.2
AC-CE9	230.8±0.8	----	257.3±0.2	279±0.4	----	201.1±1.9	215.8±1.6	261±1.2
AC-CE10								
AC-CE11	103.2±1.1	248±0.4	112±0.8	284.7±0.4	----	142±21.4	213±0.1	288±1.2
AC-CE12	68.9±1.3	245±2.7	76.9±0.0	273.1±0.8	313.6±6.8	75±3.2	86.9±3.5	277±0.8
AC-CE13	242.8±2.4	----	128.4±8.8	266.5±5.2	319.8±6.0	208±7.7	232.4±5.4	271±4.8
AC-CE14	244.5±0.6	----	262.9±1.6	326.1±0.4	----	213.4±5.4	236.4±2.8	266±1.2

Analyzing the Table 25 it is possible observe that for the samples that only present one T_{on} value the thermal stability is quite similar. For the samples that present two T_{on} values, the first value can be attributed to the evaporation of moisture present in the samples.

If one compares the thermal stability of the LA oligomers and co-oligomers (Table 24) with that of the chain extension products (Table 25), it is possible to see that the latter have values of T_{on} very close to that of the LA oligomers. This result is quite surprising, since chain extension contributes to an increase of molecular weight, and one should expect the thermal stability to increase as well. This fact can be related to the type of chain extenders used, that may contribute to a *premature* thermal degradation of the products of chain extension. Another reason may be related to the fact that the molecular weight has not increase sufficiently to promote significant differences in the thermal stability.

DSC

Figure 30 shows the DSC curves (second heating cycle) of the LA oligomers.

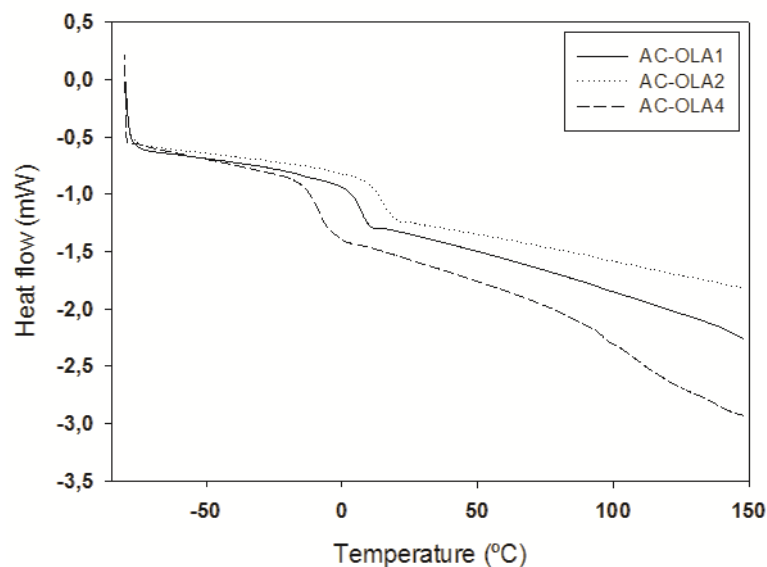


Figure 30 - DSC curves of the LA oligomers.

All the LA oligomers (AC-OLA1, AC-OLA2 and AC-OLA4) show a similar thermal behavior (Figure 30). For the three samples is only possible to verify one thermal event, a glass transition, revealing the amorphous character of the samples, which can be related with the low molecular weight of the samples.

Figure 31 presents the DSC curves obtained for the products of chain extension with the LA oligomer. The DSC curves of the remaining products of chain extension are presented in Annex E.

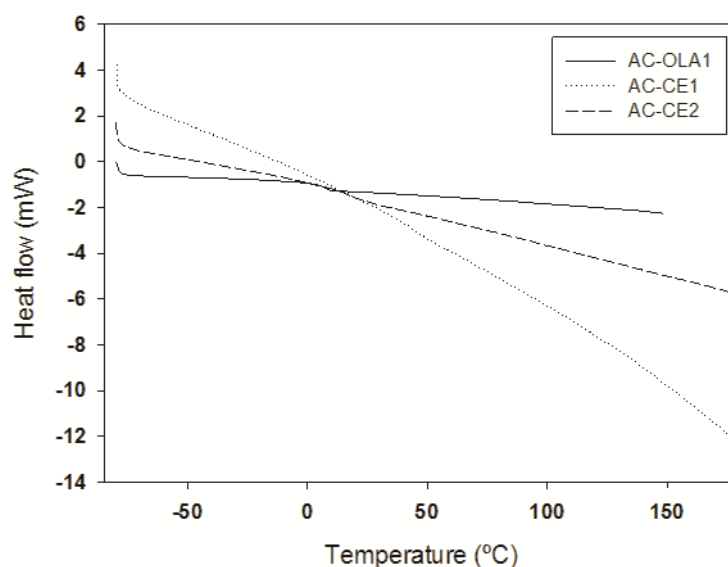


Figure 31 – DSC thermograms of LA oligomer and products of chain extension.

All the samples present a similar thermal behavior (Figure 31). The samples do not present a melting endotherm peak, indicating their amorphous character. In the case of product of chain extension with IPDI (AC-CE1), the introduction of the asymmetric IPDI which contains a hexamethyl ring and a methyl side group cause alterations the polymer structure and consequently disturb the samples crystallinity^[40]. In the case of HMDI, the reason behind the amorphous character of the sample, is not well clarified at the moment and no information on this matter is available in literature.

DMTA

Figure 32 shows the DMTA curves in glass transition zone obtained for the LA oligomers and co-oligomers. The DMTA curves of the remaining LA oligomers and co-oligomers are shown in Annex F.

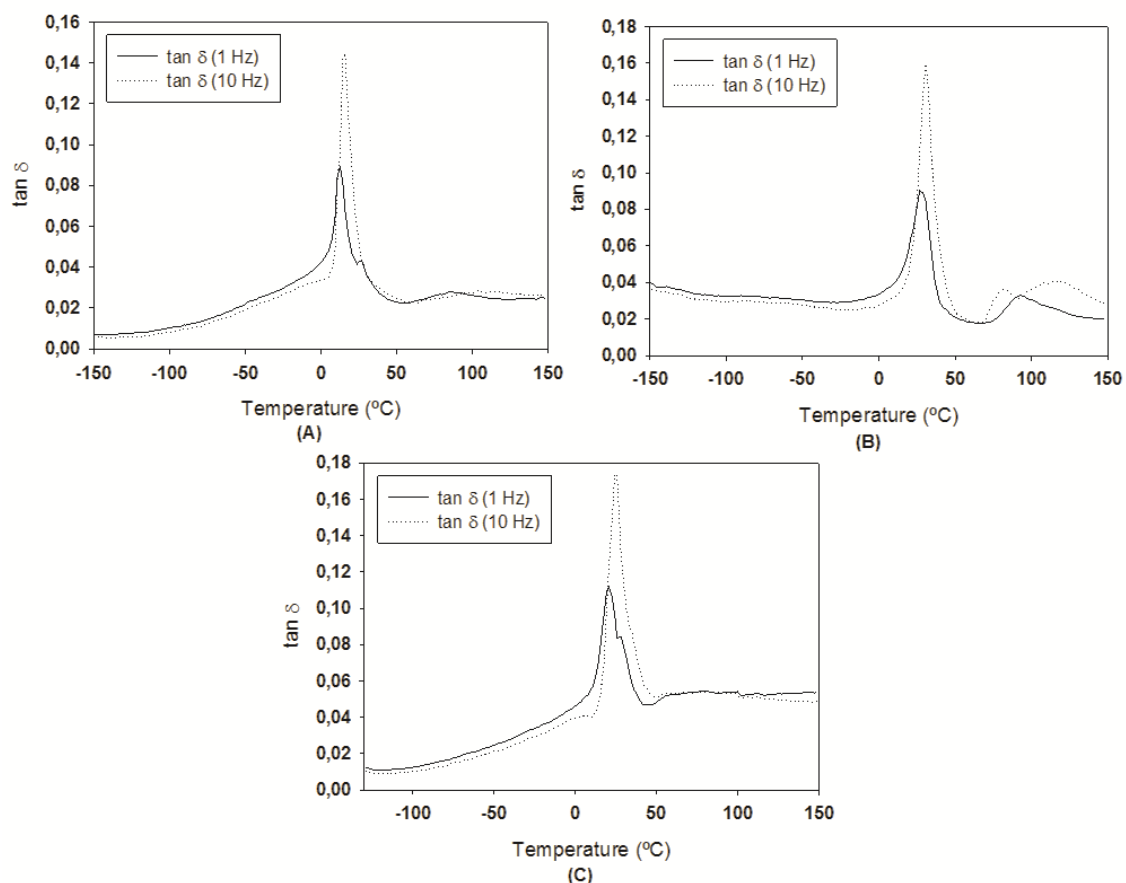


Figure 32 - DMTA traces (glass transition zone) of the LA oligomers. (A) LA oligomer (AC-OLA1); (B) O(LA-co-MA) (AC-OLA2); (C) O(LA-co-VA) (AC-OLA4), at two frequencies.

Analyzing Figure 32 it is possible to verify the peak corresponding to the T_g for the three samples. In the right side of the T_g peak it is possible to note a slight shoulder in the three samples, but at this moment it is not possible to advance with a plausible explanation for such behavior.

Table 26 presents the values of T_g obtained from the DMTA analysis.

Table 26 – T_g values for the LA oligomers obtained by DMTA.

Samples	T_g (°C)
AC-OLA1	12.6
AC-OLA2	26.9
AC-OLA3	22.3
AC-OLA4	20.6
AC-OLA5	50.5
AC-OLA6	62
AC-OLA7	46.2

Comparing the T_g values of the oligomers with lower molecular weight (AC-OLA 1, AC-OLA 2, AC-OLA3 and AC-OLA 4) with those from the oligomers of higher molecular weight (AC-OLA 5, AC-OLA 6 and AC-OLA7), it is possible to see that the former group of oligomers has lower T_g values, which is in accordance with their lower values of molecular weight. Interesting to note that the oligomers presenting the aromatic rings in the structure (AC-OLA 2, AC-OLA 3, AC-OLA 4, AC-OLA 6 and AC-OLA 7) have a higher T_g value than the oligomers containing only LA (AC-OLA 1 and AC-OLA5). This is due to the stiffening effect provided by the aromatic rings presented in the structure of MA and VA.

Figure 33 present the DMTA traces for the LA oligomer AC-OLA 1 and products of chain extension (AC-CE 1 and AC-CE 2).

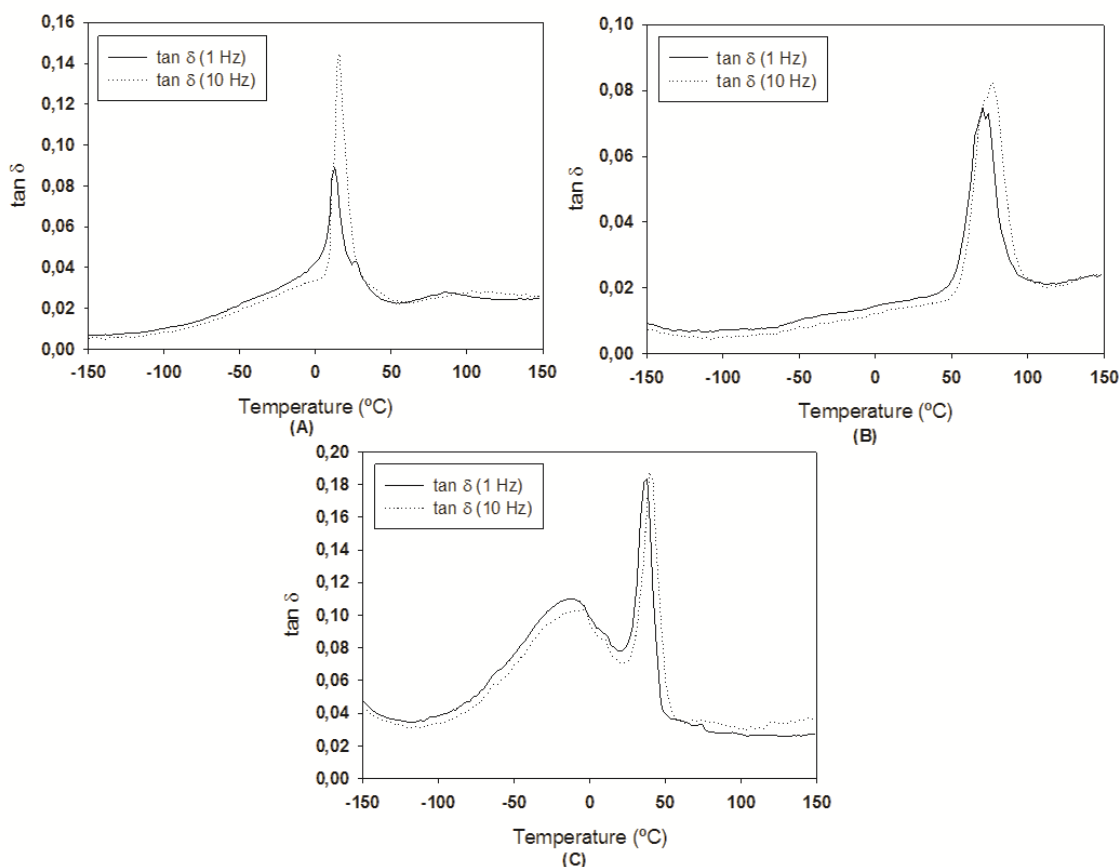


Figure 33 - DMTA traces (glass transition zone) of products of chain extension. (A) LA oligomer (AC-OLA1); (B) product of chain extension with IPDI (AC-CE1); (C) product of chain extension with HMDI (AC-CE2), at two frequencies.

Figure 33 presents the variation of the $\tan \delta$ with the temperature for the products of chain extension. It is possible to verify that the three samples present the peak corresponding to the

T_g . In AC-OLA1 and AC-CE1 it is possible to note a shoulder at the right of the T_g peak. As seen above, this is an unexpected outcome and no reasonable explanation can be given at the moment. In the AC-CE2 sample it is possible to note an additional defined peak at the left of the T_g peak. This peak is related to β -relaxation (second relaxation) and can be ascribed to local movements of the polymer main chain or lateral groups movements or rotation/vibration of terminal groups ^[60].

The T_g values of the products of chain extension obtained from the DMTA are summarized in Table 27.

Table 27 - T_g values for the products of chain extension obtained by DMTA.

Samples	T_g (°C)
AC-CE1	70.2
AC-CE2	41.8
AC-CE3	63.8
AC-CE4	50.2
AC-CE5	84
AC-CE6	57.3
AC-CE7	37.4
AC-CE8	76.4
AC-CE9	64
AC-CE10	52
AC-CE11	49.9
AC-CE12	63.9
AC-CE13	59.5
AC-CE14	55.8

Table 27 shows that products of chain extension exhibits a higher T_g values than its corresponding oligomer, which can be a direct consequence of the increase in molecular weight. Additionally, the increase in T_g can also be explained presence of urethane group, that confer some rigidity to the polymer chain ^[59, 63].

The chain extension products where HMDI was used as a chain extender lead to lower T_g values, when compared to the T_g of the products chain extended with IPDI. The aliphatic methylene groups present in the HMDI structure increase the chain flexibility and mobility leading a decrease in T_g values, whereas the cyclic structure of IPDI contributes to the increase in chain stiffness ^[41, 61].

5 Final remarks

5.1 Conclusions

In the past few years, the scientific community has sorely concentrated its research on the study of biodegradable polymers that could replace petroleum-based polymers in various applications. The use of biodegradable polymers has become one of the most important challenges of our society on the 21st century and should systematically be integrated in the design of new plastic products by industrial companies.

PLA is a biodegradable polymer that has attracted particular attention to replace the petroleum-based polymers due to its good properties. However, PLA present some poor features that have leaded the researchers to develop different PLA modifications, to make it suitable for a wider range of applications.

In this work, the main objective was the development of PLA copolymers with MA and VA, in view of improving some of the properties of PLA (e.g., thermo-mechanical) homopolymer.

The first part of the work concerned the development of PLA homopolymers and PLA copolymers with MA and VA by direct polycondensation, in order to evaluate the structure/properties relationships of the homopolymers and copolymers. The structural analysis indicated that the main functional group, ester group, was present in the PLA homopolymers and copolymers. Also the ¹H NMR revealed that almost all the co-monomer used in the feed was quantitatively incorporated in the final copolymer. The results obtained for the MWD analysis showed that the PLA copolymers have a lower molecular weight than the homopolymers, which can be due to the different reactivities of the monomers used. The SDT analysis indicated that the introduction of aromatic compounds in copolymers structure increases their thermal stability. The DSC results showed that PLA homopolymers present a semi-crystalline character and the copolymers exhibit an amorphous character. Through the DMTA analysis it was possible verify that the PLA homopolymers have a higher T_g than the PLA copolymer, most probably because the latter have a lower molecular weight when compared with the homopolymers.

In the second part of the work, chain extension reactions of LA oligomers and LA copolymers reactions with IPDI and HMDI were performed, in order to obtain polymers with high

molecular weight. The structural analysis showed that the chain extension was successful, even though the molecular weight obtained was not as high as one would expect. This result can be a consequence of the stoichiometric unbalance during the reaction. Comparing the thermal stabilities of L-LA (co-) oligomers and products of chain extension, it was possible to verify that the products of chain extension have similar values to the L-LA oligomers. The DSC analysis showed that both L-LA oligomers and products of chain extension present an amorphous character. The obtained results of DMTA proved that the products of chain extension present a higher T_g which can be a direct consequence of the increase in molecular weight.

To sum up, this work allowed the development of new PLA copolymers with co-monomers from renewable origin. Although some improvements are still needed to further increase the molecular weight of the copolymers, the results obtained during this work showed that this should be an area which is worth continuing to investigate.

5.2 Future work

This work allowed exploring new formulations of PLA based polymers, by direct polycondensation method. Among several possibilities to continue on the work, those described below can be considered of particular relevance:

- Optimization of the direct polycondensation conditions (*e. g.* use of different natural monomers and percentage of added monomer, use of different catalysts, use of a system with vacuum), and also of the chain extension reactions, in order to obtain PLA based polymers with high molecular weight;
- Processing of the obtained polymers and evaluation of their mechanical properties (*e.g.*, tensile);
- Evaluation of the biodegradability of the PLA based polymers.

References

1. Siracusa, V., et al., *Biodegradable polymers for food packaging: a review*. Trends in Food Science & Technology, 2008. **19**(12): p. 634-643.
2. Madhavan Nampoothiri, K., N.R. Nair, and R.P. John, *An overview of the recent developments in polylactide (PLA) research*. Bioresource Technology, 2010. **101**(22): p. 8493-8501.
3. <http://en.european-bioplastics.org>. [cited 2012 15 November].
4. Razza, F. and F.D. Innocenti, *Bioplastics from renewable resources: the benefits of biodegradability*. Asia-Pacific Journal of Chemical Engineering, 2012. **7**: p. S301-S309.
5. *Biobased Packaging materials for food industry*. 2000. 136.
6. Luckachan, G.E. and C.K.S. Pillai, *Biodegradable Polymers- A Review on Recent Trends and Emerging Perspectives*. Journal of Polymers and the Environment, 2011. **19**(3): p. 637-676.
7. Maharana, T., B. Mohanty, and Y.S. Negi, *Melt–solid polycondensation of lactic acid and its biodegradability*. Progress in Polymer Science, 2009. **34**(1): p. 99-124.
8. Singh, B. and N. Sharma, *Mechanistic implications of plastic degradation*. Polymer Degradation and Stability, 2008. **93**(3): p. 561-584.
9. Shah, A.A., et al., *Biological degradation of plastics: a comprehensive review*. Biotechnol Adv, 2008. **26**(3): p. 246-65.
10. <http://greenanswers.com/>.
11. *Poly(lactic acid): Synthesis, Structures, Properties, Processing, and Applications*, ed. R. Auras, et al. 2010: John Wiley & Sons, Inc.
12. Vink, E.T.H., et al., *Applications of life cycle assessment to NatureWorks™ polylactide (PLA) production*. Polymer Degradation and Stability, 2003. **80**(3): p. 403-419.
13. Vink, E.T., et al., *The sustainability of NatureWorks polylactide polymers and Ingeo polylactide fibers: an update of the future*. Macromol Biosci, 2004. **4**(6): p. 551-64.
14. Gupta, A.P. and V. Kumar, *New emerging trends in synthetic biodegradable polymers – Polylactide: A critique*. European Polymer Journal, 2007. **43**(10): p. 4053-4074.
15. Lunt, J., *Large-scale production, properties and commercial applications of polylactid acid polymers*. Polymer Degradation and Stability, 1998. **59**: p. 145-152.
16. Wee, Y.-J., J.-N. Kim, and H.-W. Ryu, *Biotechnological production of lactic acid and its recent applications*. Food Technol. Biotechnol., 2006. **44**(2): p. 163-172.
17. Hyon, S.-H., K. Jamshidi, and Y. Ikada, *Synthesis of polylactides with different molecular weights*. Biomaterials, 1997. **18**: p. 1503-1508.
18. Mehta, R., et al., *Synthesis of Poly(Lactic Acid): A Review*. Journal of Macromolecular Science, Part C: Polymer Reviews, 2005. **45**(4): p. 325-349.
19. Ajoka, M., et al., *Basic properties of polylactic acid produced by the direct condensation polymerization of lactic acid*. Bull. Chem. Soc. Jpn., 1995. **68**: p. 2125-2131.
20. Kim, S.H. and Y.H. Kim, *Direct condensation polymerization of lactic acid*. Macromol. Symp., 1999. **144**: p. 277-287.
21. Chen, G.-X., et al., *Synthesis of high-molecular-weight poly(l-lactic acid) through the direct condensation polymerization of l-lactic acid in bulk state*. European Polymer Journal, 2006. **42**(2): p. 468-472.
22. Cheng, Y., et al., *Polylactic acid (PLA) synthesis and modifications: a review*. Frontiers of Chemistry in China, 2009. **4**(3): p. 259-264.
23. Auras, R., B. Harte, and S. Selke, *An overview of polylactides as packaging materials*. Macromol Biosci, 2004. **4**(9): p. 835-64.
24. Marques, D.A.S., et al., *Poly(lactic acid) Synthesis in Solution Polymerization*. Macromolecular Symposia, 2010. **296**(1): p. 63-71.

25. S.-I. Moon, et al., *Melt/solid polycondensation of L-lactic acid - an alternative route to poly(L-lactic acid) with high molecular weight*. *Polymer Degradation and Stability*, 2001. **42**: p. 5059-5062.
26. Stridsberg, K.M., M. Ryner, and A.-C. Albertsson, *Controlled Ring-opening polymerization - polymers with designed macromolecular architecture*.
27. Kohn, F.E., J.G.V. Ommen, and J. Feijen, *The mechanism of the ring-opening polymerization of lactide and glycolide*. *European Polymer Journal*, 1983. **19**: p. 1081-1088.
28. Rasal, R.M., A.V. Janorkar, and D.E. Hirt, *Poly(lactic acid) modifications*. *Progress in Polymer Science*, 2010. **35**(3): p. 338-356.
29. Dorgan, J.R., H. Lehermeier, and M. Mang, *Thermal and Rheological Properties of Commercial-Grade Poly(Lactic Acid)s*. *Journal of Polymers and the Environment*, 2000. **8**
30. Hiljanen-Vainio, M., T. Karjalainen, and J. Seppala, *Biodegradable lactone copolymers: Characterization and mechanical behaviour of ϵ -caprolactone and lactide copolymers*. *Applied Polymer Science*, 1996. **59**.
31. Grijpma, D.W. and A.J. Pennings, *Polymerization temperature effects on the properties of L-lactide and ϵ -caprolactone copolymers*. *Polymer Bulletin*, 1991. **25**: p. 335-341.
32. Storey, R.F. and T.P. Hickey, *Degradable polyurethane networks based on d,l-lactide, glycolide, ϵ -caprolactone, and trimethylene carbonate homopolyester and copolyester triols*. *Polymer*, 1994. **35**(4): p. 830-838.
33. Reed, A. and D. Gilding, *Biodegradable polymers for use in surgery — poly(glycolic)/poly(lactic acid) homo and copolymers: 2. In vitro degradation*. *Polymer*, 1981. **22**(4): p. 494-498.
34. Fukuzaki, H., et al., *Direct copolymerization of l-lactic acid with δ -valerolactone in the absence of catalysts*. *European Polymer Journal*, 1988. **24**(11): p. 1029-1036.
35. Buchholz, B., *Analysis and characterization of resorbable dl-lactide-trimethylene carbonate copolyesters*. *Journal of Materials Science: Materials in Medicine*, 1992.
36. Xiao, L., et al., *Polylactic acid based biomaterials synthesis modification and applications*. *Biomedical Science, Engineering and Technology*.
37. Fukuzaki, H., et al., *Synthesis of biodegradable Poly(L-lactic Acid-co-D,L-mandelic Acid with relatively low molecular weight*. *Makromol. Chem.*, 1989. **190**: p. 2407-2415.
38. Edlund, U. and A.C. Albertsson, *Polyesters based on diacid monomers*. *Advanced Drug Delivery Reviews*, 2003. **55**(4): p. 585-609.
39. Zeng, J.-B., et al., *A novel biodegradable multiblock poly(ester urethane) containing poly(l-lactic acid) and poly(butylene succinate) blocks*. *Polymer*, 2009. **50**(5): p. 1178-1186.
40. Sikorska, W., et al., *Synthesis and physicochemical properties of new (bio)degradable poly(ester-urethane)s containing polylactide and poly[(1,4-butylene terephthalate)-co-(1,4-butylene adipate)] segments*. *Polymer*, 2011. **52**(21): p. 4676-4685.
41. Touminen, J., J. Kylma, and J. seppala, *Chain extending of lactic acid oligomers. effect of 2,2-bis(2-oxazoline) on 1,6-hexamethylene diisocyanate linking reaction*. *Polymer*, 2002. **43**.
42. Touminen, J. and J.V. Seppälä, *Synthesis and characterization of lactic acid based poly(ester-amide)*. *Macromolecules*, 1999: p. 3530-3535.
43. Sheth, M., et al., *Biodegradable polymer blends of poly(lactic acid) and poly(ethylene glycol)*. 1996.
44. Jacobsen, S. and H.G. Fritz, *Plasticizing poly(lactide) - the effect of different plasticizers on the mechanical properties*. *Polymer*, 1999. **39**.
45. Peesan, M., P. Supaphol, and R. Rujiravanit, *Preparation and characterization of hexanoyl chitosan/polylactide blend films*. *Carbohydrate Polymers*, 2005. **60**(3): p. 343-350.
46. Gajria, A.M., et al., *Miscibility and biodegradability of blends of poly(lactic acid) and poly(vinyl acetate)*. *Polymer*, 1996. **37**.
47. Nijenhuis, A.J., et al., *High molecular weight poly(L-lactide) and poly(ethylene oxide) blends_ thermal characterization and physical properties*. *Polymer*, 1996. **37**: p. 5849-5857.

48. Ohkoshia, I., H. Abeb, and Y. Doib, *Miscibility and solid state structures for blends of poly((S)-lactide) with atactic poly((RS)-3-hydroxybutyrate)*. *Polymer*, 2000. **41**: p. 5985–5992.
49. Labrecque, L.V., et al., *Citrate esters as plasticizers for poly(lactic acid)*. *Polymer*, 1997. **66**: p. 1507-1513.
50. Martin, O. and L. Alvérous, *Poly(lactic acid) - plasticization and properties of biodegradable multiphase systems*. *Polymer*, 2001. **42**: p. 6209-6219.
51. Ren, Z., L. Dong, and Y. Yang, *Dynamic mechanical and thermal properties of plasticized poly(lactic acid)*. *Journal of Applied Polymer Science*, 2006. **101**(3): p. 1583-1590.
52. Boonfaung, P., P. Wasutchanon, and A. Somwangthanaroj, *Development of packaging film from bioplastic polylactic acid (PLA) with plasticizers*, in *Pure and Applied Chemistry International Conference 2011*.
53. Cheremisinoff., N.P., *Polymer characterization: laboratory techniques and analysis*. 1996, United States of America: United States of America.
54. Stuart, B., *Polymer Analysis*. 1st ed, ed. C. David J. Ando, Dartford, Kent, . 2003. 289.
55. Fonseca, A.C., et al., *Novel poly(ester amide)s from glycine and L-lactic acid by an easy and cost-effective synthesis*. *Polymer International*, 2013. **62**(5): p. 736-743.
56. Karikari, A.S., et al., *Influence of Peripheral Hydrogen Bonding on the Mechanical Properties of Photo-Cross-Linked Star-Shaped Poly(d,l-lactide) Networks*. *Biomacromolecules*, 2005. **6**(5): p. 2866-2874.
57. J., S. and L.T. E., *Modern Polyesters Chemistry and Technology of Polyesters and Copolyesters*, ed. J.W. Sons. 2003.
58. Nalbandi, A., *Kinetics of thermal degradation of polylactic acid under N₂ Atmosphere*. *Iranian polymer journal*, 2001. **10** (**6**): p. 371-376.
59. Kylma, J., M. Harkonen, and J.V. Seppala, *The modification of lactic acid based poly(ester urethanes) by copolymerization*. 1996.
60. Mendieta-Taboada, O., *Análise Dinâmico-mecânica: aplicações em filmes comestíveis*. *Quimica Nova*, 2008. **31**: p. 384-393.
61. Touminen, J., J. Kylma, and J. Seppala, *Chain extending of lactic acid oligomers. 2. Increase of molecular weight with 1,6-hexamethylene diisocyanate and 2,2'-bis (2-oxaline)*. *Polymer*, 2002. **43**: p. 3-10.
62. Hojabri, L., et al., *Synthesis and physical properties of lipid-based poly(ester-urethane)s, I: Effect of varying polyester segment length*. *Polymer*, 2012. **53**(17): p. 3762-3771.
63. Michell, R.M., et al., *Novel poly(ester-urethane)s based on polylactide: From reactive extrusion to crystallization and thermal properties*. *Polymer*, 2012. **53**(25): p. 5657-5665.

Annexes

A. FTIR analysis

PLA homopolymers and copolymers

Melt polycondensation

Erro! A origem da referência não foi encontrada. presents the FTIR spectra for PLA homopolymers (AC3 and AC4) and PLA copolymer (AC6) obtained by melt polycondensation, where it is possible observe the characteristic bands of main functional group, ester group, located among $1750\text{-}1725\text{cm}^{-1}$.

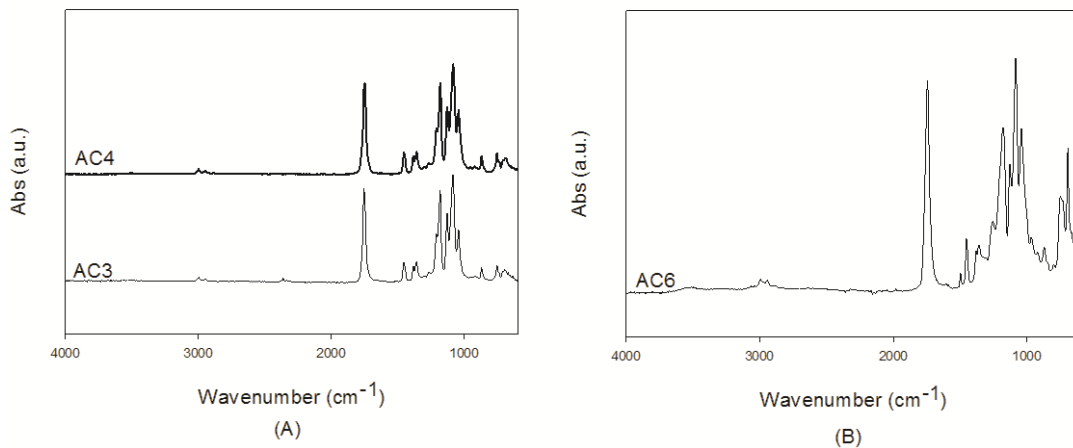


Figure A1 - FTIR spectra for PLA samples obtained by melt polycondensation; (A) PLA homopolymers; (B) PLA copolymer.

Through the **Erro! A origem da referência não foi encontrada.** (B) is not possible observe the characteristic bands of the aromatic ring ($1615\text{-}1580\text{ cm}^{-1}$) present in the mandelic acid (AC6).

Erro! A origem da referência não foi encontrada. summarizes the main bands present in the spectra of Figure A1 and respective assignments.

Table A1 - Main IR bands of PLA homopolymer and copolymers and respective assignments.

Samples	Infrared bands (cm^{-1})		
	ν -CH ₃ , -CH ₂ , -CH	ν C=O _{ester}	ν C-O-C _{ester}
AC3	2925-3052	1754	1085
AC4	2941-3026	1748	1083
AC6	2850-3127	1746	1085

Azeotropic dehydration condensation

FTIR spectra for PLA homopolymers (AC8.1 and AC9) and copolymers (AC10 and AC11.1) obtained by azeotropic dehydration condensation are shown in Figure A2.

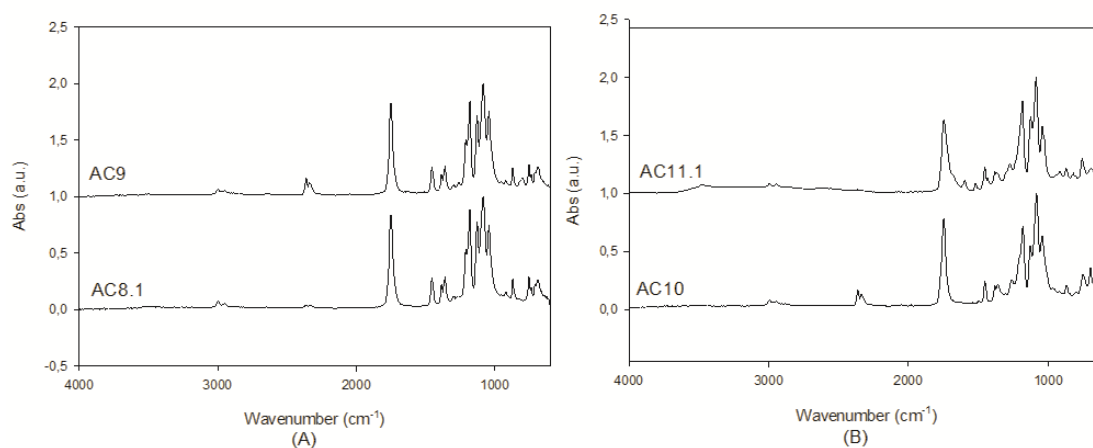


Figure A2 - FTIR spectra for PLA samples obtained by azeotropic dehydration condensation; (A) PLA homopolymers; (B) PLA copolymers.

It is possible to observe in Figure A3 the presence of the main characteristic band of ester group, situated among $1750\text{-}1725\text{cm}^{-1}$.

Table A2 summarizes the main bands present in the spectra of Figure A2 and respective assignments.

Table A2 - Main IR bands of PLA homopolymers and copolymers and respective assignments.

Samples	Infrared bands (cm^{-1})		
	ν -CH ₃ , -CH ₂ , -CH	ν C=O _{ester}	ν C-O-C _{ester}
AC8.1	2924-3034	1747	1084
AC9	2868-3029	1747	1084
AC10	2850-3080	1747	1083
AC11.1	2838-3043	1745	1086

PLA chain extension

Figure A3 shows the FTIR spectra of L-LA oligomers and co-oligomers with hydroxyl end groups and the corresponding products of chain extension with IPDI and HMDI.

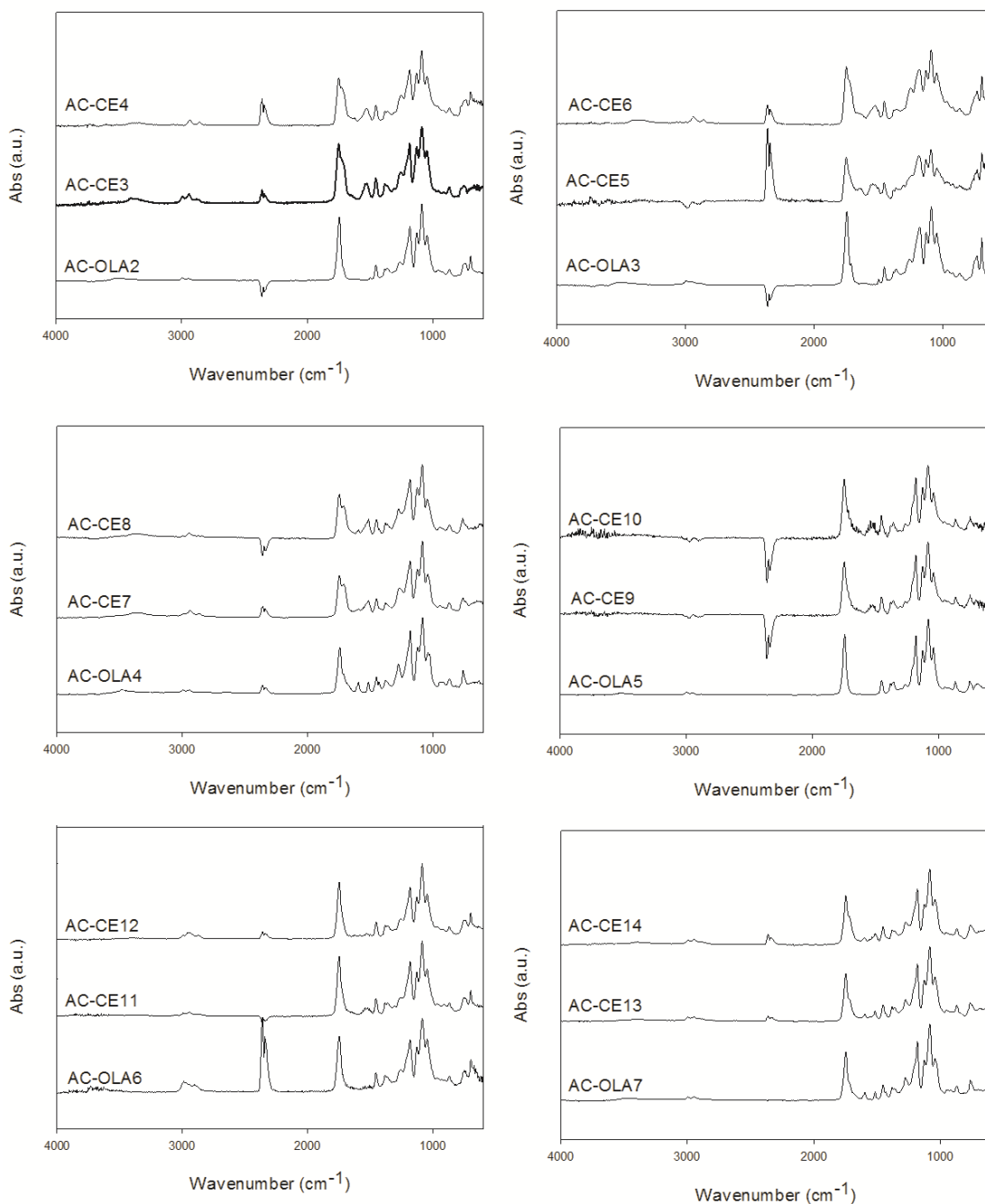


Figure A3 - FTIR spectra of the PLA oligomers and products of chain extension.

It is possible to observe in Figure A3 the main characteristic bands of the ester group, located among $1750\text{-}1725\text{cm}^{-1}$.

The Table A3 lists the other bands present in the PLA oligomers spectra of Figure A3 and respective assignments.

Table A3 - Main IR bands of PLA oligomers and respective assignments.

Samples	Infrared bands (cm ⁻¹)			
	$\nu_{\text{-CH}_3, \text{-CH}_2, \text{-CH}}$	$\nu_{\text{C=Oester}}$	$\nu_{\text{C-O-Cester}}$	$\nu_{\text{-OH}}$
AC-OLA2	2972-3019	1743	1085	3501
AC-OLA3	2890-3023	1743	1087	3515
AC-OLA4	2923-3018	1745	1085	3503
AC-OLA5	2936-3022	1745	1082	3505
AC-OLA6	2934-3006	1748	1083	3524
AC-OLA7	2917-3010	1747	1082	3513

The Table A4 summarizes the main bands present in products of chain extension spectra of Figure A3 and respective assignments.

Table A4 - Main IR bands of products of chain extension and respective assignments.

Samples	Infrared bands (cm ⁻¹)					
	$\nu_{\text{-NH}}$	$\nu_{\text{-CH}_3, \text{-CH}_2, \text{-CH}}$	$\nu_{\text{C=Oester}}$	$\nu_{\text{C=Ourethane}}$	$\nu_{\text{NH}} + \nu_{\text{CN}}$	$\nu_{\text{C-O-Cester}}$
AC-CE3	3303	2818-3038	1748	1731-1705 (sh)	1523	1085
AC-CE4	3302	2805-3027	1748	1734-1710 (sh)	1529	1087
AC-CE5	3305	2943-3073	1748	1739-1683 (sh)	1524	1090
AC-CE6	3301	2838-3114	1748	1740-1695 (sh)	1522	1088
AC-CE7	3306	2845-3013	1748	1737-1690 (sh)	1522	1086
AC-CE8	3305	2832-3014	1749	1739-1689 (sh)	1515	1087
AC-CE9	3305	2989-3168	1748	1744-1702 (sh)	1521	1085
AC-CE10	3305	2901-3009	1748	1741-1708 (sh)	1521	1085
AC-CE11	3307	2889-3008	1748	1740-1706 (sh)	1521	1084
AC-CE12	3303	2919-3027	1747	1739-1698 (sh)	1529	1084
AC-CE13	3303	2897-3013	1748	1738-1692 (sh)	1514	1083
AC-CE14	3305	2911-3016	1747	1737-1695 (sh)	1515	1083

B. ^1H NMR Analysis

PLA homopolymers and copolymers

Melt polycondensation

Figure B1 presents the ^1H NMR spectra of the PLA homopolymers and copolymer obtained by melt polycondensation.

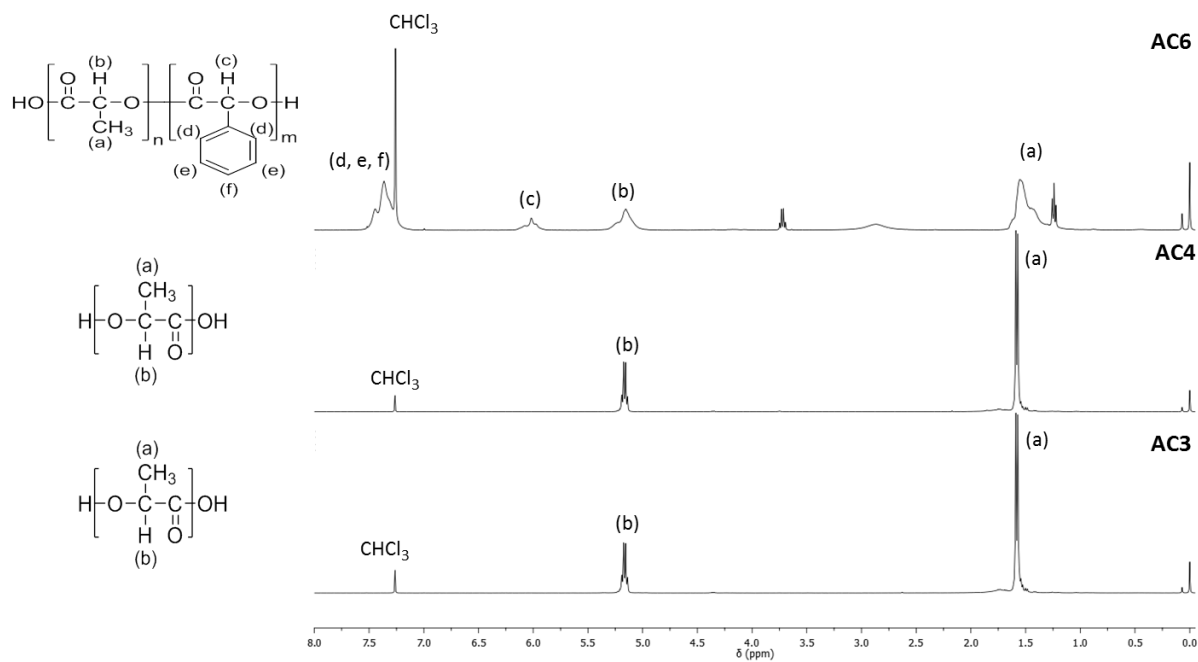


Figure B1 - ^1H NMR of the PLA homopolymers (AC3 and AC4) and copolymer (PLA-co-MA) (AC6).

Azeotropic dehydration condensation

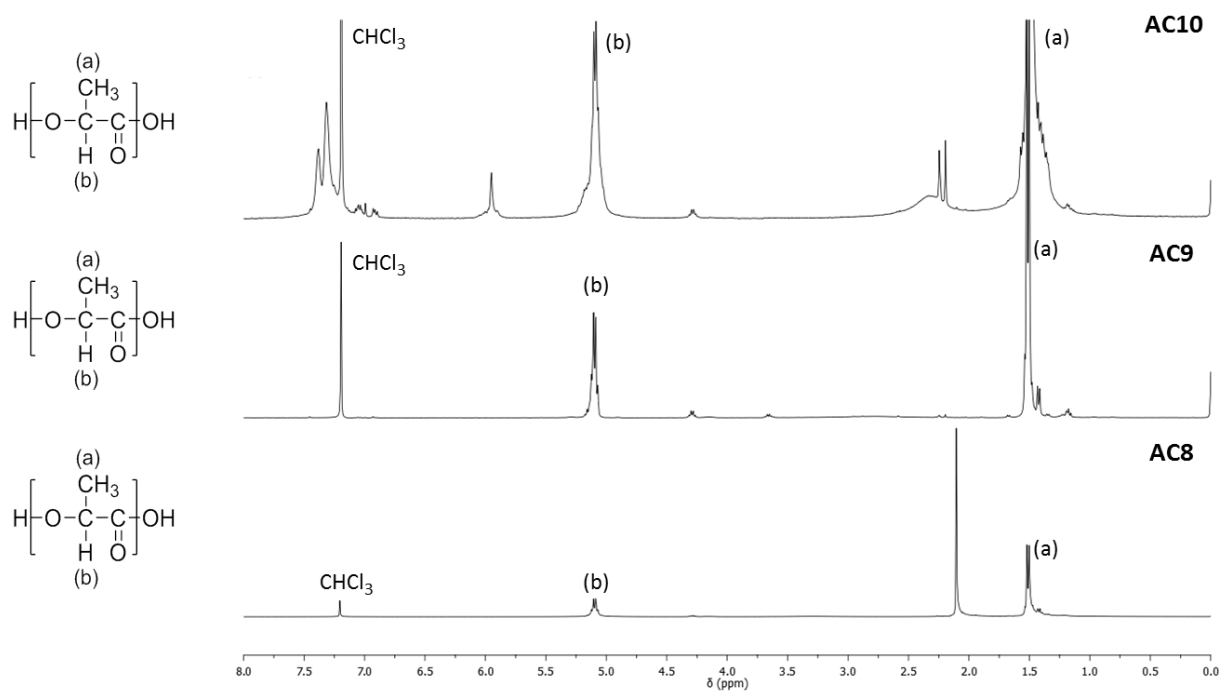


Figure B2 - ¹H NMR of the PLA homopolymers obtained by Azeotropic dehydration condensation

Chain extension

In order to clarify the structures of the LA oligomer (AC-OLA2) and products of chain extension (AC-CE3 and AC-CE4) it was performed a ^1H NMR analysis (Figure B3).

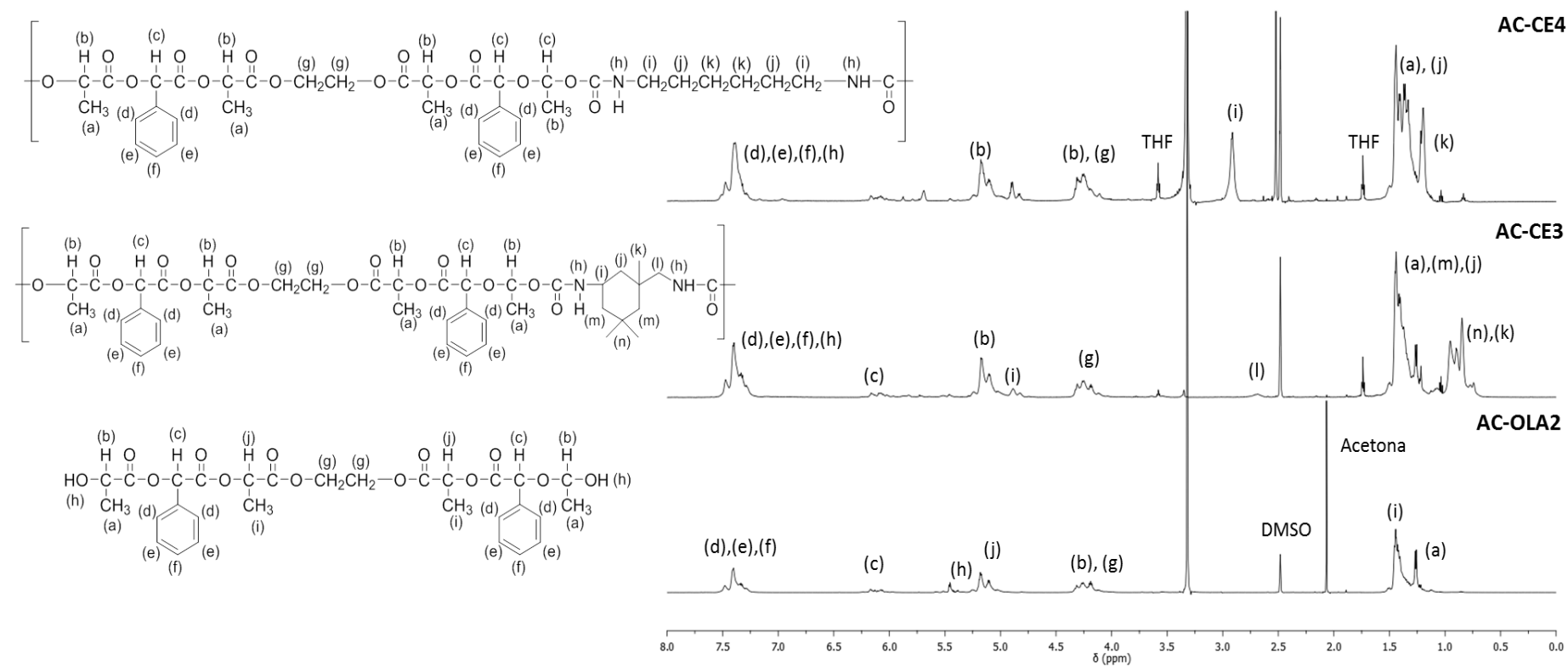


Figure B3 - ^1H NMR of the PLA oligomer (AC-OLA2) and products of chain extension (AC-CE3) and AC-CE4).

Figure B4 shows the ^1H NMR of the LA oligomer (AC-OLA3) and products of chain extension (AC-CE5 and AC-CE6) with IPDI and HMDI, respectively.

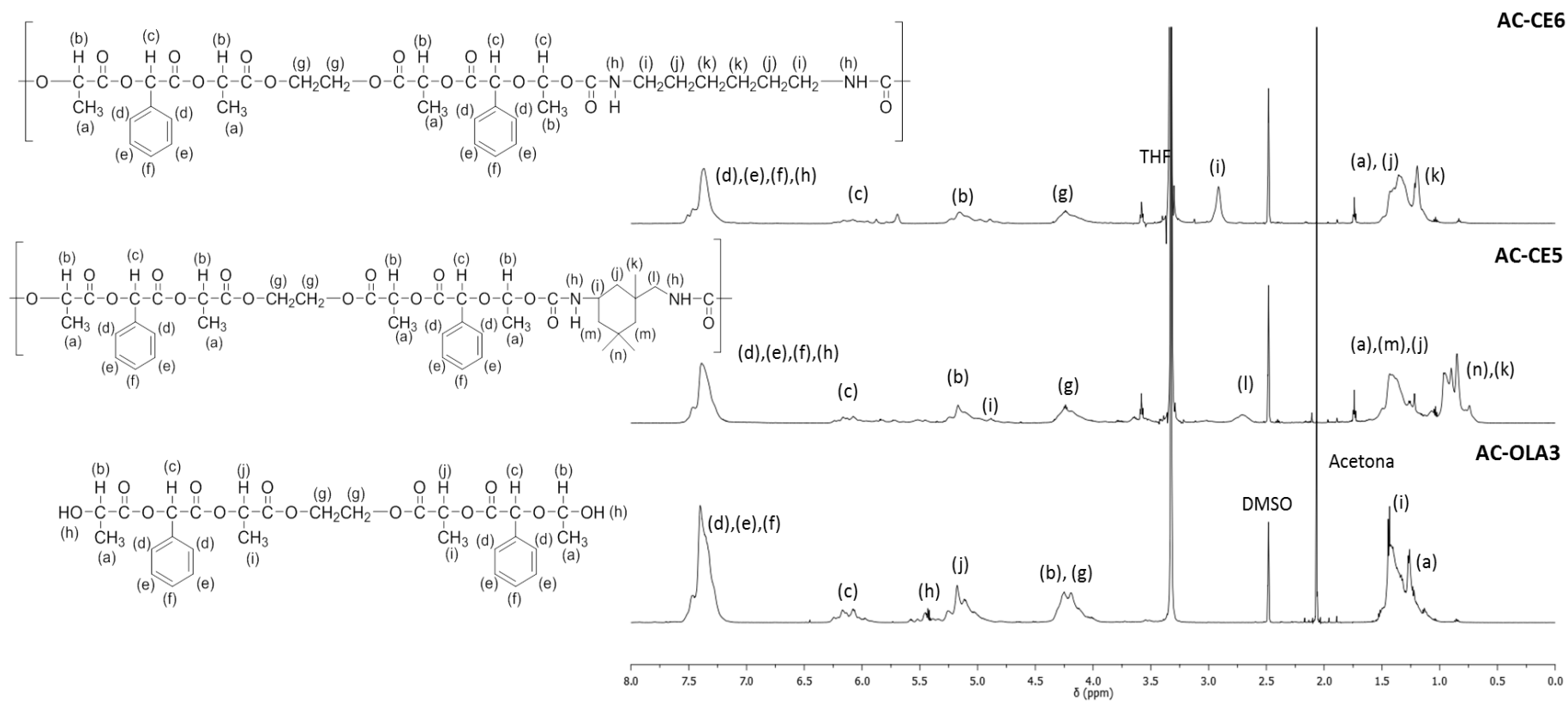


Figure B4 - ^1H NMR of the PLA oligomer (AC-OLA3) and products of chain extension (AC-CE5) and AC-CE6).

Figure B5 presents the ^1H NMR of the LA oligomer (AC-OLA4) and products of chain extension (AC-CE7 and AC-CE8) with HMDI and IPDI, respectively

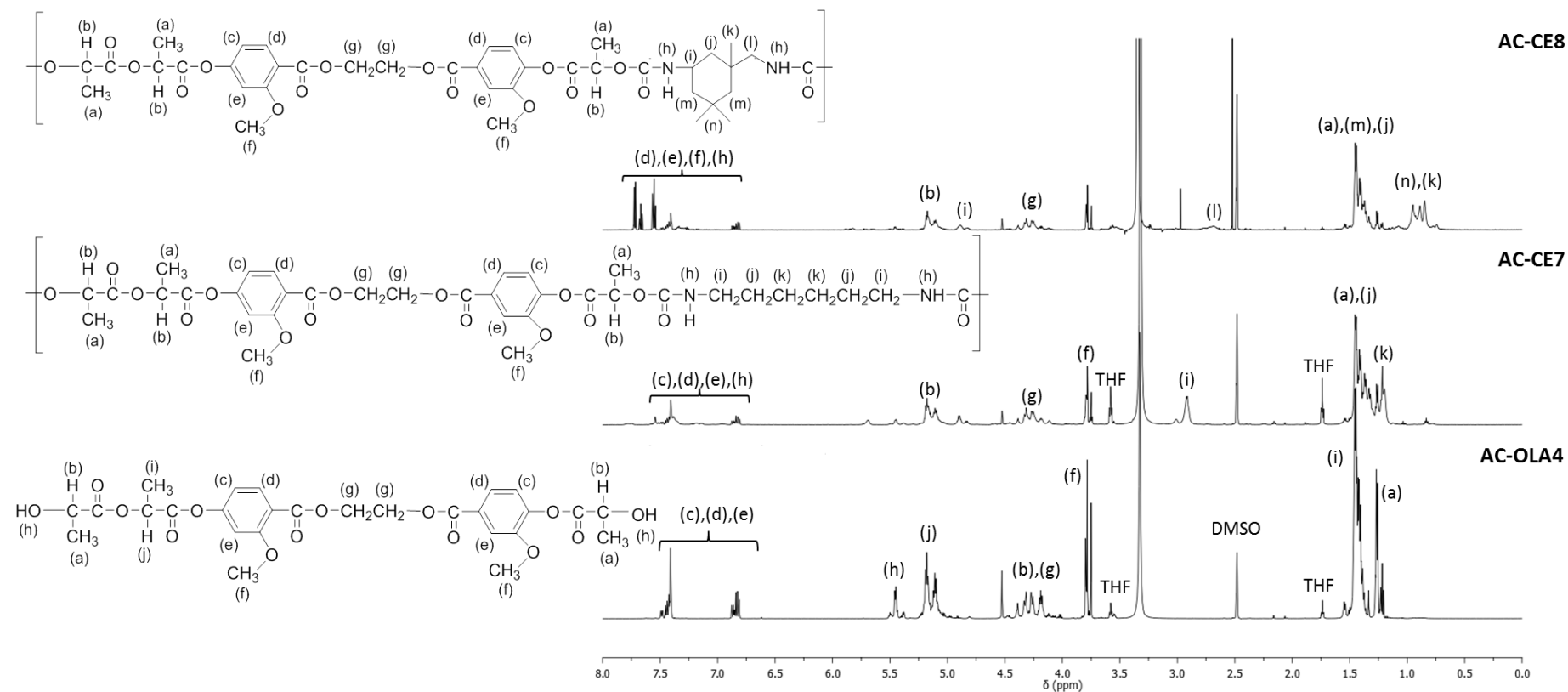


Figure B5 - ^1H NMR of the PLA oligomer (AC-OLA4) and products of chain extension (AC-CE7) and AC-CE8).

Figure B6 shows the ^1H NMR of the LA oligomer (AC-OLA5) and products of chain extension (AC-CE9 and AC-CE10) with IPDI and HMDI, respectively

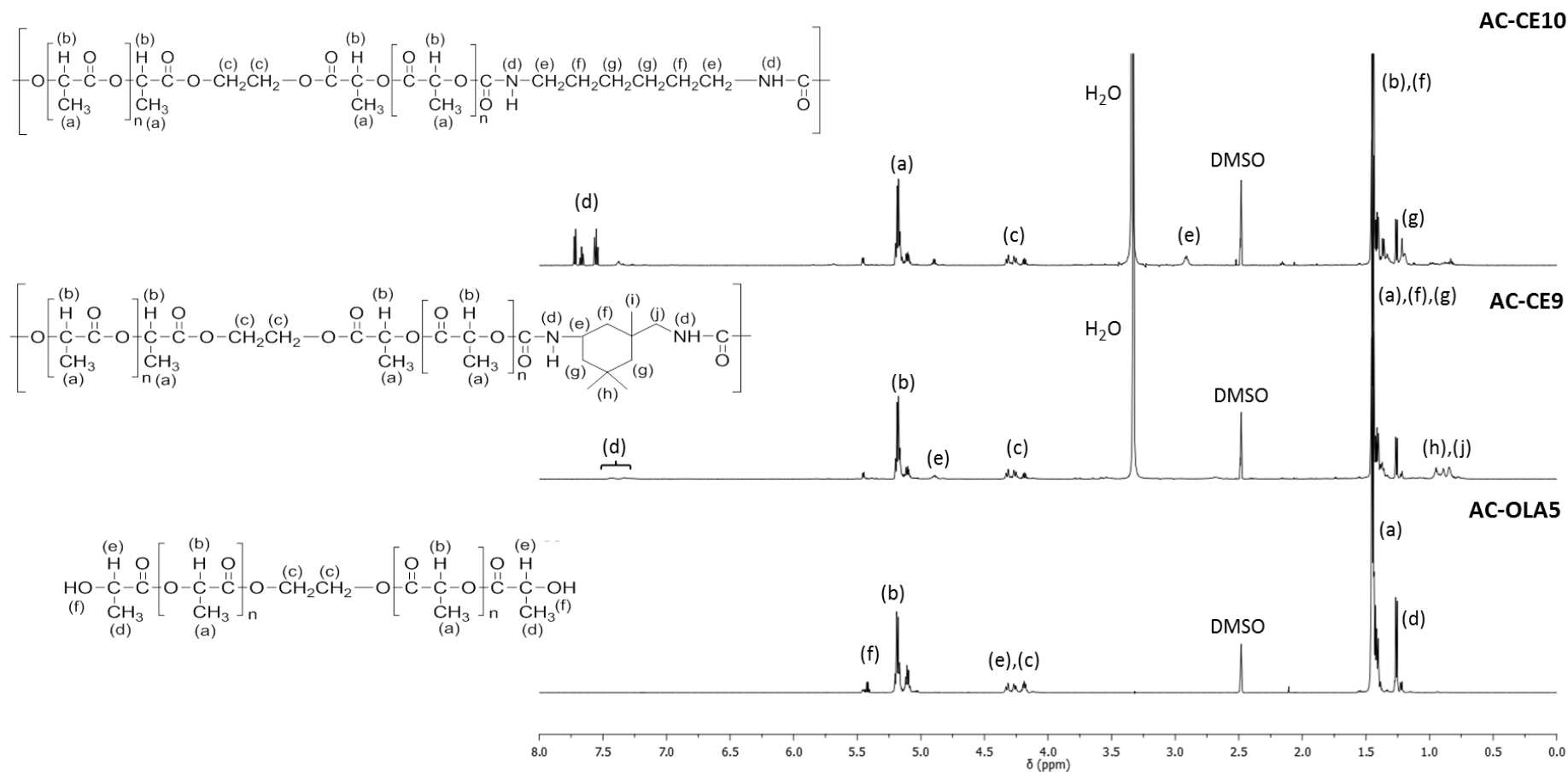


Figure B6 - ^1H NMR of the PLA oligomer (AC-OLA5) and products of chain extension (AC-CE9) and AC-CE10).

Figure B7 presents the ^1H NMR of the LA oligomer (AC-OLA6) and products of chain extension (AC-CE11 and AC-CE12) with IPDI and HMDI, respectively

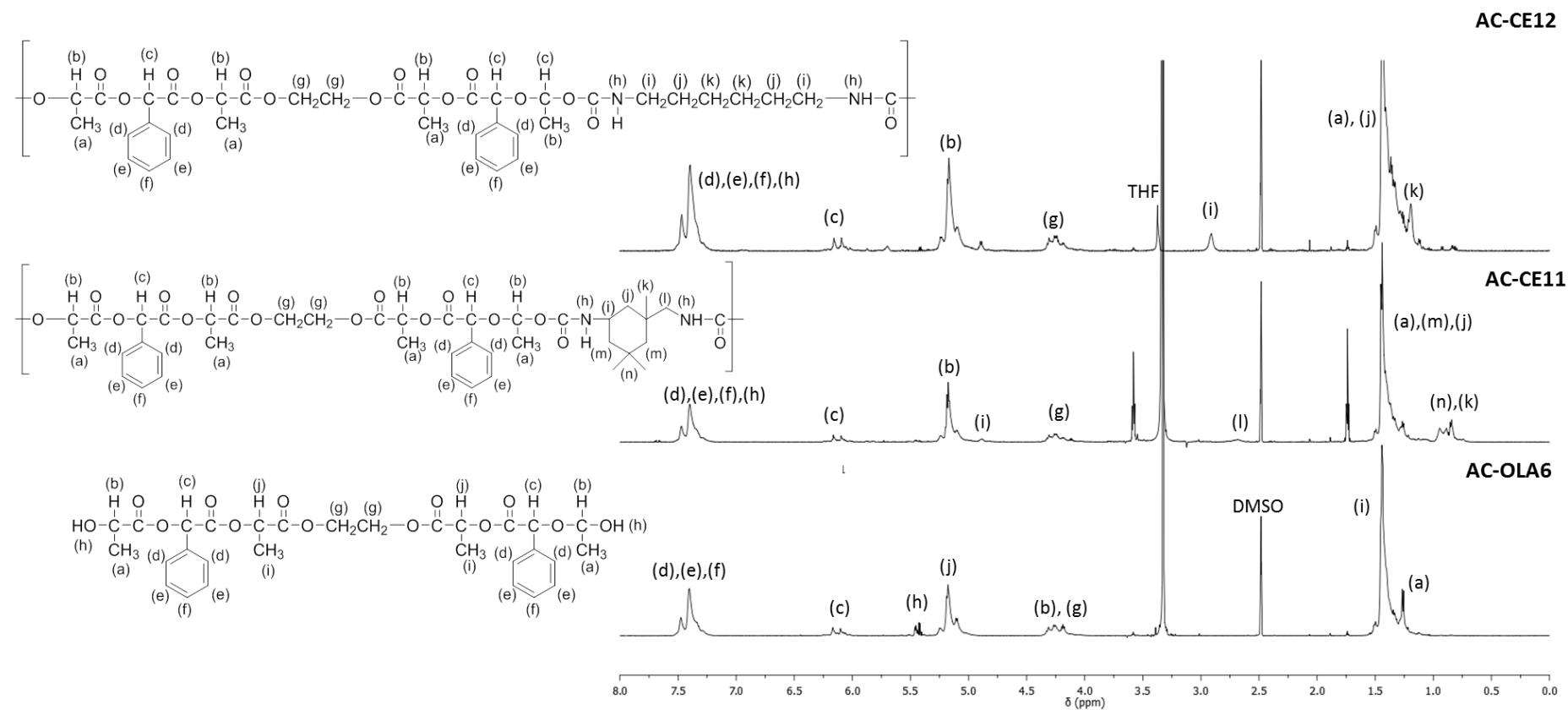


Figure B7 - ^1H NMR of the PLA oligomer (AC-OLA6) and products of chain extension (AC-CE11) and AC-CE12).

Figure B8 shows the ^1H NMR of the LA oligomer (AC-OLA7) and products of chain extension (AC-CE13 and AC-CE14) with IPDI and HMDI, respectively

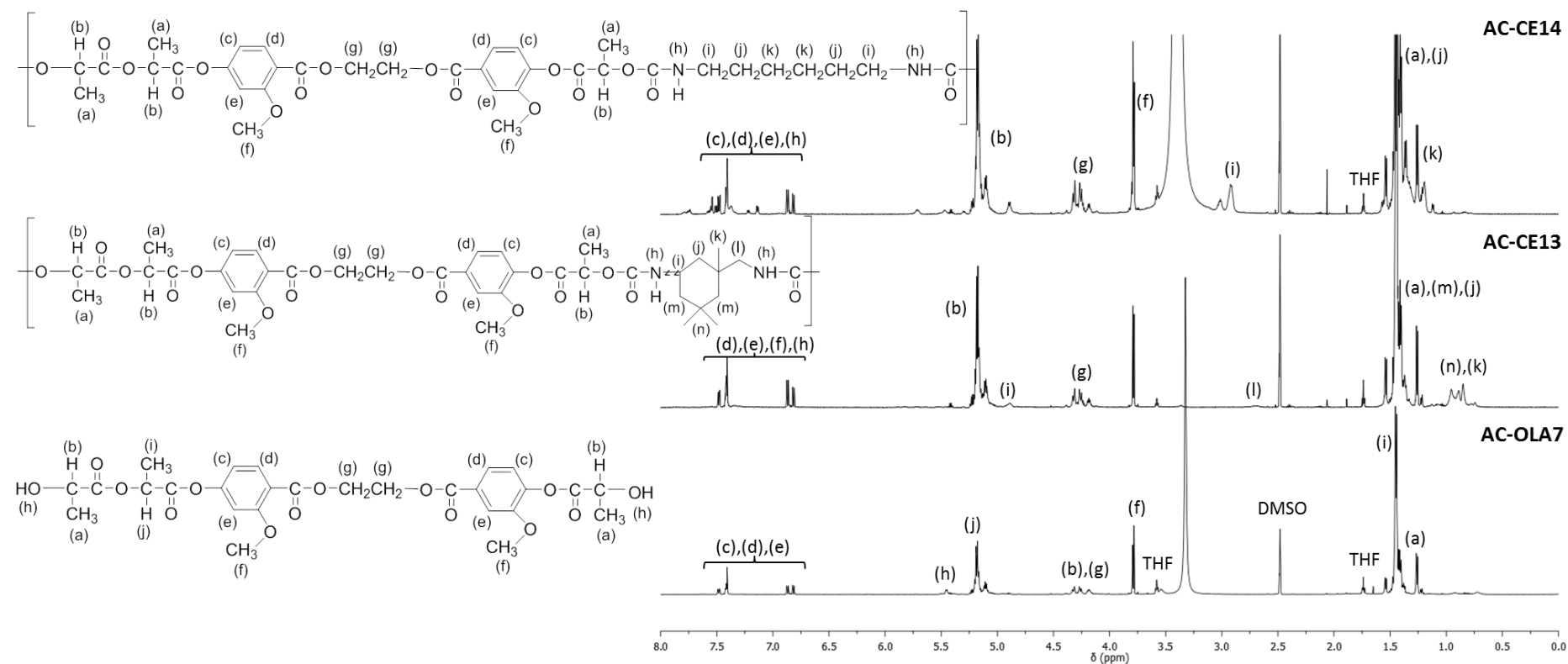


Figure B8 - ^1H NMR of the PLA oligomer (AC-OLA7) and products of chain extension (AC-CE13) and AC-CE14).

C. GPC Analysis

PLA homopolymers and copolymers

Melt polycondensation

Figure C1 shows the molecular weight distribution (MWD) of the PLA homopolymers (AC3 and AC4) and copolymers (AC6) measured by SEC, using the conventional calibration.

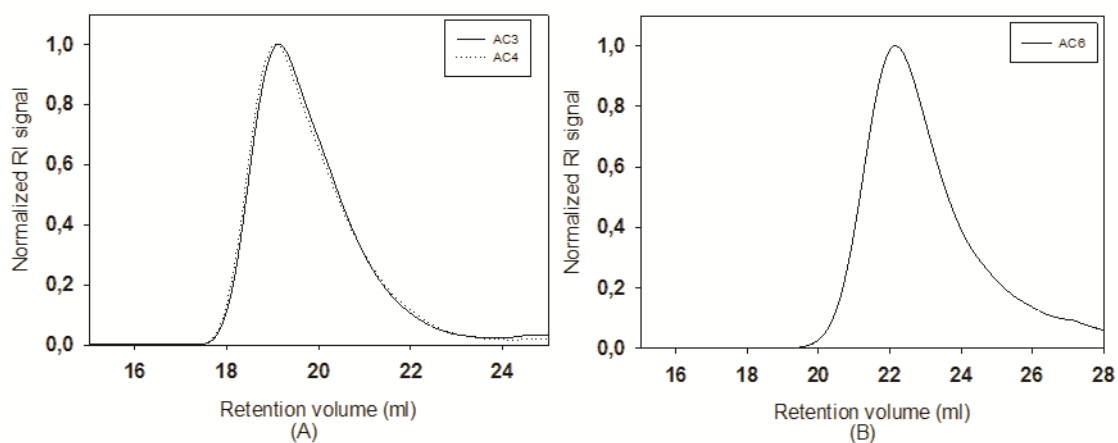


Figure C1- Normalized RI signal vs. retention volume for PLA samples obtained by melt polycondensation; (A) PLA homopolymers; (B) PL-co-MA.

Azeotropic dehydration condensation

Figure 18 presents the SEC trace (RI signal) for PLA homopolymer (AC9) and copolymer (AC10) obtained through azeotropic dehydration condensation.

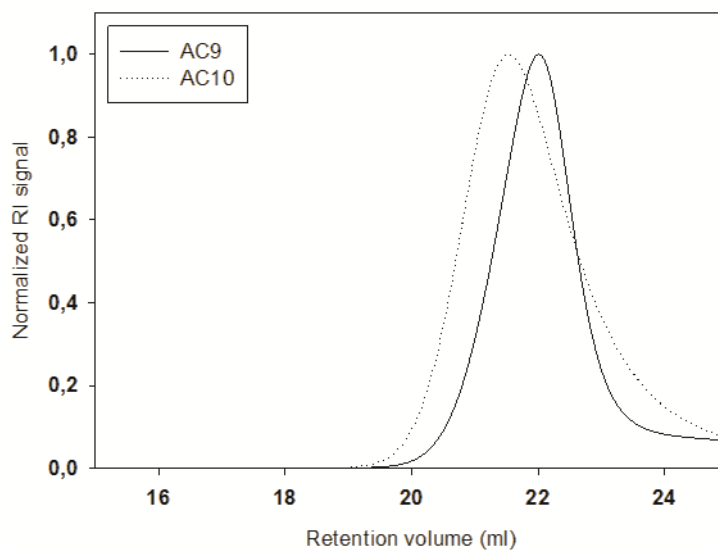


Figure C2 - Normalized RI signal vs. retention volume for PLA homopolymer and copolymer obtained by azeotropic dehydration condensation.

PLA chain extension

Figure C3 presents the SEC trace (RI signal) obtained for all the LA oligomers synthesized along the work and all the corresponding products of chain extension with IPDI and HMDI.

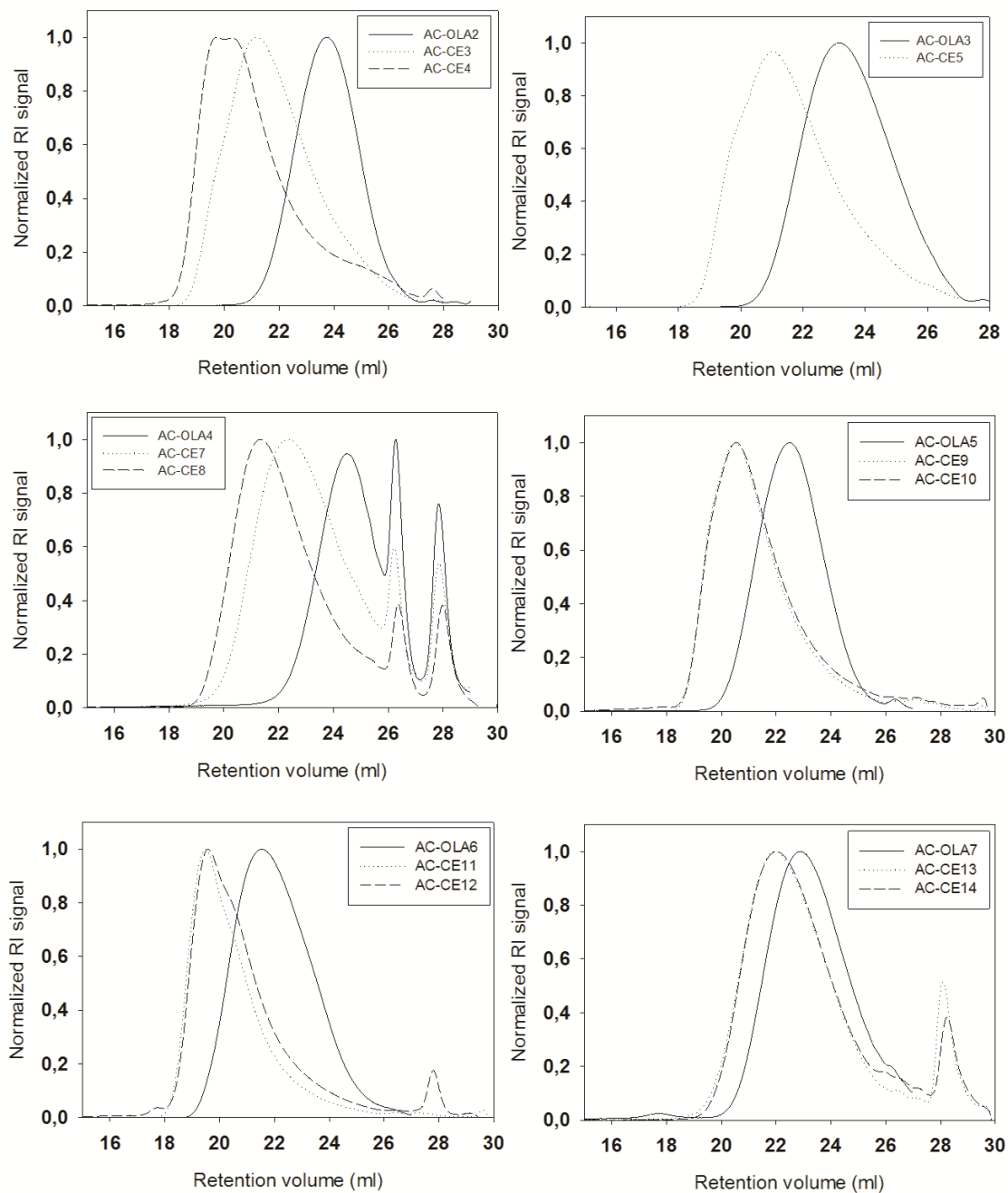


Figure C3 - Normalized RI signal vs. retention volume for LA oligomers and products of chain extension.

D. SDT Analysis

Monomers

Figure D1 shows the thermoanalytical curves of the monomer used in the PLA synthesis.

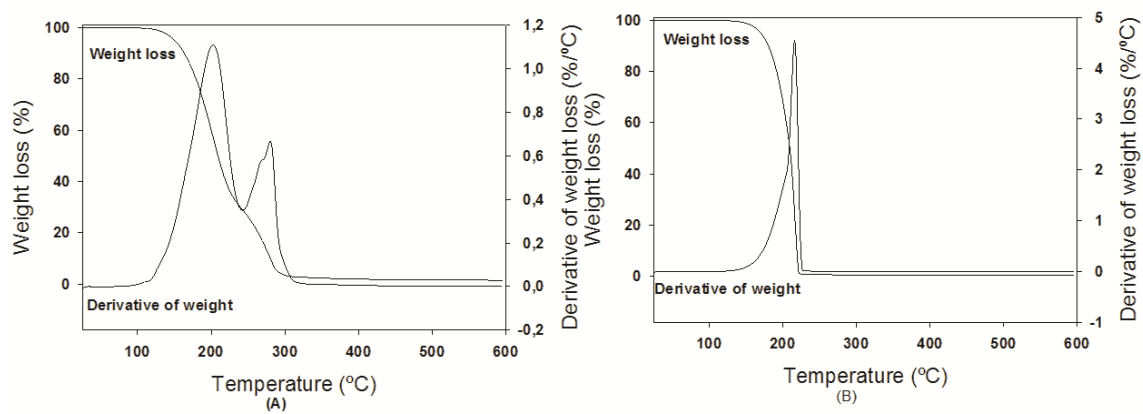


Figure D1 - Simultaneous thermoanalytical curves of monomers; (A) Mandelic acid; (A) Vanillic acid.

PLA homopolymers and copolymers

Melt polycondensation

The thermal behaviors and thermal stabilities of PLA homopolymers and copolymer obtained by melt polycondensation were determined by simultaneous thermal analysis (Figure D2).

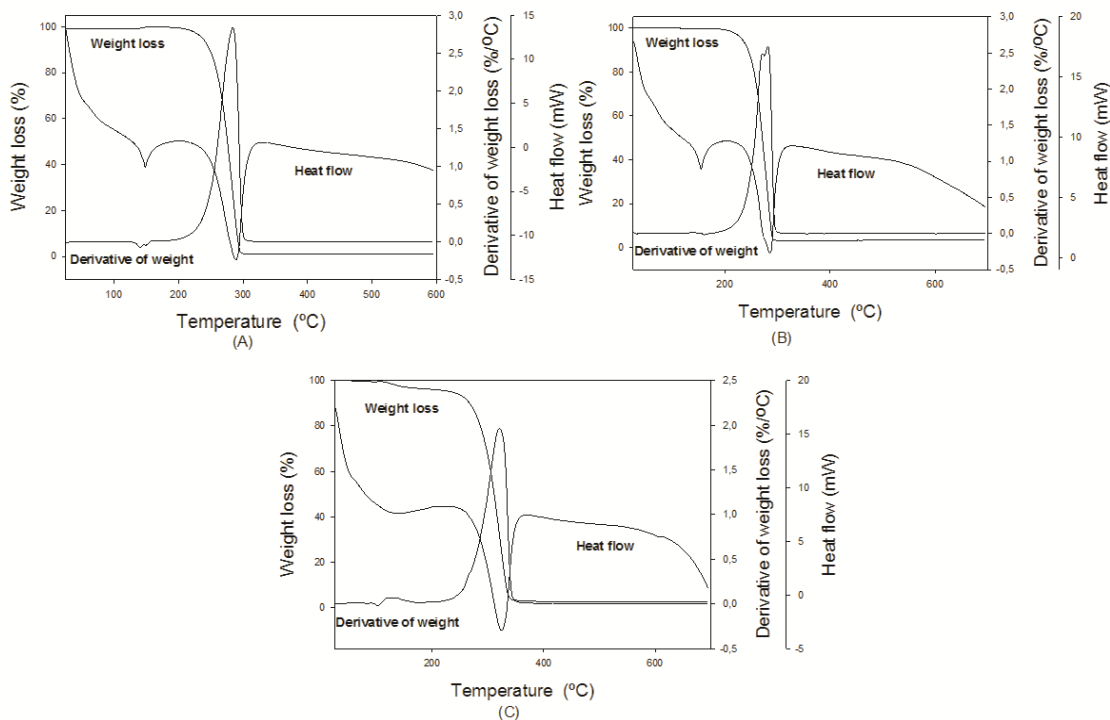


Figure D2 - Simultaneous thermoanalytical curves of PLA homopolymers and copolymers; (A) PLA homopolymer; (B) PLA homopolymer; (C) PLA-co-MA.

PLA chain extension

The thermal behaviors and thermal stabilities of products of chain extension were determined by simultaneous thermal analysis. Figure D3 gives the thermoanalytical curves for LA oligomer (AC-OLA2) and products of chain extension with IPDI (AC-CE 3) and HMDI (AC-CE 4).

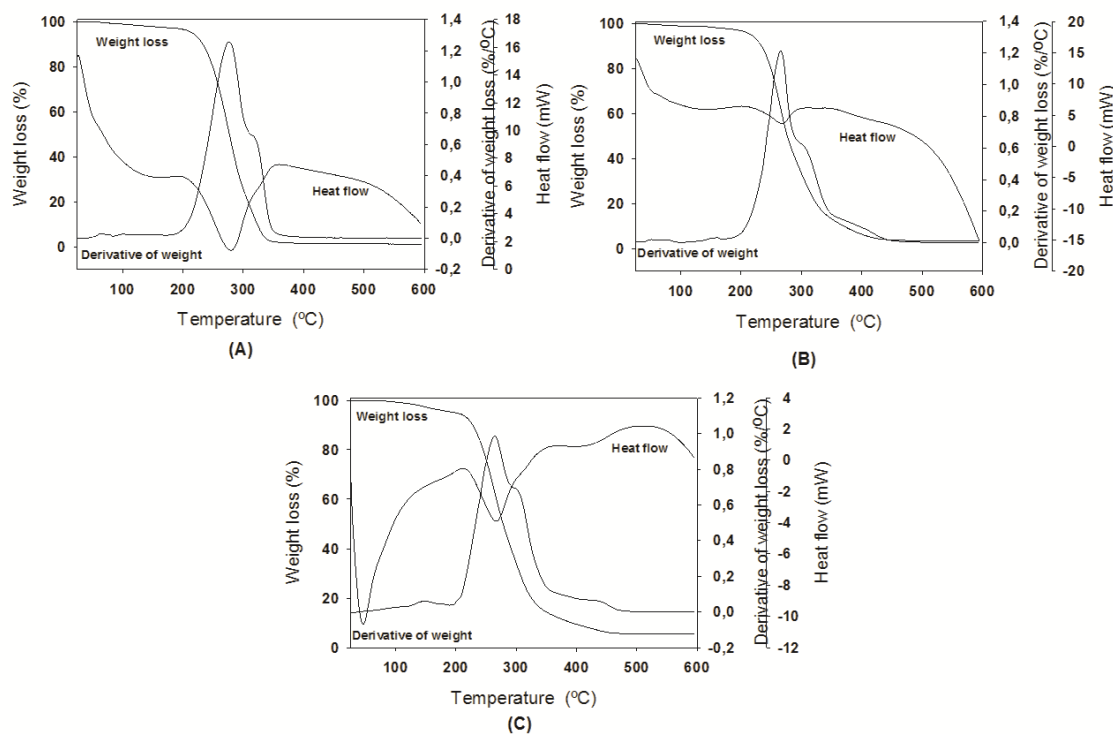


Figure D3 Simultaneous thermoanalytical curves of LA co-oligomer and products of chain extension; (A) OLA-co-MA (AC-OLA2); (B) Product of chain extension (AC-CE3); (C) Product of chain extension (AC-CE4)

Figure D4 gives the thermoanalytical curves for LA oligomer (AC-OLA3) and products of chain extension with IPDI (AC-CE 5) and HMDI (AC-CE 6).

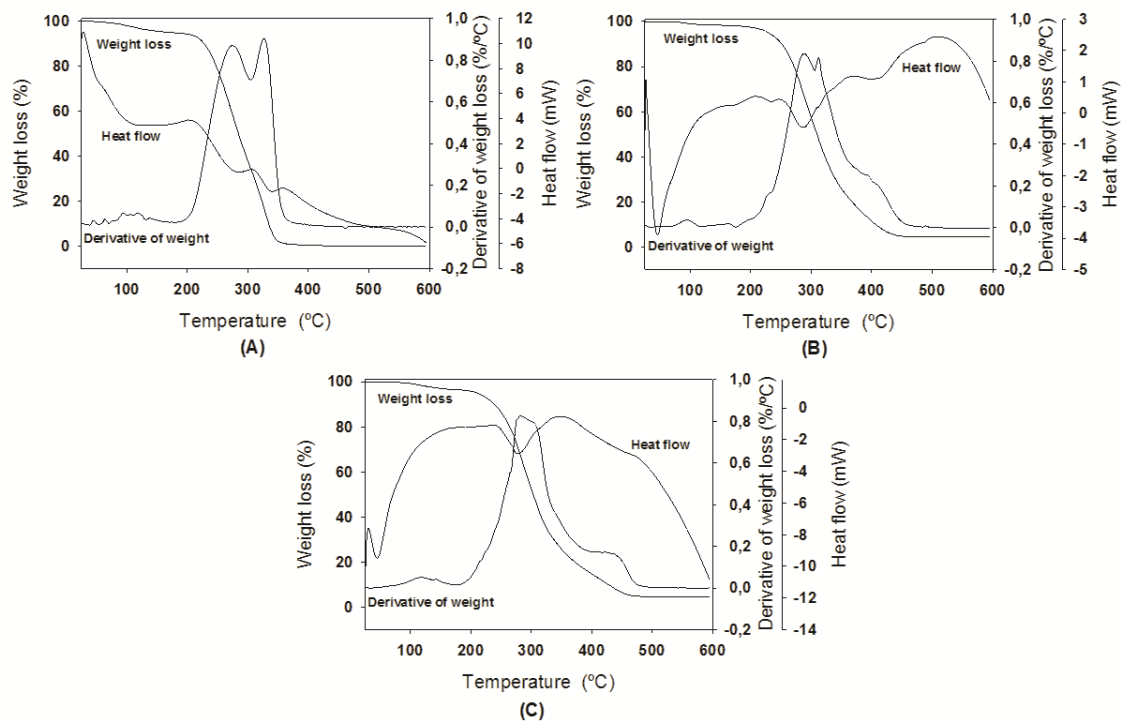


Figure D4 - Simultaneous thermoanalytical curves of LA co-oligomer and products of chain extension; (A) OLA-co-MA (AC-OLA3); (B) Product of chain extension (AC-CE5); (C) Product of chain extension (AC-CE6).

Figure D5 shows the thermoanalytical curves for LA oligomer (AC-OLA4) and products of chain extension with IPDI (AC-CE 7) and HMDI (AC-CE 8).

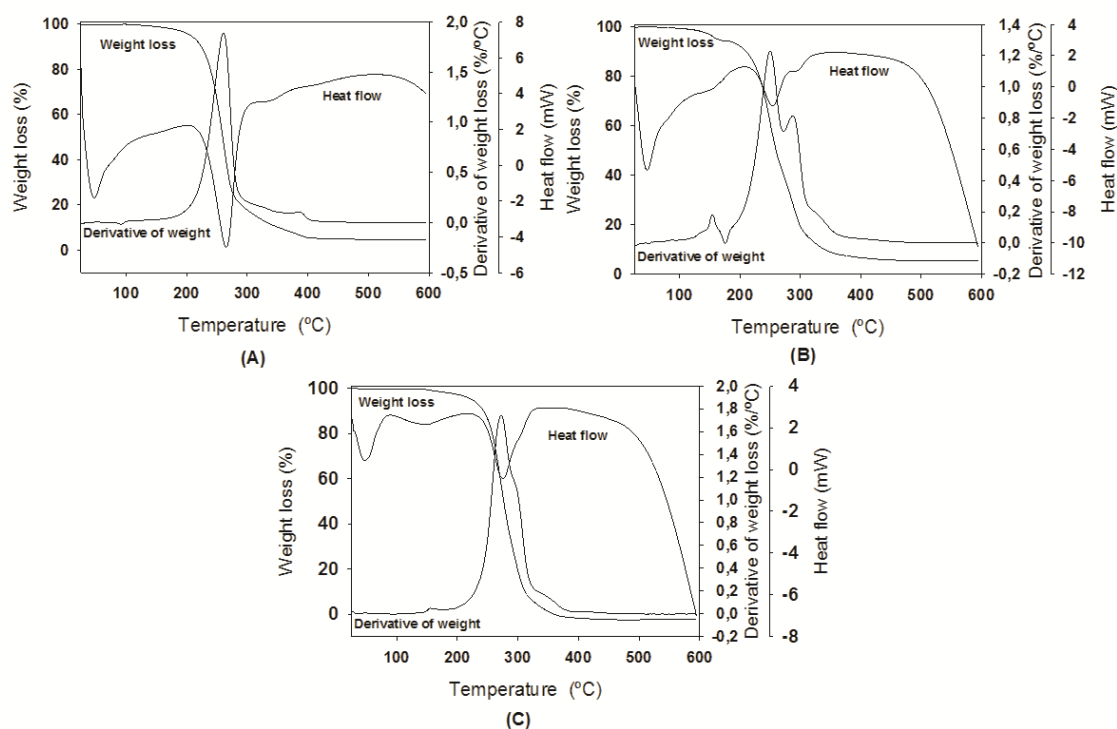


Figure D5 - Simultaneous thermoanalytical curves of LA co-oligomer and products of chain extension; (A) OLA-co-VA (AC-OLA4); (B) Product of chain extension (AC-CE7); (C) Product of chain extension (AC-CE8).

The thermoanalytical curves of LA oligomer (AC-OLA5) and products of chain extension with IPDI (AC-CE 9) and HMDI (AC-CE 10) are present in Figure D6.

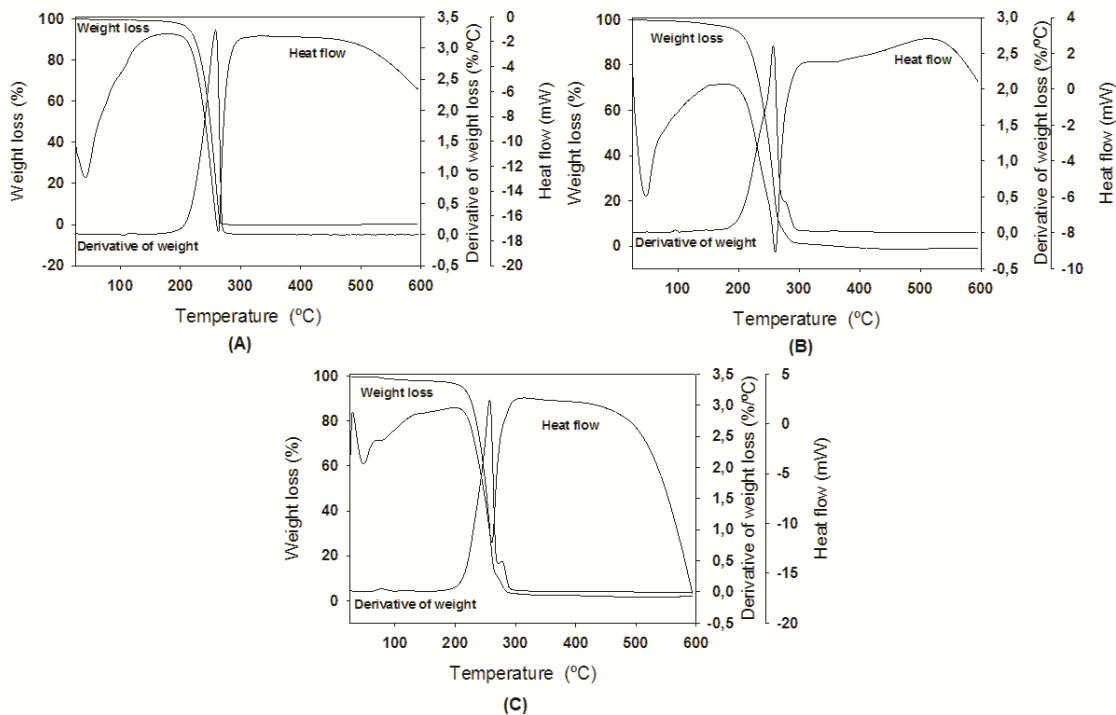


Figure D6 - Simultaneous thermoanalytical curves of LA oligomer and products of chain extension; (A) LA oligomer (AC-OLA5); (B) Product of chain extension (AC-CE9); (C) Product of chain extension (AC-CE10).

Figure D7 presents the thermoanalytical curves for LA oligomer (AC-OLA6) and products of chain extension with IPDI (AC-CE 11) and HMDI (AC-CE 12).

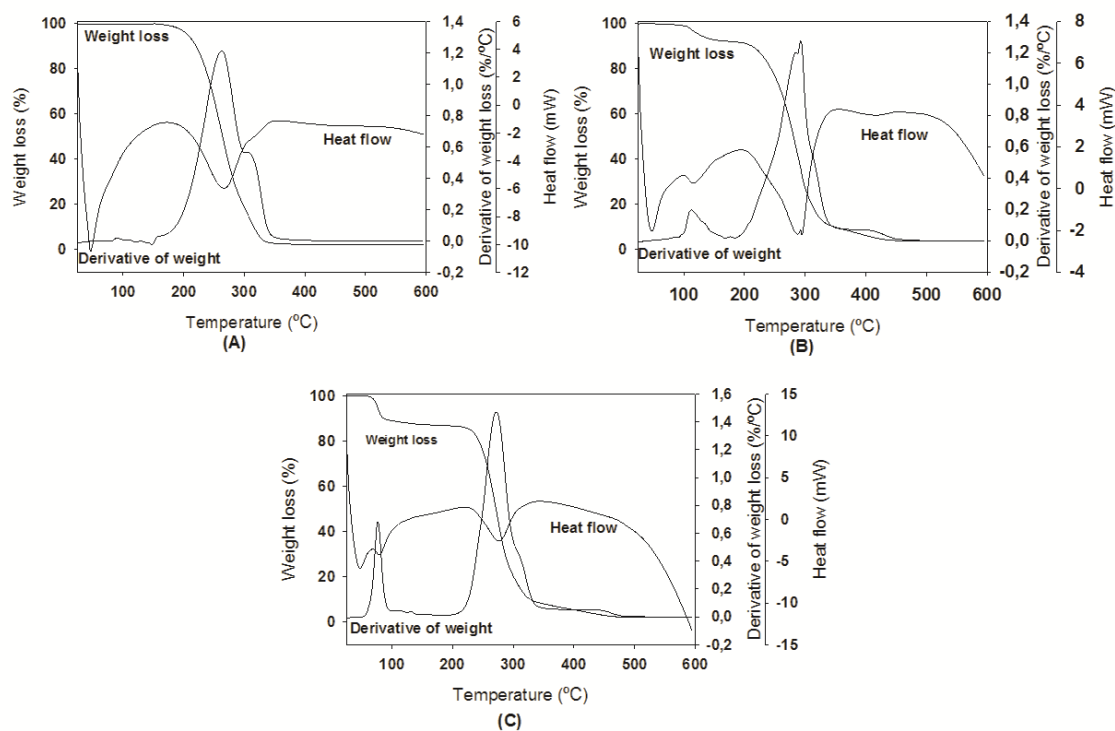


Figure D7 - Simultaneous thermoanalytical curves of LA co-oligomer and products of chain extension; (A) OLA-co-MA (AC-OLA6); (B) Product of chain extension (AC-CE11); (C) Product of chain extension (AC-CE12).

Figure D8 gives the thermoanalytical curves for LA oligomer (AC-OLA7) and products of chain extension with IPDI (AC-CE 13) and HMDI (AC-CE 14).

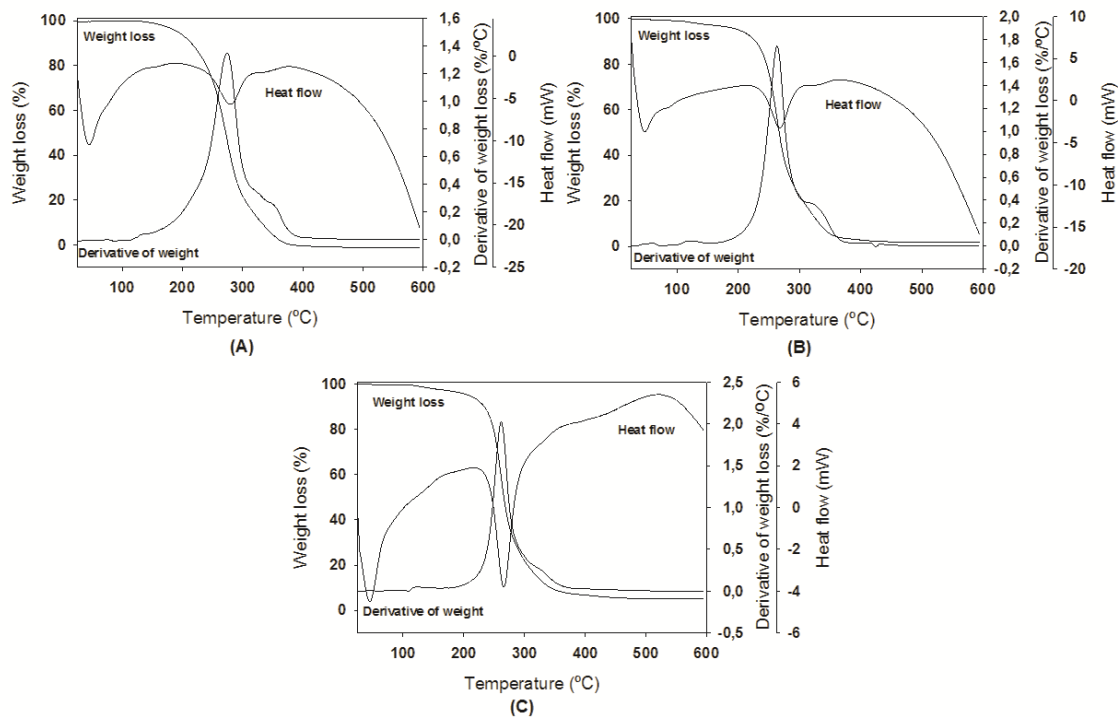


Figure D8 - Simultaneous thermoanalytical curves of LA co-oligomer and products of chain extension; (A) OLA-co-VA (AC-OLA7); (B) Product of chain extension (AC-CE13); (C) Product of chain extension (AC-CE14).

E. DSC Analysis

PLA homopolymers and copolymers

Melt polycondensation

Figure E1 shows the DSC thermogram (second heating cycle) of the PLA homopolymers and copolymer obtained by melt polycondensation.

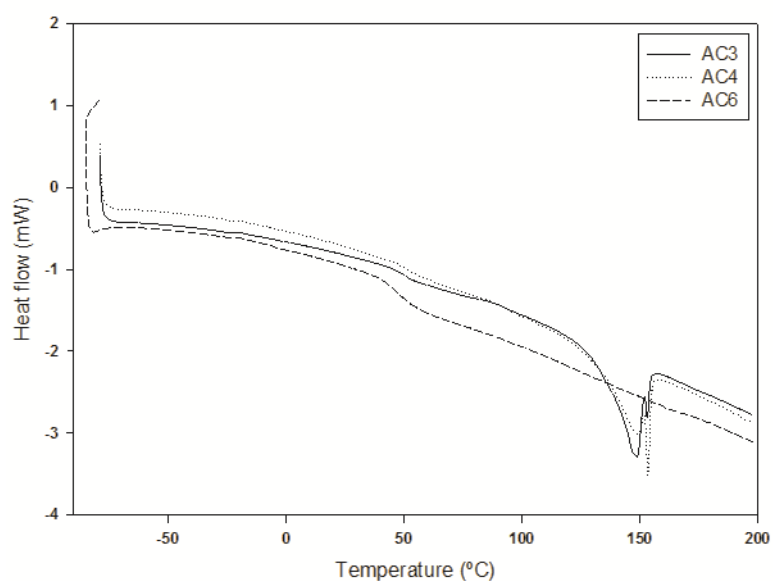


Figure E1 - DSC thermogram (second heating cycle) of the PLA homopolymers (AC3 and AC4) and copolymer (AC6) obtained by melt polycondensation.

Azeotropic dehydration condensation

The thermal behavior of PLA homopolymers (AC8 and AC9) and copolymer (AC10) obtained by azeotropic dehydration condensation has been studied by DSC (Figure E2) present the DSC thermogram obtained for PLA homopolymers and copolymers.

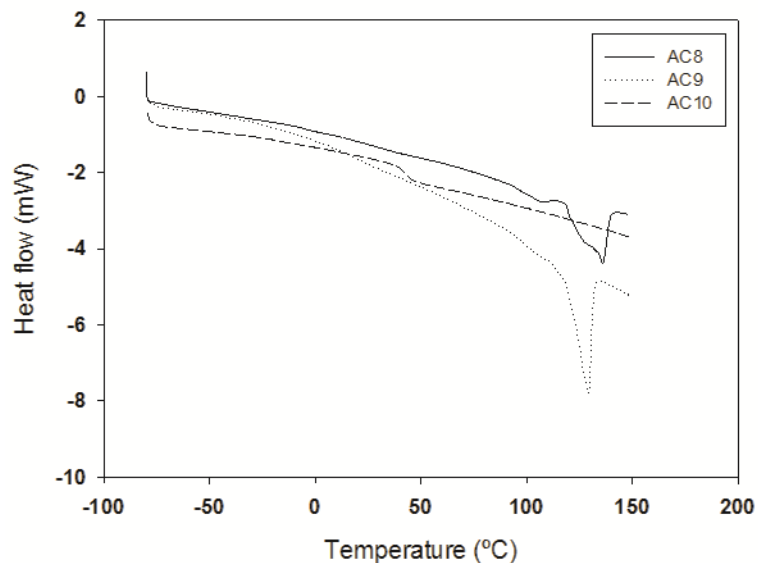


Figure E2 – DSC thermogram (second heating cycle) of the PLA homopolymers (AC8 and AC9) and copolymer (AC10) obtained by azeotropic dehydration condensation.

PLA chain extension

Figure E3 present the DSC curves (second heating cycle) obtained for the LA oligomers and products of chain extension.

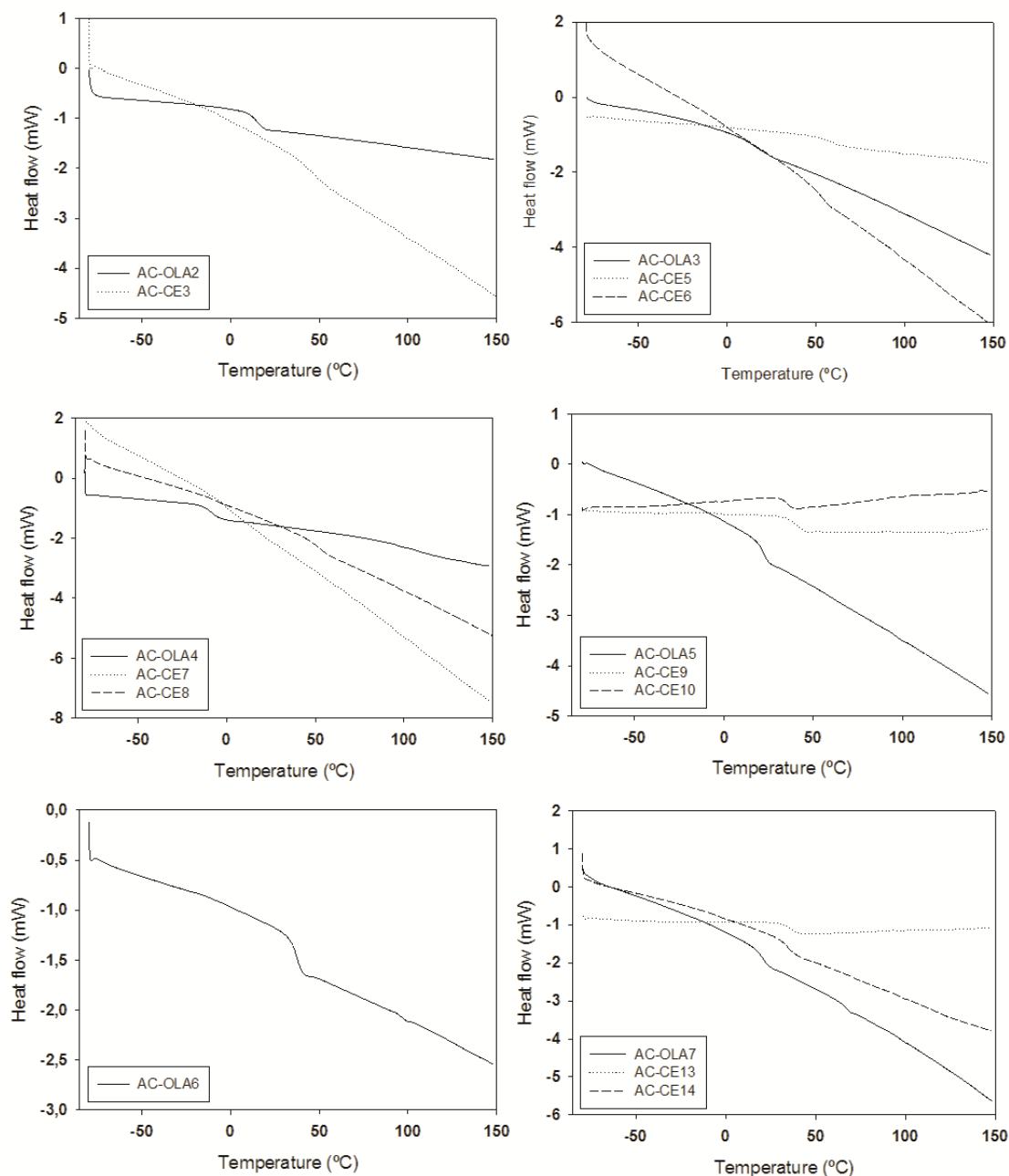


Figure E3 – DSC curves of LA oligomers and products of chain extension.

F. DMTA Analysis

PLA homopolymers and copolymers

Melt polycondensation

In order to investigate the thermal transitions of the PLA homopolymers (AC3 and AC4) and copolymer (AC6) obtained by melt polycondensation it was performed the DMTA analysis, using frequency of 1 Hz and 10 Hz (Figure F1).

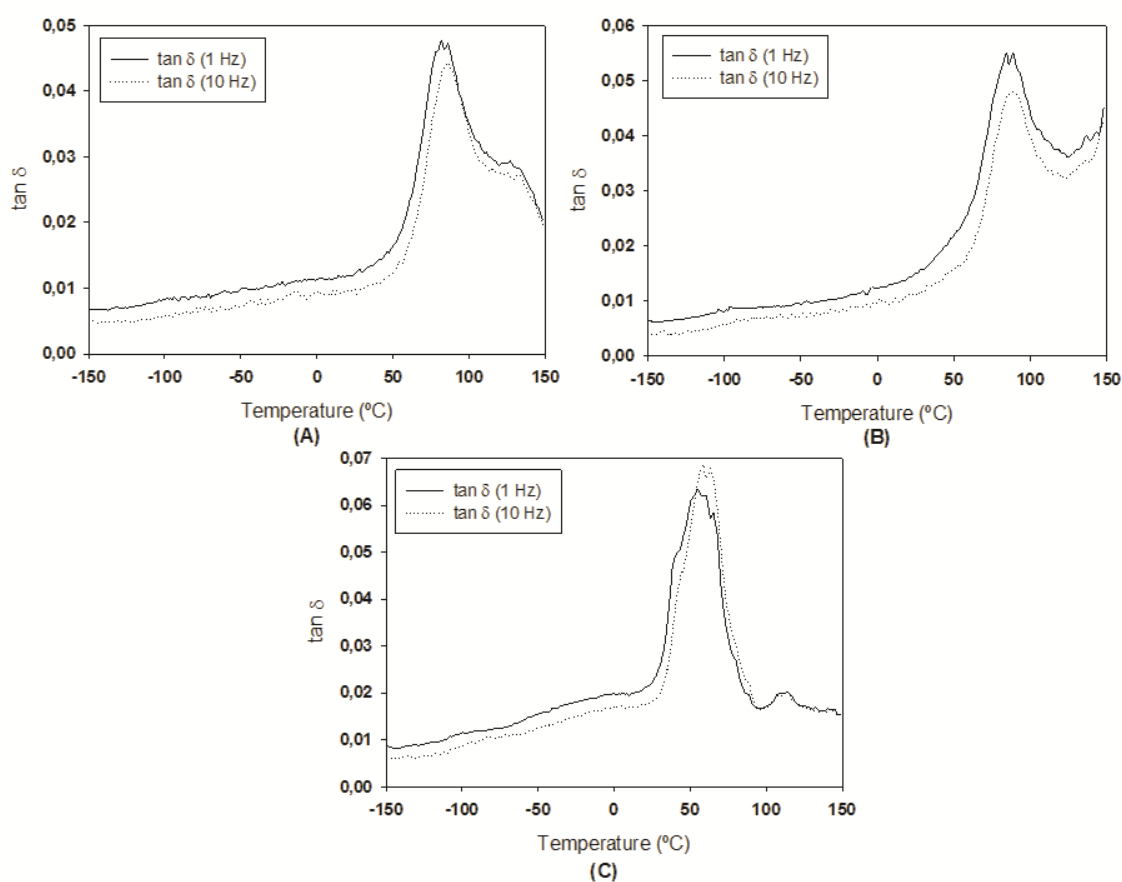


Figure F1 - DMTA traces (glass transition zone) of PLA homopolymers and copolymer, at two frequencies; (A) PLA homopolymer (AC3); (B) PLA homopolymer (AC4); (C) PLA-co-MA (AC6).

Azeotropic dehydration condensation

The thermal transitions of PLA homopolymers (AC8 and AC9) and copolymer (AC10) obtained by azeotropic dehydration condensation were evaluated by DMTA analysis using frequency of 1 Hz and 10 Hz (Figure F2).

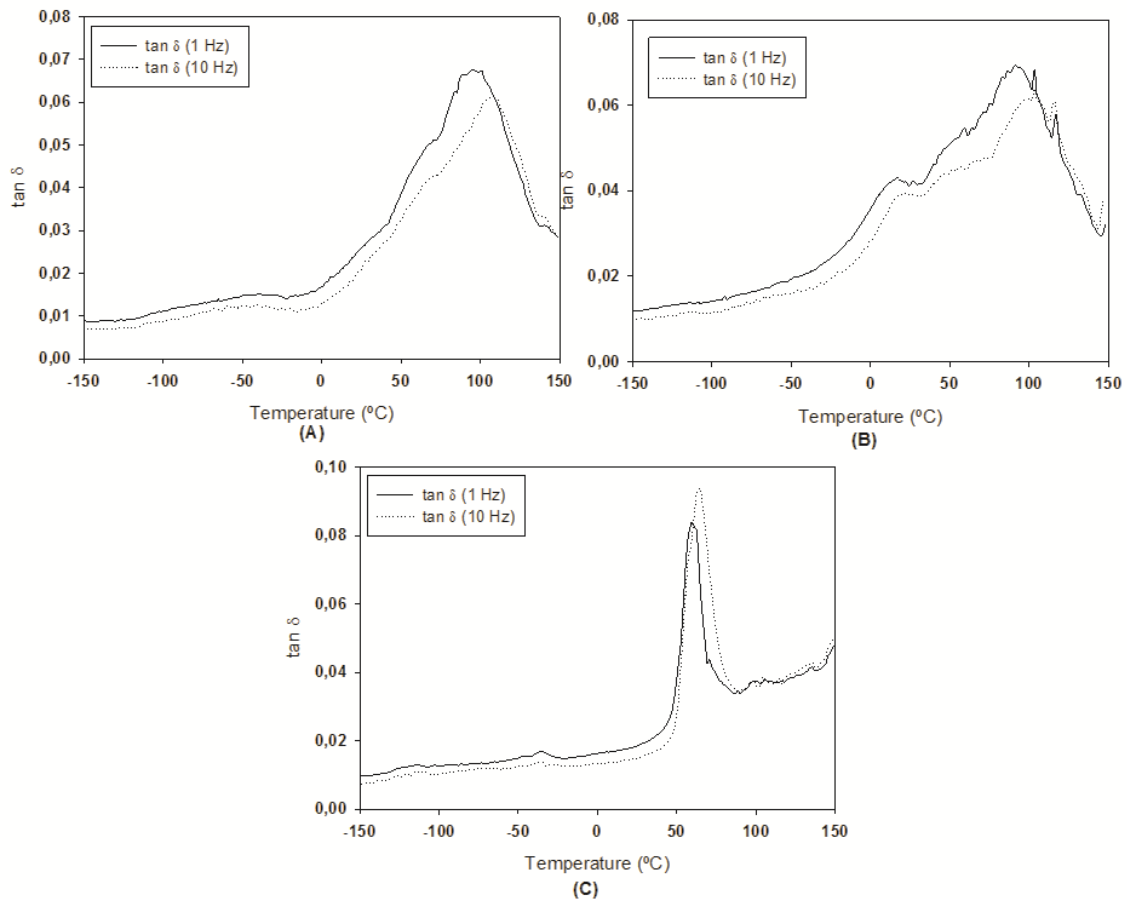


Figure F2 - DMTA traces (glass transition zone) of PLA homopolymers and copolymer, at two frequencies; (A) PLA homopolymer (AC8); (B) PLA homopolymer (AC9); (C) PLA-co-MA (AC10).

PLA chain extension

LA oligomer (AC-OLA2) and products of chain extension (AC-CE3 and AC-CE4) thermal events were also evaluated by DMTA analysis. Figure F3 present the DMTA traces for the LA oligomer and products of chain extension

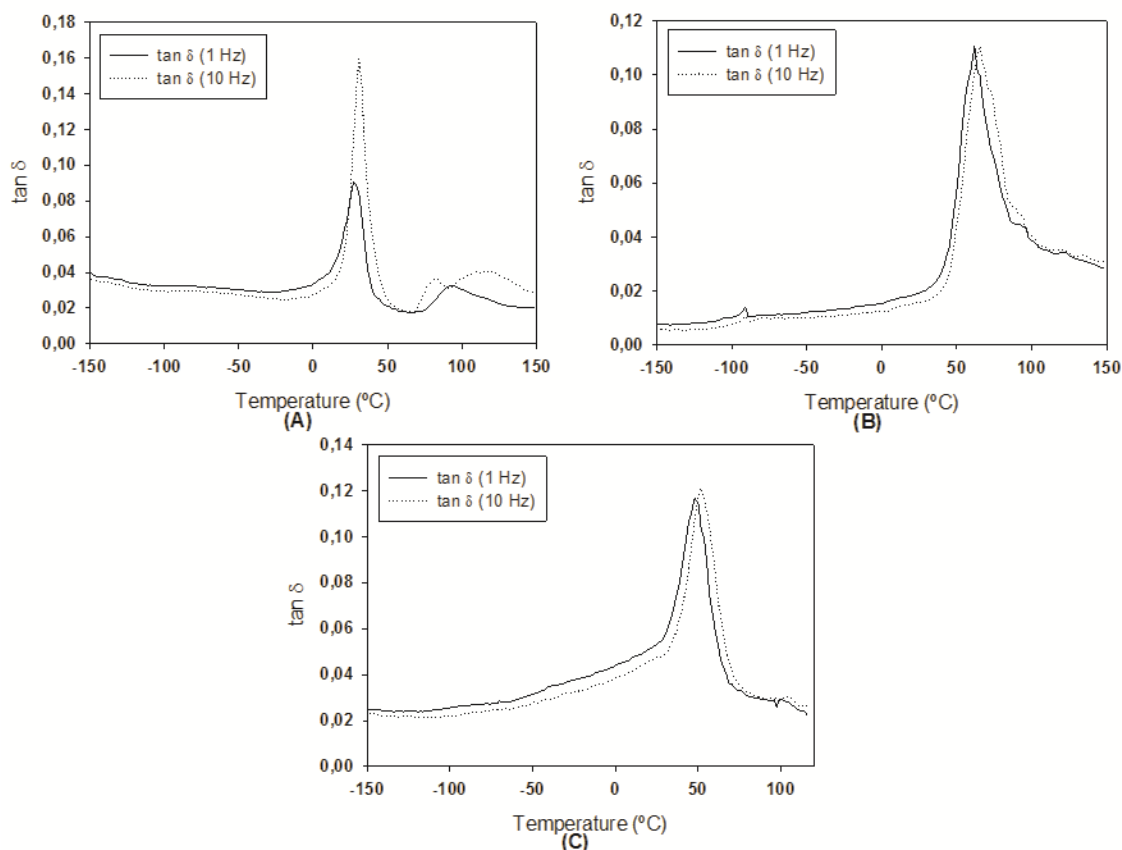


Figure F3 - DMTA traces (glass transition zone) of LA oligomer and products of chain extension, at two frequencies; (A) LA oligomer (AC-OLA2); (B) Product of chain extension (AC-CE3); (C) Product of chain extension (AC-CE4).

The thermal transitions of LA oligomer (AC-OLA3) and products of chain extension (AC-CE5 and AC-CE6) were investigated by DMTA analysis. Figure F4 present the DMTA traces for the LA oligomer and products of chain extension

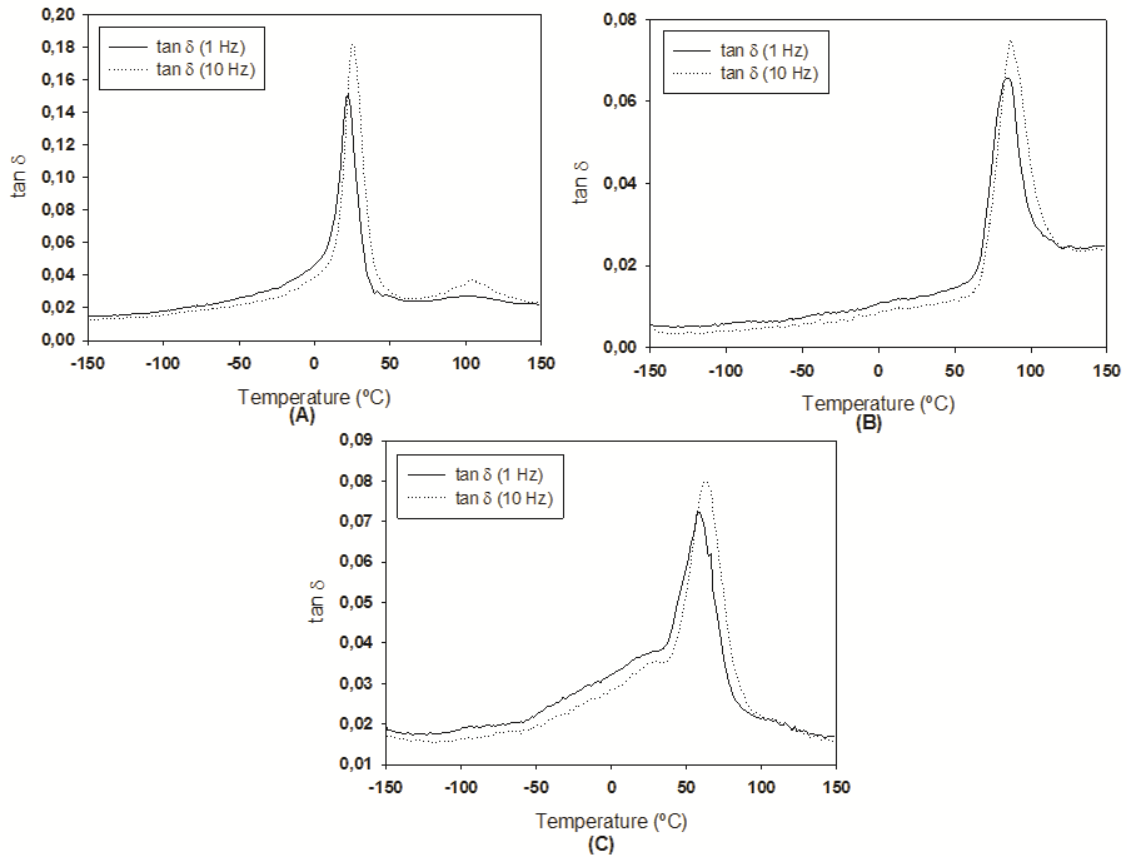


Figure F4 - DMTA traces (glass transition zone) of LA oligomer and products of chain extension, at two frequencies; (A) LA oligomer (AC-OLA3); (B) Product of chain extension (AC-CE5); (C) Product of chain extension (AC-CE6).

The thermal behaviors of LA oligomer (AC-OLA4) and products of chain extension (AC-CE7 and AC-CE8) were evaluated by DMTA analysis. Figure F5 present the DMTA traces for the LA oligomer and products of chain extension using, at 1 Hz and 10 Hz.

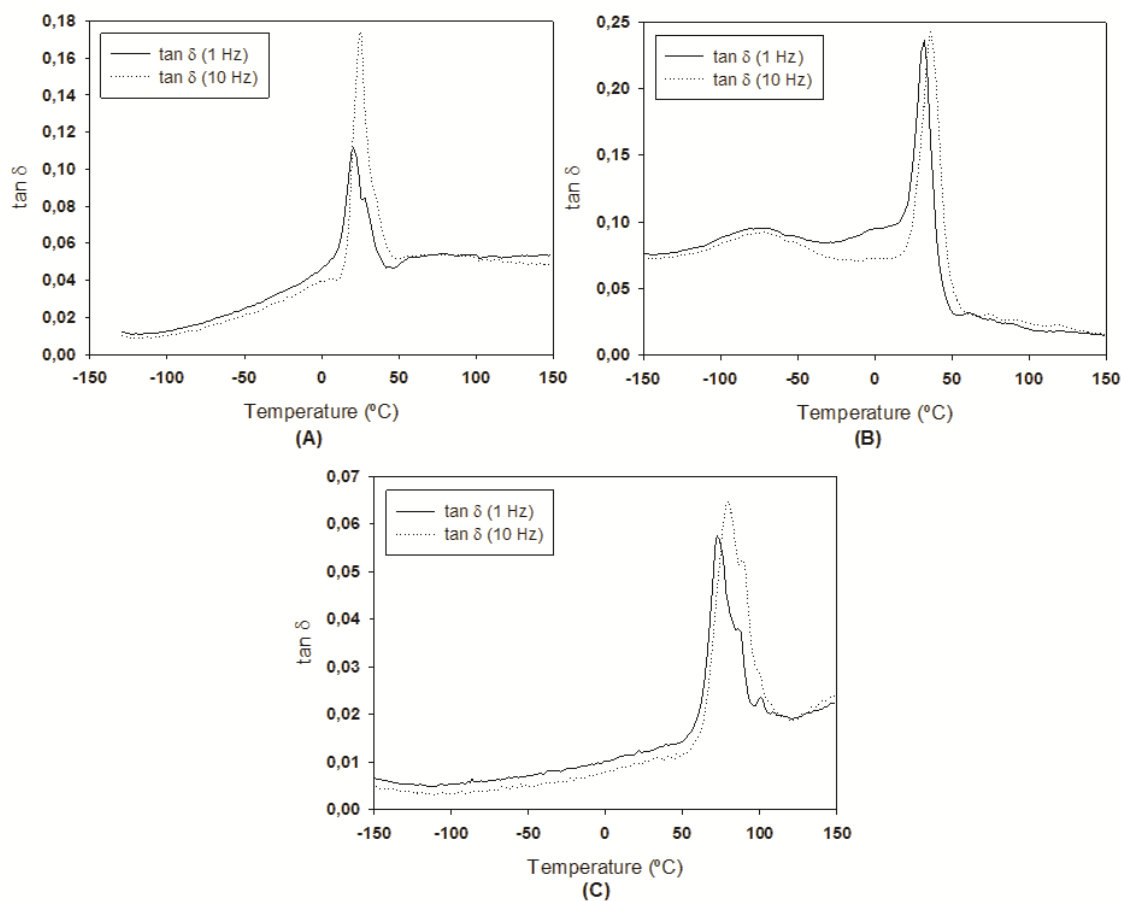


Figure F5 - DMTA traces (glass transition zone) of LA oligomer and products of chain extension, at two frequencies; (A) LA oligomer (AC-OLA4); (B) Product of chain extension (AC-CE7); (C) Product of chain extension (AC-CE8).

Figure F6 present the DMTA traces for the LA oligomer (AC-OLA5) and products of chain extension (AC-CE9 and AC-CE10) using frequency 1 Hz and 10 Hz.

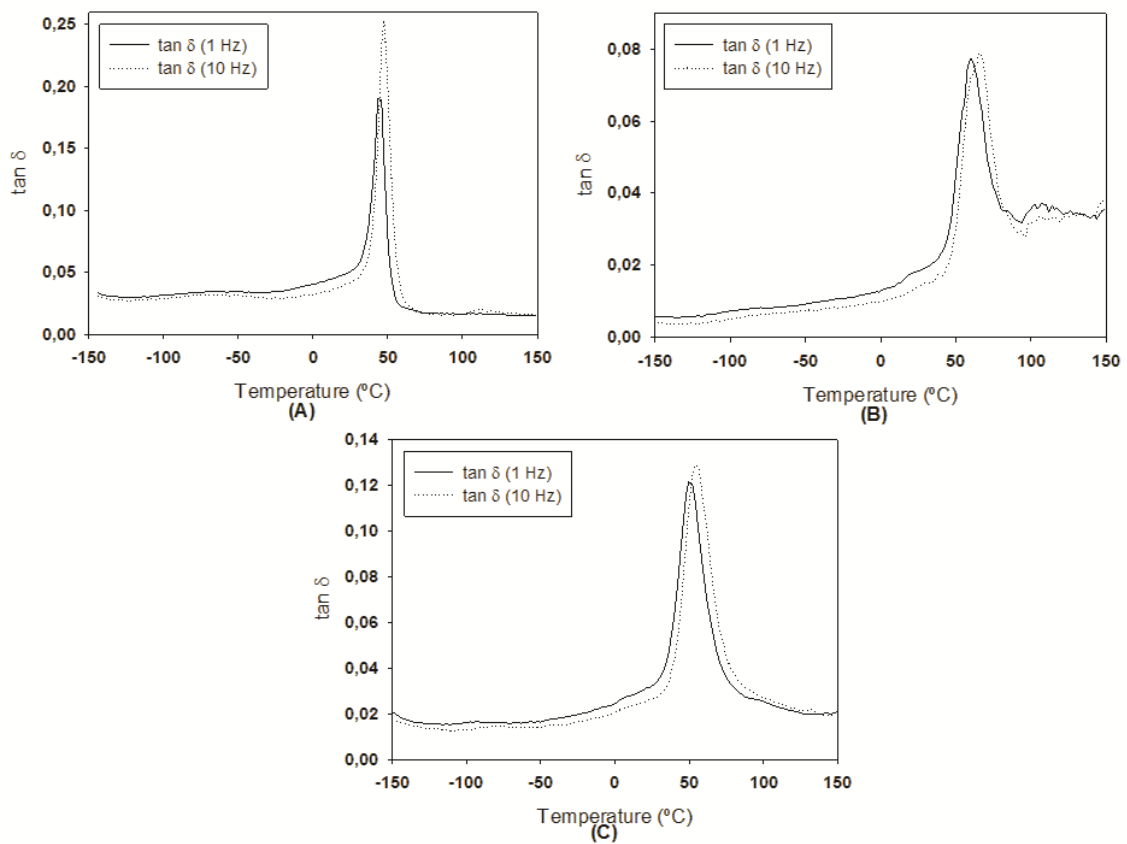


Figure F6 - DMTA traces (glass transition zone) of LA oligomer and products of chain extension, at two frequencies; (A) LA oligomer (AC-OLA5); (B) Product of chain extension (AC-CE9); (C) Product of chain extension (AC-CE10).

Figure F7 gives the DMTA traces for the LA oligomer (AC-OLA6) and products of chain extension (AC-CE11 and AC-CE12) using frequency 1 Hz and 10 Hz.

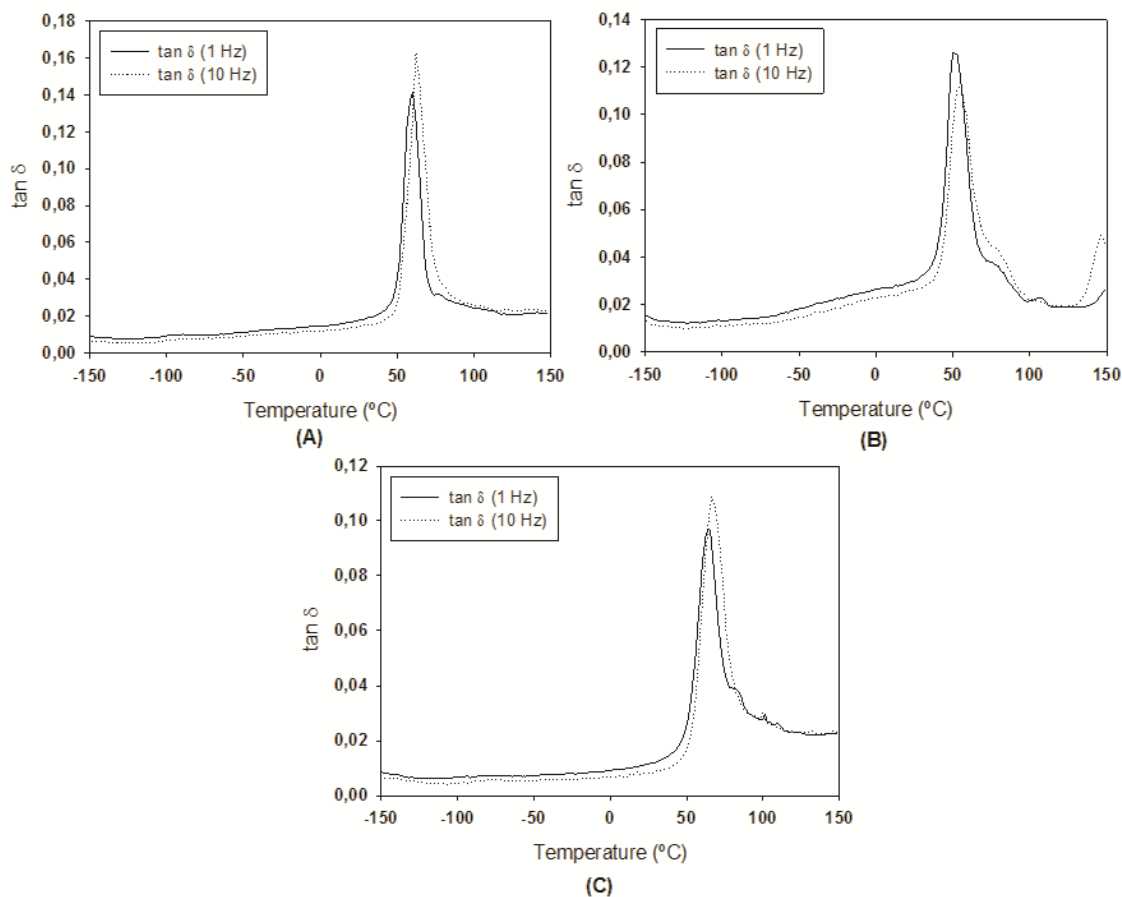


Figure F7 - DMTA traces (glass transition zone) of LA oligomer and products of chain extension, at two frequencies; (A) LA oligomer (AC-OLA6); (B) Product of chain extension (AC-CE11); (C) Product of chain extension (AC-CE12).

The T_g of LA oligomer (AC-OLA7) and products of chain extension (AC-CE13 and AC-CE14) were determined by DMTA analysis in multifrequency mode (1 Hz and 10 Hz).

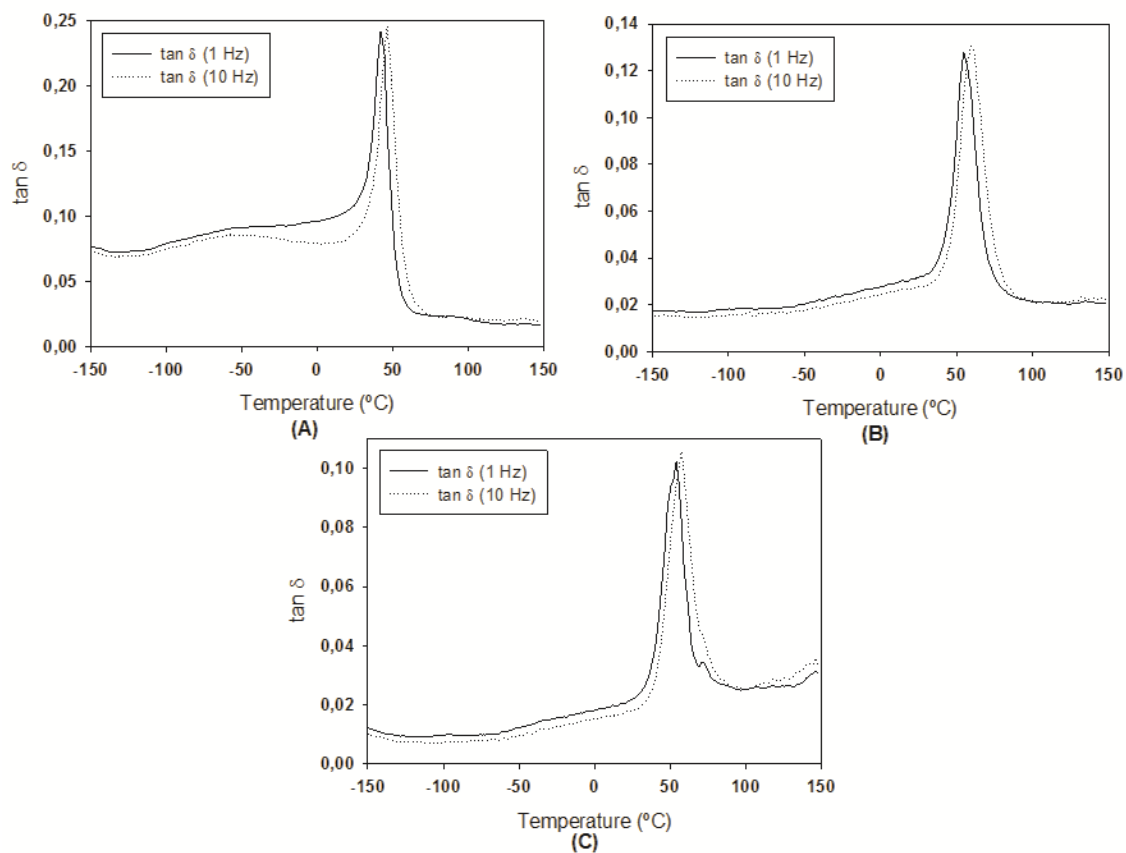


Figure F8 - DMTA traces (glass transition zone) of LA oligomer and products of chain extension, at two frequencies; (A) LA oligomer (AC-OLA7); (B) Product of chain extension (AC-CE13); (C) Product of chain extension (AC-CE14).